UNIVERSITEIT GENT

Faculteit Bio-ingenieurswetenschappen

Academiejaar 2009 – 2010

Monotemporal assessment of amount of *Acacia*'s (individuals, tree groups) and estimation of crown diameter classes of *Acacia raddiana* in Bou-Hedma National Park, Tunisia

Kevin Delaplace

Promotor: Prof. dr. ir. Robert De Wulf
Promotor: Prof. dr. ir. Donald Gabriels
Tutor: Dr. ir. Frieke Van Coillie
Tutor: Dr. Mohamed Ouessar
Tutor: Dr. Azaiez Ouled Belgacem
Tutor: Dr. Houcine Taamallah

Masterproef voorgedragen tot het behalen van de graad van
Master in de bio-ingenieurswetenschappen: land – en waterbeheer

Gent, June 2010

De auteur | De promotoren

Kevin Delaplace | Prof. dr. ir. R. De Wulf | Prof. dr. ir. D. Gabriels

ACKNOWLEDGEMENTS

This work was carried out at the Laboratory of Forest Management and Spatial Information Techniques (FORSIT) and the Department of Soil Management, Faculty of Bioscience Engineering, Ghent University. In Tunisia, the *Institut des Régions Arides* (IRA) provided a place to sleep, access to their library and transport from and to Bou-Hedma National Park. I wish to thank both institutes for affording me access to their research facilities. It was a great experience to perform research abroad.

I would like to thank FORSIT, to give me the opportunity to work with very high resolution satellite imagery (obtained specifically for this project) and to work with the newest software for image analysis. I would specifically like to thank prof. dr. ir. Robert De Wulf for his guidance and expertise on the forestry parts of my thesis. I am also pleased to thank dr. ir Frieke Van Coillie for guiding me through the image analysis part. Their enthusiasm was a driving force to continue and increased my interest in research.

I am grateful for the detailed revisions, performed by prof. dr. ir. Donald Gabriels, whose knowledge of (semi-)arid regions is a valuable addition for this work. Moreover, he is very familiar with the IRA, facilitating international research possibilities for students. In this context, it is also a great opportunity to express my respect to dr. ir. Koen De Smet (Flemish Government; Environment, Nature and Energy Department). His knowledge of the study area and efforts concerning the reforestation program, created excellent opportunities for research.

It is a pleasure to thank people from Tunisia, who supported me during the field survey. Special thanks go to ir. Lazhar Hamdi (head of the National Park), for his enthusiasm and efforts in managing the National Park. He taught me how to recognize local fauna and flora. Moreover, we had fascinating conversations and he allowed me to participate in religious holidays and local habits. Following persons (IRA) took care of the general organization of the project: dr. Mohamed Ouessar, dr. Azaiez Ouled Belgacem and dr. Houcine Taamallah. I would like to thank them for the necessary assistance. “Choukran!”

Literature on certain parts of this thesis is not always available or very hard to find. Hence, I express a warm thanks to Sahraoui Bensaid and Zouhaier Noumi for sending me articles and sharing their perspectives.

Last but not least, I would like to thank my family, especially my parents for they continued confidence and support. Many thanks go to my fellow students and friends, for a great study period in Gent. More specifically, Ken De Sadeleer (with whom I went to Tunisia), Frederik De Bruyn, Stijn De Lausnay, Stijn De Brabandere and Jef De Clerck.

Kevin Delaplace

Gent, June 2010

SUMMARY

Forest ecosystems influence human well-being. About 30 % of the world's forests have ground covers between 10 % and 30 %. Although these forests are essential resources for millions of rural people in developing countries, they are badly and often under-inventoried. Moreover, these open forests have special features that provide excellent opportunities for remote sensing-based forest inventory. In this study we focus on the *Acacia raddiana* forest steppe in Bou-Hedma National Park, Tunisia. *A. raddiana* is a keystone species in the pre-Saharan Tunisia zone, as it is the only tree persisting on the edge of the desert. In cooperation between the Flemish Government and the Direction Générale des Forêts of Tunisia, reforestation of 50,000 ha with *A. raddiana* is planned. In the fields of phenology and ecophysiology some studies have already been conducted. However, dynamics have not been studied in detail. Hence, in this study the aim is to perform a monotemporal assessment of the amount of *Acacia raddiana* and their crown diameter classes, with the use of a GeoEye-1 satellite image.

For image processing of the GeoEye-1 image, ground truth is required for classification and calibration of empirical models to estimate attributes of individual *Acacia raddiana* trees. In order to cover different spatial arrangements of trees, a random sampling scheme was selected. For each tree or tree group different tree attributes were measured: bole diameter at the base (0.10 – 0.15 m above the ground), bole diameter at breast height (1.30 m above the ground), total tree height and crown diameter. For each tree, a habit image was also taken in two directions, together with vertical images in each of the four cardinal directions (to obtain an estimate of tree crown density). Stages of phenology (leaf, flower and fruit), soil stoniness, erosion crust under and outside the tree canopy were visually determined using distinctive classes. Finally, vegetation under the tree canopy and outside the tree canopy was identified, together with the presence of animal faeces. Data were normalized and compiled in a relational database.

A general analysis of dendrometric and ancillary variables was performed. As no directional variation was found in crown diameter, the arithmetic mean of both directions was used for further analysis. Significant differences ($p < 0.05$) between tree individuals and tree groups were found for all tree attributes, with higher values for tree groups. This result is likely to be influenced by an age factor, as the majority of plantations are established in linear formations of individual trees, whereas tree groups are probably old relicts of the ancient forest steppe.

Analysis of erosion crust classes revealed a difference between the % cover of an erosion crust under and outside the tree canopy, indicating soil protection by tree cover. Stoniness classes were consistent with field observations, with a gradient from the mountain towards the sandy plain. Moreover, the dataset was grouped, based on the presence of animal faeces. Statistical significant differences ($p < 0.05$) were found for all tree attribute values, indicating a clear preference for rumination by the herbivorous fauna (*Oryx* sp., *Addax* sp. and *Gazella* sp.) near larger trees. This is mainly driven by the amount of shade casted by larger trees.

A. raddiana shows a large variation of appearances in the field, with sometimes a more bushy appearance. We tested the hypothesis that young individuals are multi-stemmed from the base and at a certain age one of the axes becomes the trunk. Significant differences between single-

and multi-stemmed trees were found, with a clear difference for tree height, mean and maximum diameter at breast height and maximum basal diameter. Single-stemmed trees showed larger attribute values. For the other tree attributes, differences were not explicit. Hence the hypothesis could not be rejected, nor accepted.

A *Geographic Object-Based Image Analysis* (GEOBIA) working strategy was used for image analysis. Through segmentation, with two subsequent algorithms (*multiresolution segmentation* and *contrast split segmentation*), objects were created. Both small and large trees were correctly delineated. After segmentation, objects were classified as *soil*, *Eucalyptus* or *Acacia* using Nearest Neighbour classification. A KIA based on the samples (biased) of 0.96 was found, using 170 *Acacia*, 37 *Eucalyptus* and 5,153 *soil* samples. Finally, over 200 object features were calculated to be used in the subsequent calibration of empirical models.

Empirical equations to estimate individual *Acacia raddiana* tree attributes were modelled. The models featured acceptable MAPE and RMSE values (based on typical forest inventory error between 15 % and 20 %). Empirical equations are given to estimate bole diameter, stem volume and tree height from crown diameter. Moreover, a strong linear relation was found between equivalent bole diameter at the base and equivalent bole diameter at breast height. Hence, stem volume could be estimated with basal diameter as only variable. Finally, the height-diameter curve was fitted. Based on the created image objects, a strong correlation was found between the object feature *area* and the tree attributes. Moreover, an exponential relation was found between *area* and *GLCM Entropy Layer 4 (90°)*. This relation makes it possible, to estimate individual tree characteristics based on a texture feature. Empirical models are presented to estimate crown diameter from the *area* feature and crown diameter, tree height and bole diameter from the *GLCM Entropy Layer 4 (90°)* feature.

With the modelled empirical equations and the classified GeoEye-1 image, the structure of the population of *Acacia raddiana* in Bou-Hedma National Park was determined. During image analysis, 21,912 segments were classified as *Acacia*. The distribution of basal diameter classes shows exponential behaviour, confirming an uneven-aged forest structure. Calculation of tree density (number of identified crowns per ha), indicated a mean density of 8.4 trees, with maximum density of 95 trees per ha.

SAMENVATTING

Bosecosystemen beïnvloeden menselijk welzijn. Ongeveer 30 % van de bossen in de wereld, hebben een bedekkingsgraad tussen de 10 % en 30 %. Deze bossen leveren essentiële natuurlijke hulpbronnen voor miljoenen mensen in ontwikkelingslanden. Nochtans zijn deze bossen vaak slecht of beperkt geïnventariseerd. Bovendien beschikken deze open bossen over speciale eigenschappen, die ze geschikt maken om met *remote sensing* technieken geïnventariseerd te worden. In deze studie behandelen we de *Acacia raddiana* steppe in Bou-Hedma Nationaal Park, Tunesië. *A. raddiana* is een sleutelsoort ten noorden en ten zuiden van de Sahara, aangezien het de enige boomsoort is, die op de rand van de woestijn kan overleven. In samenwerking met de Vlaamse Overheid en de Direction Générale des Forêts van Tunesië, wil men in de nabije toekomst 50,000 ha aanplanten met *A. raddiana*. Er is al wat onderzoek verricht in Bou-Hedma Nationaal Park, voornamelijk op vlak van fenologie en ecofysiologie. De dynamiek werd echter nog niet in detail bestudeerd. In deze studie is het doel dan ook, om monotemporeel het aantal *Acacia raddiana* bomen te bepalen, samen met hun diameterklassen, door gebruik te maken van een GeoEye-1 satellietbeeld.

Voor de verwerking van het satellietbeeld, zijn er data op het veld noodzakelijk. Deze data zijn noodzakelijk voor beeldclassificatie en de calibratie van empirische modellen om boom attribuutwaardes van *Acacia raddiana* te schatten. Om de verschillende vormen van voorkomen te bemonsteren, werd een random samplingschema gebruikt. Voor elke boom (of groep van bomen) werden meerde attributen opgemeten: stamdiameter aan de basis (0.10 – 0.15 m boven de grond), stamdiameter op borsthoogte (1.30 m boven de grond), totale boomhoogte en kroondiameter. Van elke boom, werd ook een habitusfoto genomen in twee richtingen. Bovendien werden ook verticale foto's genomen, om de kroondensiteit te schatten. Verschillende fenologische stadia (blad, bloei en vrucht), bodemstenigheid en het voorkomen van een erosiekorst onder en buiten de kroon, werden visueel bepaald, gebruik makend van verschillende klassen. Vegetatie onder en buiten de verticale kroonprojectie werd ook geïdentificeerd, samen met de aanwezigheid van dierlijke uitwerpselen. De data werden genormaliseerd en samengevoegd in een relationele database.

Een algemene dendrometrische analyse werd uitgevoerd. Er werd geen directionele variatie gevonden in kroondiameter, dus werd het rekenkundig gemiddelde gebruikt verdere analyse. Significante verschillen ($p < 0.05$) werden gevonden tussen boomindividuen en boomgroepen, met hogere waardes voor boomgroepen. Dit resultaat is hoogstwaarschijnlijk beïnvloed door een leeftijdsfactor. De meeste plantages werden namelijk aangeplant in lineaire formaties van individuen, waarbij boomgroepen vermoedelijk relicten zijn van het oude bos.

De procentuele bedekking met een erosiekorst, vertoonde duidelijke verschillen onder en buiten de kroonprojectie, wat de bescherming van de bodem door boombedekking aantoont. Klassen van stenigheid, waren consistent met de veldwaarnemingen, met een gradiënt van de bergketen naar de zandige vlakte. Verder werd de dataset gesplitst, op basis van de aanwezigheid van dierlijke uitwerpselen. Er werden statistisch significante verschillen gevonden voor alle boom attribuutwaardes, wat een duidelijke voorkeur aantoont voor grotere bomen, voor herkauwing door de herbivoren in het park. (*Oryx* sp., *Addax* sp. and *Gazella* sp.). Dit is vooral veroorzaakt door de hoeveelheid schaduw van deze individuen.

A. raddiana vertoont veel variatie in voorkomen in het veld, met soms een eerder struikachtig uitzicht. We hebben de hypothese getest dat jonge individuen meerstammig zijn aan de basis en dat vanaf een zeker leeftijd, één van de stammen de hoofdas wordt. Significante verschillen werden gevonden tussen eenstammige en meerstammige individuen, met een duidelijk verschil in boomhoogte, gemiddelde en maximale stamdiameter op borsthoogte en maximale basale diameter. Enkelstammige bomen vertoonden grotere attribuutwaardes. Voor de andere boom attributen, waren de verschillen niet uitdrukkelijk aanwezig. De hypothese kon dus niet verworpen, noch aanvaard worden.

Een *Geographic Object-Based Image Analysis* (GEOBIA) strategie werd gebruikt voor de beeldanalyse. Door het beeld te segmenteren, met twee opeenvolgende algoritmes (*multiresolution segmentation* en *contrast split segmentation*), werden objecten gecreëerd. Zowel kleine als grote bomen, werden correct afgelijnd. Na deze segmentatie, werden deze objecten geclassificeerd als *bodem, Eucalyptus* of *Acacia* met een Nearest Neighbour classifier. Uiteindelijk werden meer dan 200 object *features* berekend, gebruikt voor de calibratie van empirische modellen. Er werd een KIA (gebaseerd op de trainingsdata, dus met *bias*) gevonden van 0.96, met 170 *Acacia*, 37 *Eucalyptus* en 5,153 *bodem* segmenten als trainingsdata.

Er werden empirische vergelijkingen opgesteld, om individuele boom attribuutwaardes te schatten. De modellen hadden aanvaardbare RMSE en MAPE waardes (gebaseerd op een typische bosinventarisatie fout tussen de 15 % en 20 %). Empirische vergelijkingen worden gegeven om de stamdiameter, stamvolume en boomhoogte te schatten op basis van de kroondiameter. Er werd bovendien een lineair verband gevonden, tussen de stamdiameter aan de basis en de stamdiameter op borsthoogte. Op deze manier kon een relatie opgesteld worden die het stamvolume bepaalt, op basis van de basale diameter. Ook de hoogte-diameter curve werd opgesteld. Gebaseerd op de gecreëerde beeldobjecten, werd een sterke correlatie gevonden tussen het object *feature area* and de boom attribuutwaardes. Bovendien werd een exponentiële relatie gevonden tussen de *features area* en *GLCM Entropy Layer 4 (90°)*. Deze relatie maakt het mogelijk, om individuele boomkenmerken te schatten, op basis van een textuurmaat. Empirische modellen worden gegeven, om de kroondiameter te schatten op basis van *area* en kroondiameter, boomhoogte en stamdiameter op basis van *GLCM Entropy Layer 4 (90°).*

Op basis van de gemodelleerde vergelijkingen en het geclassificeerde beeld, werd de structuur van de populatie *Acacia raddiana* bepaald in Bou-Hedma National Park. De beeldanalyse leverde 21,912 segmenten op, die werden geclassificeerd als *Acacia*. De distributie van de basale diameter klassen, vertoont exponentieel gedrag, die de ongelijkjarige structuur bevestigt. Berekenen van de densiteit (als het aantal afgelijnde kronen per ha), geeft een gemiddelde waarde van 8.4 bomen per ha, met een maximum van 95 bomen per ha.

CONTENTS

LIST OF ABBREVIATIONS

ANOVA	Analysis Of Variances
AZ	Agricultural Zone
BC	Before Christ
BD	Basal Diameter
BZ	Buffer Zone
CDM	(Kyoto) Clean Development Mechanism
DBH	Diameter at Breast Height
DGF	Direction Générale des Forêts
DN	Digital Number
FAO	Food and Agricultural Organization of the United Nations
FDI	Forest Discrimination Index
FSO	Feature Space Optimization
GEOBIA	Geographic Object-Based Image Analysis
GIS	Geographic Information System
GLCM	Grey Level Co-occurrence Matrix
GMT	Greenwich Mean Time
IPZ	Integral Protection Zone
IRA	Institut des Régions Arides
KIA	Kappa Index of Agreement
LAI	Leaf Area Index
MAPE	Mean Absolute Percentage Error
NIR	Near Infrared
NN	Nearest Neighbour
RGB	Red Green Blue
RMSE	Root Mean Square Error
SAVI	Soil Adjusted Vegetation Index
TCD	Tree Crown Density
TTA	Training and Test Area
UNESCO	United Nations Educational, Scientifical and Cultural Organization
UTM	Universal Transverse Mercator
VHR	Very High Resolution
WGS	World Geodetic System

LIST OF TABLES

LIST OF FIGURES

INTRODUCTION

Forest ecosystems provide natural resources, as well as other economic and ecological benefits; hence they influence human well-being (Falkowski et al., 2009). About 30 % of the world's forests have ground covers between 10 % and 30 %. These forests are essential resources for millions of rural people in developing countries; however they are badly and often under-inventoried. Hence, future trends in these forests are hard to predict (Ozdemir, 2008). In the past, (semi-)arid zones did not receive the necessary attention, concerning their biodiversity, protection and use. As a result, tree populations are nowadays threatened by overexploitation. However, the use of local species to combat desertification is gaining interest (Grouzis and Le Floc'h, 2003).

Acacia raddiana is an important woody species in the pre-Saharan Tunisia zone. The species is able to tolerate extreme drought (in the range of 20 to 200 mm), through special adaptations such as a deep lateral root and partial shedding of leaves in the dry season. It is the only forest tree persisting on the edge of the desert and is therefore considered a keystone species (Abdallah et al., 2008; Grouzis & Le Floc'h, 2003). The restoration of the original woodland combating desertification, particularly by afforestation and reforestation, is therefore an important research activity in the Bou-Hedma region (Bou-Hedma National Park, part of the network of Biosphere Reserves of UNESCO). Some studies have been conducted on this population of *A. raddiana,* particularly in the fields of phenology and ecophysiology (Grouzis & Le Floc'h, 2003; Mihidjay, 1999; Wahbi, 2006). However, dynamics have not been studied in detail, although knowledge of the dynamics may be useful to test the efficiency of different management scenarios (Noumi et al., 2010).

In cooperation between the Flemish Government and the Direction Générale des Forêts (DGF) of Tunisia, reforestation of 50,000 ha with *Acacia raddiana* is planned in the historical geographic range of the species (from Sidi Toui to the region of Tozeur). These reforestation programs are part of a larger project (Kyoto Clean Development Mechanism (CDM)), requiring scientific follow up of the plantations, their ecological and their socio-economical consequences. Reforestation of *A. raddiana* is hypothesised to induce local climatic change, by a change in vegetation cover and hence a change in

ecosystem *albedo* and *surface roughness*. Consequences likely to occur include (De Smet[1], personal communication):

- Change of soil temperature
- Formation of humus by partial leaf shedding in summer
- Influence on the cloud formation process, inducing precipitation
- Interception of water by tree leaves and trunks, influencing erosion processes

Although consequences of reforestation programs are likely to occur, scientific data remains scarce. When large areas are considered, a regional climate change might be observed. The impact of this local climate change will also be felt outside the Biosphere Reserve, where the local rural population depends on rain fed agriculture and the water resources originating from water infiltrated on the mountains of the Bou-Hedma mountain chain.

In order to evaluate future trends, it is important to assess the current situation at Bou-Hedma National Park. Hence, the objective of this MSc. thesis is the monotemporal assessment of amount of *Acacia raddiana* (tree groups and tree individuals) in Bou-Hedma National Park and estimation of crown diameter classes of *Acacia raddiana.* Following research questions were postulated:

i. Which allometric relations can be modelled to estimate individual tree attributes? What are the associated error margins?
ii. What is the most appropriate (semi-)automated image processing procedure to estimate the amount and crown diameter classes of *Acacia raddiana*? What are the associated error margins?
iii. What is the contribution of multispectral wavebands in addition to panchromatic (1 channel) data? What are the associated error margins?
iv. What time of acquisition is optimal to estimate the amount and crown diameter classes of *Acacia raddiana*? What are the associated error margins?
v. What is the contribution of soil characteristics (e.g. stoniness, texture) to enhance results? What are the associated error margins?
vi. What is the morphology and structure of the *Acacia raddiana* forest steppe at Bou-Hedma National Park?

[1] dr. ir. Koen De Smet, Flemish Government, Environment, Nature and Energy Department, Belgium

In order to solve these research questions, field measurements were performed in Bou-Hedma National Park (from September to October 2009). With the aid of a GeoEye-1 image and Google Earth Imagery, it could be noticed that, at Bou-Hedma, *Acacia'*s appear in two different forms. First, there are plantations wherein trees are found in linear formations, scattered over the entire National Park. Secondly, there are also *Acacia* trees located in depressions and dried (temporal) riverbeds (*wadi* or *oued*). In order to sample both *Acacia* tree forms including different tree diameter classes, a random sampling scheme was selected.

This work mainly consists of two inter-related topics: forestry and remote sensing. The forestry part consists of the analysis of the field measurements and the estimation of amount of *Acacia raddiana* and their tree attributes. However in order to estimate the amount of *Acacia'*s, image analysis is necessary. These two topics are also reflected in the structure of this work. In a first chapter (*Literature study)*, a summary is given of the different visions and methods described in literature. This chapter mainly focuses on the remote sensing part. In a second chapter (*Materials and methods)*, Bou-Hedma National Park and its current organization is discussed, followed by a detailed description of the measured tree attributes and ancillary variables. We also describe the GeoEye-1 characteristics and the software used for analysis. The last part of this chapter, treats the methodology followed for image analysis and a detailed description of the algorithms used. In the third chapter (*Results and discussion*), the obtained results are presented and discussed. The first part gives a general analysis of the field data. Next, the results of the image segmentation and classification are discussed, followed by empirical equations to estimate individual *Acacia raddiana* tree attributes. Finally, based on the modelled equations and the classification of the GeoEye-1 image, we determine the structure of Bou-Hedma National Park.

Chapter 1: LITERATURE STUDY

In this first section, a summary of literature relevant for this work is given. By means of introduction, the importance of forest inventory data, as described in literature, is briefly discussed. Next, the contribution of remotely sensed data is emphasized, followed by a comparison between a Geographic Object-Based Image Analysis (GEOBIA) and a pixel-based working strategy. Thereafter, forest attribute estimation with Very High Resolution (VHR) data is discussed. Finally, some frequently used biometric relationships are listed.

1 FOREST INVENTORY

Forests ecosystems provide natural resources (and other economic and ecological benefits), which influence human well-being. The inventory and monitoring of these ecosystems, has been a research topic for many years (Chubey et al., 2006). However, the impact of forest upon the global environment (e.g. through storage of carbon) is less clear (Wulder, 1998). Therefore general forest information and knowledge of forest dynamics are required to understand the interaction between ecosystems and human activities (IPCC, 2000; Wulder 1998). Monitoring forests over large areas is necessary for the development (and evaluation) of sustainable forest practices and policies (Falkowski et al., 2009; Leckie et al., 2005).

Forest structure is the above-ground organization of plant materials, being the result of competition for light, water and nutrients at a given location (Wulder, 1998). Understanding the forest structure, gives us the opportunity to monitor, model and predict important biophysical processes, such as the interaction between the forest and the atmosphere (Running et al., 1994). Changes in forest structure may also provide information related to forest vigour, harvests, burns, stocking level and diseases (Wulder, 1998). Forests can be characterized in terms of inventory measures (e.g. height and volume) or biophysical parameters (e.g. LAI and biomass). These biophysical parameters are often used as they correlate with climate conditions and physiological processes, such as photosynthesis (Wulder, 1998).

Historically, forest inventory data was mainly collected through *in situ* measurements in order to estimate timber quality and quantity over smaller areas. The increasing attention for environmental issues, have increased the need for spatial, temporal and categorical details demanded of forest inventories (Falkowski et al., 2009). Forest inventories can provide information for various (long-term) objectives, such as biodiversity monitoring, carbon accounting, habitat protection and sustainable timber production. To attain these objectives, timely forest inventory data is often required across large spatial extents. Both spatial and timely data can easily be provided through remote sensing (Falkowski et al., 2009; Palace et al., 2008).

2 THE CONTRIBUTION OF REMOTELY SENSED DATA

Since the launch of the first earth observation satellite, Landsat-1, in 1972, satellite remote sensing has played an important role in forest monitoring (Hirata, 2008). However, the efficacy of large-area forest inventories with remotely sensed data depends upon the relationship between the scale of the object of interest (individual trees or forest stands) and sensor-specific characteristics (spatial, spectral and temporal resolution). Remote sensing systems that provide images with large spatial extents will measure less spatial detail compared to images acquired by higher spatial resolution sensors that provide more details, across a smaller spatial extent (Falkowski et al., 2009).

The use of remotely sensed data to augment traditional field-based forest inventories is not new. Manually deriving forest inventory data from analogue aerial photography has historically been the primary application of remotely sensed data (Chubey et al., 2006; Falkowski et al., 2009; Kayitakire et al., 2006; Palace et al., 2008). Human assessment is however time-consuming and the results may vary between analysts (Wulder, 1998). Nevertheless, analogue aerial photography remains an attractive data source for forest inventory and assessment, because of the high spatial resolution (Falkowski et al., 2009).

The lack of direct relationships between remotely sensed reflectance values and the forest parameters of interest to forest managers (e.g. tree height and diameter at breast height (DBH)), has limited the applications to support forest management decisions (Suarez et al., 2005). Trees are in general much smaller than the pixel size of common medium spatial resolution (10 to 30 m) remotely sensed data (Palace et al., 2008). This

prohibits the direct measurement of object properties (such as tree location and crown dimensions) (Hirata, 2008) and therefore the data do not provide information at scales relevant to meet particular forest management and planning needs (Falkowski et al., 2009). But, when very high resolution (VHR) sensors are considered, the objects (more specific, the trees) are larger than the image pixel size, making it possible to directly measure certain object properties (Falkowski et al., 2009; Hirata, 2008; Leckie et al., 2005).

Remotely sensed images from VHR sensors (spatial resolution <1 m) are able to resolve individual trees, thereby enabling more accurate estimates of detailed forest inventory attributes (Bunting and Lucas, 2006; Chubey et al., 2006; Gougeon and Leckie, 2006; Kayitakire et al., 2006; Ozdemir, 2008). Through the fusion of digital image analysis techniques with ground-based forestry, the new generation of high resolution, space borne satellites have potential to generate biomass estimates (Greenberg et al., 2005; Popescu, 2007). The spatial detail of VHR data could facilitate the characterization of subtle changes in forest structure through time as well (Falkowski et al., 2009; Palace et al., 2008).

3 GEOBIA VERSUS PIXEL-BASED WORKING STRATEGY

The conventional approach of deriving forest inventory information through manual interpretation of aerial photographs has proven very useful. Crown area (and subsequently diameter at breast height, DBH) can be estimated on an individual tree basis through manual photo interpretation (Greenberg et al., 2005). The process of acquiring, processing, and interpreting air photos is well established, understood and relative cost effective (Blaschke et al., 2008). A major drawback in manual delineation is subjectivity, with different results for different interpreters, or the same interpreter at different times (Blaschke et al., 2008). Therefore, it has long been anticipated that manual photo-based forest inventory procedures will be replaced with semi-automated, digital remote sensing approaches, with greater efficiency and consistency (Chubey et al., 2006), making them more suitable for monitoring (Blaschke et al., 2008). However, the use of these semi-automated methods (involving other data sources), have to be shown effective and more efficient than the existing workflow, or provide information currently not available (Blaschke et al., 2008). For these analyses to be operational, an entirely different approach to digital image analysis, such as one based on image objects

rather than pixels, is needed (Chubey et al., 2006). This has lead to a new discipline, called GEOBIA, defined as follows (Hay & Castilla, 2008):

> *Geographic Object-Based Image Analysis* (GEOBIA) is a subdiscipline of *Geographic Information Science (GIScience)* devoted to developing automated methods to partition remote sensing imagery into meaningful image-objects, and assessing their characteristics through spatial, spectral and temporal scales, so as to generate new geographic information in GIS-ready format.

Using this approach aggregates (image objects) of the individual pixels are created, representing the forest stand (or the individual tree) (Chubey et al., 2006). The recent release of new commercial object-based image analysis software, such as eCognition® (Definiens, 2009a), coupled with the limitations of pixel-based methods, has led to new interest in object-based image analysis of remotely sensed data (Chubey et al., 2006).

A major advantage of object-based image analysis is the multitude of additional information that can be derived. Pixels typically contain a vector of information representing each band or layer in a data set. For digital imagery, the sensors measure energy that is reflected largely from the upper surface of canopies and hence a two dimensional view is provided (Bunting & Lucas, 2006). The spectral response information is related as digital numbers (DN). This spectral response is influenced by shadowing within and between crowns and reflectance from non-photosynthetic material such as bare soil (Bunting & Lucas, 2006; Wulder, 1998). In contrast, image objects are generally composed of multiple pixels, enabling the calculation of statistics, such as mean, standard deviation and others (Chubey et al., 2006). The higher spectral variance in VHR imagery also limits the classification accuracy of traditional pixel-based methods (Hay & Castilla, 2006). In addition to spectral-based information, information on object size, shape and context can be calculated (Chubey et al., 2006; Greenberg et al., 2005), which are also useful to increase classification accuracy (Hay & Castilla, 2006). These object features can then be related to forest parameters. Although relationships between explanatory variables and deduced forest inventory parameters allow for biophysical interpretation, these relationships are empirical and may not be applicable for other data sets (Chubey et al., 2006). The final result of the object based image analysis, can be exported as polygons and used in *Geographic Information Systems* (GIS) (Schiewe et al., 2001; Hay & Castilla, 2006).

4 FOREST ATTRIBUTE ESTIMATION WITH VERY HIGH RESOLUTION (VHR) DATA

VHR satellite sensors are promising data sources for forest inventory and assessment. The submetre spatial resolution of these new sensors (e.g. GeoEye-1; 0.41 m panchromatic resolution[2]) allows the detection of individual tree characteristics such as tree crown diameter and shadow length (Ozdemir, 2008), leading to improved estimates of many forest inventory attributes including crown closure, tree density and stand volume (Wulder, 1998). Current studies have focused on analysis of temperate forests, boreal forests and plantations, so a strong bias exists towards systems with low species diversity and relatively regular geometric crown shapes (Palace et al., 2008). This is not surprising as these open forests have special features that provide excellent opportunities for remote sensing-based forest inventory (Ozdemir, 2008). Moreover, thirty percent of the world's forest resources are open forests and there remains a clear lack of reliable inventory data to allow sustainable management of this valuable resource from (semi-)arid areas. Therefore, there is a clear need for better inventory data, generated at relatively low cost (Ozdemir, 2008). As the development of VHR sensors and associated data processing continues, this will likely improve the ability to conduct spatially detailed forest inventories across large spatial extents (Falkowski et al., 2009).

Numerous satellite platforms (e.g. QuickBird, GeoEye-1) acquire imagery with spatial resolutions less than 1 m (Falkowski et al., 2009). These systems are able to provide consistent, timely data with a high degree of geometric fidelity, making them an attractive data source for forestry applications. However, the use of VHR imagery is subject to a number of challenges. When large areas need to be characterized, many scenes are required, which leads to high data acquisition costs (Falkowski et al., 2009; Wulder et al., 2008). If cost is not a major limitation, the off-nadir view angles and differing solar and atmospheric conditions associated with multiple scenes would require image processing to reduce effects.

Other challenges are associated with image processing of VHR imagery. Relatively new processing techniques are specifically developed for analysing VHR data (Chubey et al., 2006). In some cases, these techniques may not be as robust as more established

[2] Resampled to 0.5 m for commercial customers (Eurimage, 2009; GIM, 2009)

methods or may not be widely available in popular image processing software (Falkowski et al., 2009). Moreover, the detection and count of decidous trees is generally not as successful as with coniferous trees, because they usually have a less conical shape (Gougeon and Leckie, 2006). Image processing techniques for the automatic extraction of forest inventory attributes from VHR images are nonetheless increasingly mature. The extraction of forest inventory information from VHR images often requires specific processing as well. Furthermore, the application of such techniques may be regionally specific or only applicable in certain forest structural types (Falkowski et al., 2009). Different approaches have been used for the estimation of forest inventory attributes: stand segmentation, crown segmentation, texture analysis, shadow analysis, spectral analysis and spectral mixture analysis (Falkowski et al., 2009). Image segmentation, texture analysis and shadow analysis are promising approaches for attribute estimation (Falkowski et al., 2009).

a IMAGE SEGMENTATION

Image segmentation refers to the use of automated algorithms to partition remotely sensed images into homogenous, mutually distinct spatial units. In terms of forest inventory applications, image segmentation can be characterized as either forest stand segmentation or individual tree segmentation. The goal of forest stand segmentation is to partition an image into spatial units that are homogenous in terms of forest composition and structure. Forest stand segmentation is outside the scope of this work. Crown segmentation (or isolation) is focused upon delineating individual tree crowns from VHR remotely sensed data. Multiple techniques have been developed to automatically isolate individual trees, e.g. local maximum filtering, multiscale (object-based) methods, valley following algorithms, and feature matching techniques (Bunting & Lucas, 2006; Falkowski et al., 2009; Palace et al., 2008).

After the delineation, individual tree crown parameters can be used to directly estimate forest inventory attributes, including stand density and canopy closure (Leckie et al., 2005; Wulder, 1998). Through allometry, other attributes such as timber volume, biomass or diameter distributions can be modeled (Palace et al., 2008; Popescu, 2007). The accuracy of many automatic crown segmentation techniques depends on the structural complexity and density of the forest stands. Greater accuracies are attained in

open single-storey stands compared to closed multistory stands (Maltamo et al., 2004). Furthermore, the efficacy is generally lower in areas exhibiting large variation in crown shapes and sizes, or where the canopy is relatively planophile (Falkowski et al., 2009; Hirata, 2008). The results can be affected by commission error (false extraction) and omission error (missing) (Hirata, 2008). Moreover, segmentation is very useful to distinguish distinct objects, but has difficulties with subtle boundaries, that can be typically found by forestry interpreters (Katoh et al., 2009). As segmentation is based on the features of objects with a particular size, form and colour, setting of the segmentation parameter will depend on the software used.

b TEXTURE ANALYSIS

Texture analysis refers to using local image patterns to characterize the spatial structure of remotely sensed imagery. Texture quantifies the spatial variation in image digital numbers and may be determined using different methods (Falkowski et al., 2009). One simple measure of texture summarizes the image digital numbers within a fixed window (called a kernel). Image texture has been identified as one of the most important visual parameters for manual photo interpretation (Lillesand & Kiefer, 2004). The digital calculation of texture is in fact analogous to how human interpreters exploit image texture when interpreting aerial photography (Falkowski et al., 2009). Simple first-order texture measures (e.g. standard deviation) can be generated directly from the digital numbers. More complex measures were presented by Haralick in 1973 by placing digital numbers in a virtual matrix, such as the *Grey Level Co-occurrence Matrix* (GLCM) (Haralick et al., 1973). These texture measures can then be used to empirically estimate forest inventory information from remotely sensed imagery (e.g. age classes) (Falkowski et al., 2009). Kayitakire et al. (2006) used several texture features to characterize numerous forest structural parameters including age, height, basal area and stand density from IKONOS imagery. Limitations of texture analysis for forest inventory purposes can occur when multiple images are used, as the relationship between texture features and forest structure often changes between images (Falkowski et al., 2009). In situ data is thereby needed for calibration. Texture analysis is also scale dependent and therefore dependent on image resolution (Wulder et al., 2004).

c *SHADOW ANALYSIS*

Shadows of tree canopies can often be related to forest inventory parameters as well as biophysical characteristics (Falkowski et al., 2009). Spectral mixture analysis and geometric-optical models, which model the fraction of shadow in a forest scene, have been applied to medium resolution remotely sensed data to deduce structural parameters (Falkowski et al., 2009). Spectral mixture analysis models pixel reflectance as linear or non-linear combinations of pure subpixel components (e.g. trees, soil, shadow) and has been used to estimate forest canopy cover, biomass and leaf area index (LAI) from medium resolution remotely sensed data (Chen et al. 2004; Hall et al., 1995). New techniques have now been used to relate shadow fraction to forest structure from VHR remotely sensed data. Leboeuf et al. (2007) use image thresholding and segmentation to create a shadow fraction map, which is then used to empirically estimate biomass. Greenberg et al. (2005) used IKONOS imagery and shadow allometry to estimate crown area, tree bole diameter, stem density and biomass. Stem volume in an open canopy juniper forest (Turkey) was estimated through shadow fraction analysis of QuickBird imagery by Ozdemir (2008). Due to variations and interactions between topography, tree spacing and tree size, the correlation between image shadows and tree attributes such as tree height and stem density can be low (Kane et al., 2008). Sun-sensor-surface geometry will also have an impact on shadow analysis. This is of particular importance when considering the use of shadow analysis to measure forest inventory attributes via VHR sensors capable of providing multiple look angles. These characteristics should be taken into account to ensure consistency (Falkowski et al., 2009).

5 BIOMETRIC RELATIONSHIPS

When a strong relationship exists between forest attributes and the features extracted from remote sensing, these forest attributes can be estimated using regression or other modeling techniques (Ozdemir, 2008). Some forest attributes can be directly measured based on the segmentation results. Stand density e.g. can easily be estimated as the number of tree crowns derived from the imagery (Hirata, 2008). Through the use of these relations, forest structure can be estimated for large areas in an efficient way (Wulder, 1998).

Allometric equations for relating measurable variables are commonly used for forest inventories and ecological studies (Hirata, 2008). Equations often used for biological variables are polynomials (Ozdemir, 2008). However power functions are also used and the equation can be expressed as follows (Ketterings, et al. 2001):

$$y = a.x^b$$

where x is an independent variable, y a dependent variable, and a and b are constants. The equation can be represented on logarithmic coordinates as follows:

$$\log y = \log a + b \log x$$

with the constant b forming the slope of the regression and log a the intercept (Hirata, 2008).

As biometric relationships are species and site specific, field data has to be collected. Based on these field data, biometric relationships can be modeled, for example between tree height and crown size (Popescu, 2007). DBH is the most frequently tree measurement made by foresters, however it is not directly visible on remotely sensed imagery. Despite the fact that it cannot be directly imaged, estimates can been made using allometric equations (Palace et al., 2008; Popescu, 2007). Studies have reported that DBH is correlated with crown radius (which can be estimated directly) and also with stem height (Hirata, 2008; Palace et al., 2008; Popescu, 2007). When the allometric relationship between e.g. crown area and DBH is modeled, the other attributes can also be estimated. Tree height measurement is always time and labour consuming. Hence, the height-diameter curve is often used to estimate tree height, instead of taking measurements (Hirata, 2008).

An example of a height-diameter curve is the *Näslund formula* (Hirata, 2008):

$$h = h_{bh} + \frac{d^2}{(a + bd)^2}$$

with h = tree height, h_{bh} = breast height, d = DBH and a,b = constants

For the estimation of aboveground biomass and carbon stocks in forests, allometric equations are used with DBH and tree height (h) as independent variables (Palace et al., 2008). The remote sensing observations of crown width can be used to estimate biomass, via DBH (Palace et al., 2008). Volume (v) can then e.g. be modeled as follows:

$$v = ph + qd^2 + rd^2h + s$$

Where v is the volume and p, q, r and s are constants to be determined for each species (and respective DBH classes) (Hirata, 2008).

Errors are always present in allometric equations: potential sources of errors include statistical errors (estimation of coefficients and form of equations), measurement and data processing errors (Popescu, 2007). It is emphasized that the modeled relationships are empirical, chosen because they 'fit' (Ketterings, et al. 2001).

Chapter 2: MATERIALS AND METHODS

In this section, general characteristics of the study area (Bou-Hedma National Park, Tunisia) are summarized, based on data in literature[3]. Next, a detailed description of the field data collection is presented. Finally, properties of the acquired GeoEye-1 image are given, followed by the methodology used for image processing.

1 BOU-HEDMA NATIONAL PARK

a LOCATION

The Djebel[4] Bou-Hedma Biosphere Reserve and National Park is situated in central Tunisia (Figure 1). It is located along the southern Tunisian mountain ranges that are extensions of the Saharan Atlas (Abdelkebir, 2005). The geographical coordinates are from 34°24' N to 34°32' N and from 09°23' E to 09°41' E. The altitude varies between 90 m and 814 m above sea level (Abdelkebir, 2005).

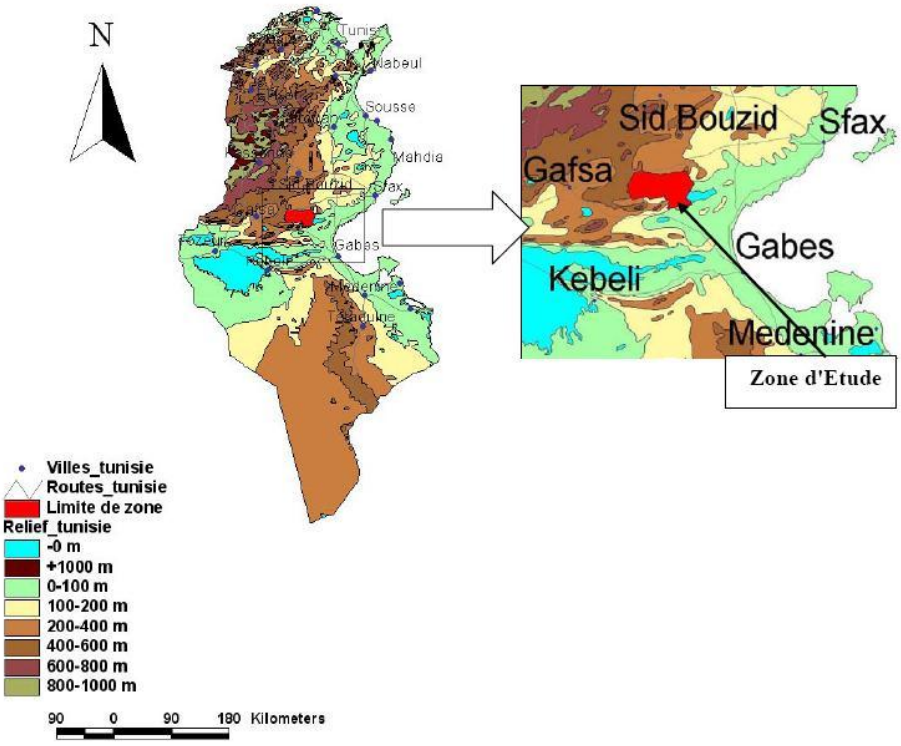

FIGURE 1: LOCATION OF BOU-HEDMA NATIONAL PARK (Abdelkebir, 2005)

[3] The section **1 Bou-Hedma National Park** was written in cooperation with Ken De Sadeleer, a fellow student who researched the influence of *Acacia raddiana* on soil and air properties (such as humidity and temperature).

[4] Arabic word used for 'mountain', 'hill' or 'slope'.

b HISTORICAL BACKGROUND

Because of its unique geographical location, the importance of its ecology was already researched since the 18th century. In the past, the whole area between Gabès and Gafsa was covered by *Acacia raddiana* forest steppe[5]. This steppe covered 38,000 hectares in the year 1853, when there was still water in the *Oued*[6] *Cherchara* and the *Sebkha*[7] *En Noual.* (Karem, 2001; Tarhouni, 2003). From this date *Bled Talah* was recognised as a unique relict of a forest steppe of *A. raddiana.* This is emphasized by the name of the region – *Bled Talah* – where *Bled* is Arabic for 'region' or 'plain' and *Talah* is the common name used for *A. raddiana*. Due to overcutting, grazing and change in climatic conditions, the area of this forest was drastically reduced. The status of a national park was proposed by Lavauden and Ahmed Bacha Bey in 1936, but there was no immediate action. Several events (the most important one is the settlement of Tunisian families, who were formerly nomadic) continued to cause damage to the environment. As a result, in 1955, only a few old trees at the *Bordj*[8] were left. A first protective measure was taken in 1957-1958 by the fencing of 700 hectares, delimited by plantations of *Eucalyptus* sp., *Prosopis juliflora* and *Parkinsonia* sp. In the sixties, actions were taken to combat erosion, after the FAO *(Food and Agricultural Organization of the United Nations)* reported that the *Djebel Bou-Hedma* was being degraded (Caron, 2001). These protective actions and measures resulted in a gradual restoration of the vegetation since the year 1970 (Tarhouni, 2003). One of the actions taken was the construction of a tree nursery and the creation of *Integral Protection Zones* (IPZ). The *Direction des Forêts du Ministère de l'Agriculture* started with the total protection of 2,400 ha in 1977. In the same year, the park became part of the network of Biosphere Reserves of the UNESCO. The Bou-Hedma National Park was officially created by decree no. 80-1606 in December 1980. In 1985, regeneration actions were undertaken and they paid off as the number of *A. raddiana* trees was multiplied with a factor of about 30 (Caron, 2001). The difference between the protection zones and the exterior of the park became (and still is) very distinct. Inside the protection zone, there is a very light browsing (about one animal per

[5] In literature, the population is also sometimes considered as a pseudo-savanna, with scattered trees or shrub individuals of *Acacia raddiana* associated with several species of grasses, shrubs and ligneous chamaephytes (Noumi et al., 2010).
[6] Derived from the Arabic word *wadi* which means 'river'. It is a name used for irregular river systems (temporary rivers when rainfall is high) in (semi-)arid regions.
[7] Salt depression
[8] Bordj or caravanserail: a stopping place for caravans

40 ha), while the neighbouring land is subjected to an intensive browsing by domestic herds (about two animals per ha) (Noumi et al., 2010). The national park provides for involvement of the local population, which is given assistance with agriculture outside the protection zones. The synergy between the protection of the natural resources and the augmentation of life conditions can be an example to use in similar regions (Caron, 2001).

c *PRESENT INFRASTRUCTURE*

The national park of Bou-Hedma covers 16,488 ha and is divided in different zones. There are three *Integral Protection Zones* (IPZ) or *Core areas*, two *Buffer Zones* (BZ) and two *Agricultural Zones* (AZ) or *Transition areas* (Table 1).

TABLE 1: ZONE DISTRIBUTION IN BOU-HEDMA (modified from Banque Mondiale (2001) cited in Caron (2001))

	Area (ha)		
Zone	Total	Plain and mountain foot	Mountain
IPZ 1	5,114	2,000	3,114
IPZ 2	2,700	1,500	1,200
IPZ 3	1,000	1,000	0
Total IPZ	8,814	4,500	4,314
BZ 1	1,774	1,019	755
BZ 2	2,000	2,000	0
Total BZ	3,774	3,019	755
AZ 1	2,400	2,400	0
AZ 2	1,500	1,500	0
Total AZ	3,900	3,900	0
Total	16,488	11,419	5,069

All field data collection was carried out in the IPZ 1, with a total area of 5,114 ha (divided in 2,000 ha of plains and 3,114 ha of mountain zones). On the mountain chain, there is only one individual tree of *A. raddiana*. The altitude of the mountain foot is 100-200 m and is considered a transition zone towards the mountain (Caron, 2001). The IPZ 1 is surrounded by a fence to prevent the wild fauna (antelopes, ostriches) from escaping and to prevent grazing by domestic animals. The Bou-Hedma mountain is considered as a natural barrier, so no fencing is established. Day and night, foresters are present at various locations in the park to patrol the fences and guard the main entrances. An important evolution is the social control exerted by civilians, who often call the chief forester when they notice a delict (Hamdi[9], De Smet, personal communication). The

[9] Lazhar Hamdi, chief forester of Bou-Hedma National Park, Tunisia

agricultural zones and buffer zones do not have a fence. Crop husbandry is scattered over the agricultural zone and not always successful (no reliable yields). Only part of the crops is irrigated, often through the use of water with a high salt content. The use of *tabias*[10] is also a common sight in the region. In the buffer zones all agricultural activities are prohibited, as is the harvesting of all natural resources (Caron, 2001).

The IPZ 1 is the core of the national park, where almost all visitors (about 4000 yearly) are welcomed in the ecomuseum. In the ecomuseum the different steps of the regeneration of the park are explained, together with other relevant information (e.g. on biodiversity). At the *Bordj* Bou-Hedma, materials are stocked, administrative tasks are conducted and rooms for researchers are provided. There is also a collection of *Opuntia inermis* (46 varieties) and an exposition enclosure with local fauna. The present chief forester[11], who lives next to the ecomuseum, emphasizes the importance of research, which can be beneficial for local families in many ways (Caron, 2001; Hamdi, personal communication). One important achievement of the national park is the creation of an institution for secondary education near the park. Bungalows for researchers will be constructed in the very near future (Hamdi, personal communication).

Research in breeding and use of plantation species, is carried out at the plant nursery. The nursery is located close to *Aïn*[12] *Noa* which provides irrigation water. Part of the water of *Aïn Cherchara* is redirected to a *seguia*[13] (relic of roman times) which flows through the park from North to South, and exits the park as a watering point for local livestock. The *seguia* is also used by the fauna in the park, as was easy to observe. The nursery features seedlings of *A. raddiana* and other local species such as *Periploca* sp. and *Rhus* sp. Part of the plants are raised for use in the park, others are donated to the local population (e.g. in schools) (Hamdi, personal communication). Seeds are harvested in the park and used in situ or at research institutes like the '*Institut des Régions Arides*' (IRA) (Hamdi, personal communication).

[10] Structure used to limit sheet erosion and to increase water retention
[11] This was ir. Lazhar Hamdi at time of writing.
[12] Arabic for 'source'
[13] Arabic for 'irrigation canal'

d CLIMATE

Arid Tunisia, or the central and southern part of Tunisia, is characterized by an extremely irregular spatiotemporal rainfall pattern, a limited amount of rain (350 mm maximum per year), a limited number of days of rain (15 to 40 days per year) and a high average annual temperature (18 to 21 °C) (Abdelkebir, 2005). The main climatic characteristics of this area during the period 1934 to 1985 (recorded by a meteorological station at Bou-Hedma) are: an average annual rainfall of 180 mm, an average temperature of 17.2 °C, a mean maximum temperature of 38.0 °C and a mean minimum temperature of 3.9 °C. Following Emberger's classification, the climate in Bou-Hedma National Park is Mediterranean arid with temperate winters (Noumi et al., 2010) (Figure 2).

More recent data of the precipitation (measured from 1994 until 2005, weather station in Haddej, Bou-Hedma National Park) show that rainfall fluctuates considerably from year to year (Table 2). This inter-annual variability in precipitation is characteristic for Mediterranean climates (Noumi et al., 2010). During the period 1994-2005, the average annual rainfall, calculated using a hydrological year (from September until August of the next year), is 146.5 mm (Boukchina et al., 2006). The average annual rainfall however varies with height from 150 mm in the plain (100 m above sea level) to 300 mm on the highest peak of the mountain range (800 m above sea level) (Noumi et al., 2010).

TABLE 2: ANNUAL FLUCTUATIONS OF THE PRECIPITATION (Boukchina et al., 2006)

Year	Precipitation (mm)
1994/1995	84
1995/1996	316
1996/1997	208
1997/1998[14]	-
1998/1999	170
1999/2000	110
2000/2001	47
2001/2002	120
2002/2003	158
2003/2004	200
2004/2005	52

[14] For the year 1997/1998, data is missing for 7 months. The rainfall measured by the rain gauge was very low.

Regarding air temperature for the same period (1994-2005; weather station in Haddej, Bou-Hedma National Park), the coldest month is January, with an average temperature of 11.5 °C. The warmest month is August, with an average temperature of 29.7 °C (Table 3).

TABLE 3: MONTHLY TEMPERATURE MEASUREMENTS OVER THE PERIOD 1994-2005 (Boukchina et al., 2006)

	T_{MIN} (°C)	T_{MAX} (°C)	T_{AVG} (°C)
January	7.5	16.3	11.5
February	9.9	17.4	13.4
March	12.1	20.9	15.7
April	12.8	23.8	18.1
Mai	17.6	28.9	22.3
June	22.7	33.1	26.8
July	25.7	34.1	29.3
August	26.4	35.0	29.7
September	21.8	32.0	26.9
October	19.2	26.1	22.5
November	12.2	22.8	16.9
December	9.2	17.5	13.1

T_{min} = absolute minimum monthly temperature (averaged over all years)
T_{max} = absolute maximum monthly temperature (averaged over all years)
T_{avg} = mean monthly temperature (averaged over all years)

The length of the dry season is an important parameter. However important differences exist whether the yearly pluviometric regime is continuous or not (monomodal versus multimodal regime) (Caron, 2001). A bimodal rainfall regime is characterized by both autumn and spring peaks of rainfall (Le Houérou, 2001). A simple method to discriminate between dry and wet season, was proposed by Bagnouls and Gaussen (1953): a season is dry when the precipitation P (mm) is lower than the temperature T (°C) multiplied with two ($P < 2T$). When P is larger than 2T, the season is considered wet. Caron (2001) applied this to Bou-Hedma National Park, with means of 1994 through 1999, resulting in 12 months of dry season, with September to December as wettest months.

e GEOMORPHOLOGY AND GEOLOGY

The northern border of the study area is formed by mountains. The mountain slopes are characterized by limestone bedrock which is exposed to severe water erosion (Karem et al., 1993). The eroded materials are transported with the water flow after rainfall and deposited at the base of the mountain. The mountains North of the study area act as a water basin that supplies water runoff downstream the foothills. The high mountain plateaus are characterized by silty soils, which are deep enough for vegetation rooting

(Karem et al., 1993). The foothills are characterized by outcropping parent material, a limestone crust topsoil and accumulation of colluvial material. Water availability increases from the *glacis* (transition zone between plain and mountain) to the sandy plain because of increasing water holding capacity in the soils, as well as increasing proximity of the water table (Noumi et al., 2010).

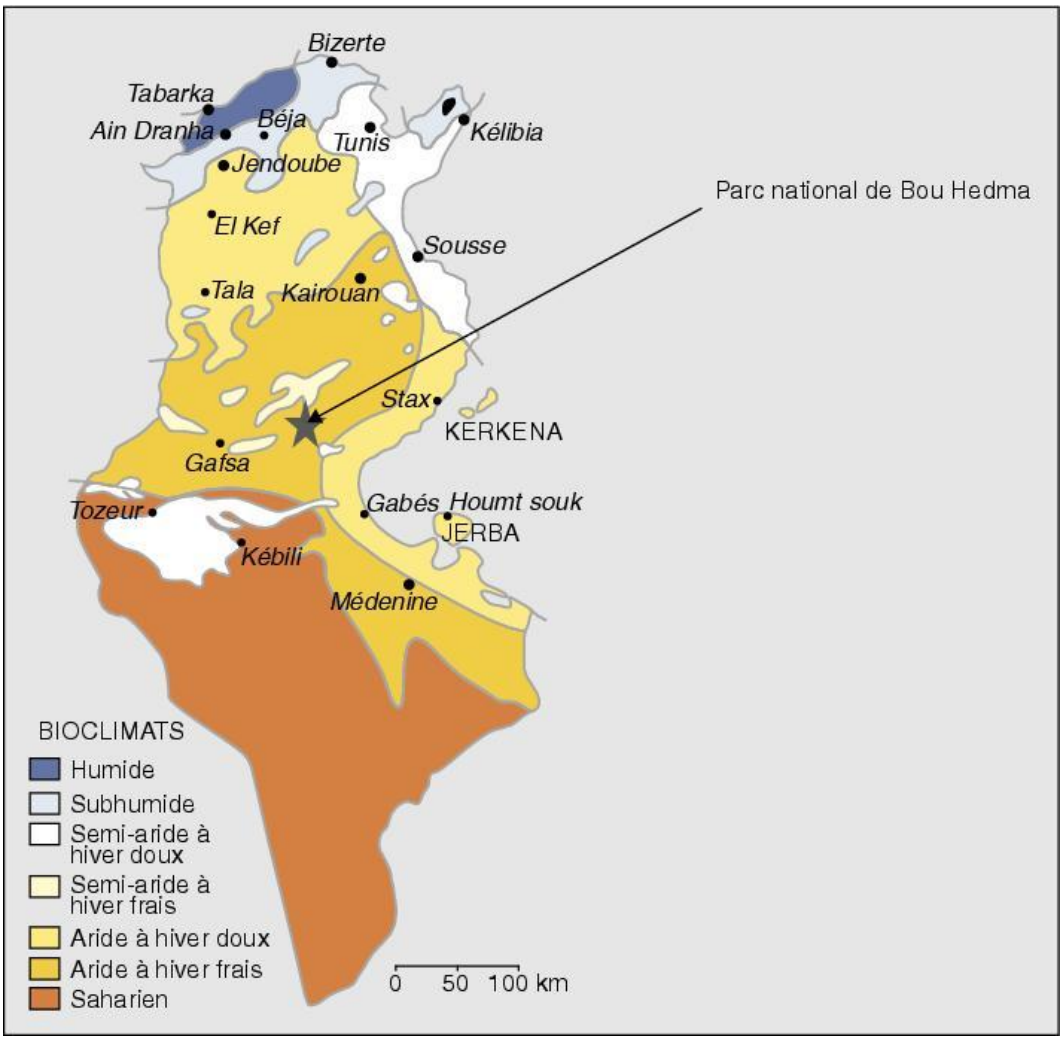

FIGURE 2: GEOGRAPHICAL LOCATION OF BOU-HEDMA NATIONAL PARK ON THE BIOCLIMATIC MAP OF TUNISIA (Tarhouni et al., 2007)

The oueds are very heterogeneous (sandy beds, rocks, pebbles) (Schoenenberger, 1987). The plain South of the mountains consists of a deep coarse sandy soil with undeveloped deposits. These deposits date from the Quaternary and originate from the mountains.

The heterogeneity in soil characteristics creates an edaphic environment (plant communities are distinguished by soil conditions rather than by climate conditions). Psammophile species, such as *Rhanterium suaveolens* and *Cleome amblyocarpa*, depend

on the fixation of sand by wind phenomena on the calcareous gypsum crust (Schoenenberger, 1987).

The *A. raddiana* steppe is considered as a remainder of tropical origin (Sghari, 2009). Much of the Mediterranean basin became more arid in the period 1,000 – 500 BC (Ouarda et al. 2009). However, it is generally agreed, that a more lush vegetation (capable of maintaining elephant populations), was present up to the second and third century of our era (Lavauden, 1928). Since the 3rd century, the development of aridity led to the gradual disappearance of tropical steppes at the northern border of the Sahara. This is also the case in Tunisia, which has lost all its *A. raddiana* steppe, except for a reduced population that survived in Bou-Hedma. According to Sghari (2009), the survival of the steppe is a consequence of a geomorphologic shelter, created by the surrounding mountain ranges. In the North, there is the Djebel Bou-Hedma, which forms a barrier for the cold, moist wind from the northwest. This barrier also creates a totally different bioclimate at both sides of the Djebel Bou-Hedma. In the South, there is also a mountain range which protects the *A. raddiana* steppe from the warm, dry Saharan winds. Other theories claim that the highly polyploidy state (tetraploid) gives the population advantages in unstable environments, which is also observed with other species (e.g. *Atriplex halimus*) (Ouarda, et al. 2009).

2 FIELD DATA COLLECTION

a GOAL OF THE FIELD WORK

With the aid of the *GeoEye-1* and *Google Earth* imagery, two kinds of *Acacia* spatial configuration were noticed in *Bou-Hedma National Park*. First, there are the plantations, where trees are in linear formations scattered over the entire National Park. Second, trees in depressions and dried (temporal) riverbeds (*wadi* or *oued*). The latter have a more natural aspect and co-occur with larger shrubs (*Periploca* sp. and *Retama* sp.). *Eucalyptus* sp. are also present, along the road (North-South orientation) and in some dense plantations close to the *Bordj*. In order to cover both spatial arrangements and different diameter classes of trees, a random sampling scheme was selected. Using a Garmin GPSMap 60Cx, tree coordinates were determined and stored in UTM units (using *World Geodetic System 84* (WGS 84)).

The measurements were limited to *Acacia raddiana* trees, as the goal is to obtain an estimate of the amount of *Acacia's* and their diameter class distribution. A printed version of a false colour composite satellite image was used as guidance in the field to determine the location of the trees. The measured trees will serve as ground truth for the classification of the image, in order to separate the *Acacia*'s from soil background and other vegetation. Moreover, ground truth is required to calibrate empirical models to estimate tree attributes of *Acacia raddiana* trees.

b MEASUREMENT OF TREE ATTRIBUTES

i Bole (trunk) diameter

The measurement of bole diameter can be performed in various ways. The use of tree calipers was ruled out because of the non uniform boles. The diameter of *Acacia raddiana* differs in different directions (Hamdi, personal communication). The dense crowns of the trees also limit the accessibility with a caliper. For these reasons, bole diameter was calculated from the girth using a calibrated measuring tape (circumference = π.diameter). To allow comparison between different trees, it is important to define a height to perform the measurements that can be reliably (re)located (Brack, 1999). Bole diameter was measured at two heights. One diameter was measured at the base of the tree at 10 to 15 cm above ground level (basal diameter, BD) as this diameter is often used for trees higher than 1.3 m without an individual trunk (Zaafouri et al., 1996). The second diameter is the diameter at 1.30 m above ground level, which is commonly known as the diameter at breast height (DBH) (Brack, 1999). The definition of ground level used (Brack, 1999), excludes litter not incorporated in the soil. For trees on sloping ground, the uphill was used as reference for ground level.

When a tree forked at the aforementioned heights, special rules were applied (Brack, 1999). When the fork was just above the reference height, the tree was considered as a single stem with multiple leaders. When the forking occurred below the reference height, the individual was treated as multi-stemmed. When swelling or other irregularities were present, subjectively a representative measuring height was used, just below the irregularity.

ii Total height

To determine the total tree height, trigonometric principles were used. Using the properties of uniform triangles, tree height can be determined in a straightforward way (Figure 3). First the highest point of the tree (A) was visually determined and the beginning of a 50 m tape measure was fixed vertically below this point (C). Second a point from where the highest point and the base were easily visible was taken (O) and the distance (|OB|) was noted. Using a clinometer (Suunto PM-5/360 S), the angle between top and base (angle 1 + angle 2) was then measured. Using the distance to the vertical projection of the tree top and angles measured, tree height (h) can be calculated:

$$h = |AB| + |BC|$$
$$= |OB|.(tan(angle\ 1) + tan(angle\ 2))$$

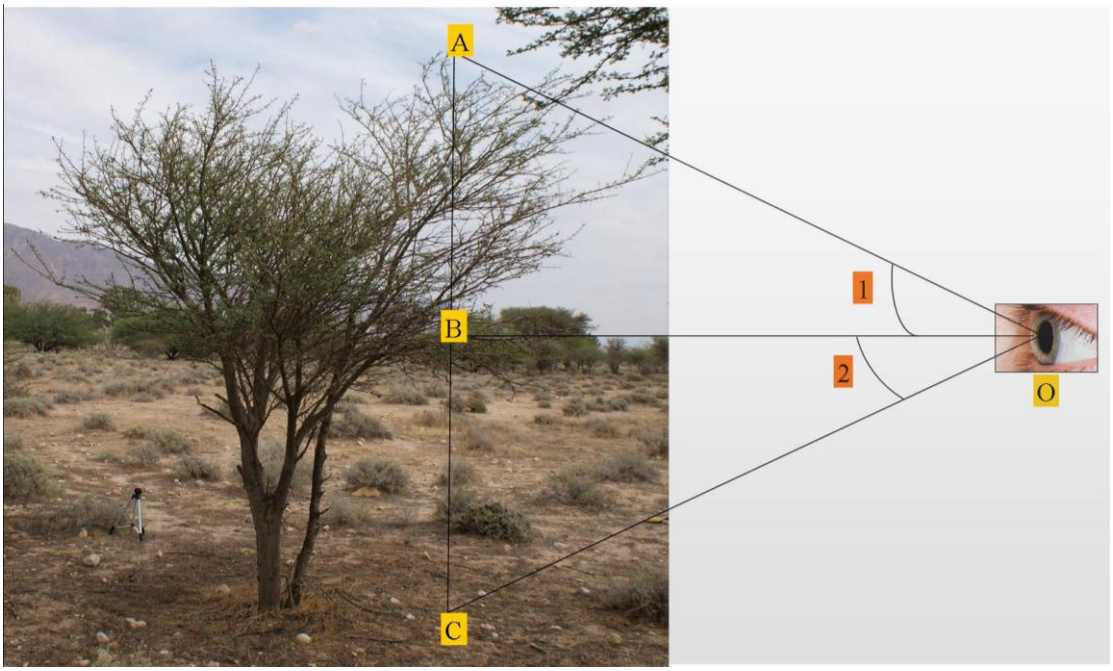

FIGURE 3: ESTIMATING TREE HEIGHT WITH A CLINOMETER

For accuracy assessment, the height of two straight objects (height to balcony of guesthouse and the stake of a swing at IRA) were measured with a measuring tape and subsequently estimated with the aforementioned clinometer. The height estimation was repeated 30 times for each object. For the stake of the swing (with a total height of 176.5 cm), an absolute error of 1.4 cm (underestimation) was noted (relative error = 0.79%). The height of the guesthouse (up to the balcony), with a total height of 460.0 cm, was also underestimated with an absolute error of 6.2 cm (relative error = 1.34%). On

average, a 2%-5% error with little bias can be expected. However this will also depend on field conditions (Needham & Peasly 2003).

iii Crown diameter

In order to include directional variation, the crown diameter was measured in two fixed (perpendicular) directions. The mean can be used as a global indication of the crown diameter. Using a compass the North-South and East-West direction was determined and the diameter was measured with a measuring tape (50 m). In the case of a group of trees, only the total crown diameter was measured, as individual crowns were not distinguishable.

c ADDITIONAL TREE INFORMATION

i Pictures

For each tree or tree group, habit images were taken using a *Sony α 200 digital mirror reflex camera*. In general, habit images were taken in two directions: the Southern side and the Eastern side of the trees. In order to obtain an estimate of the tree crown density, vertical images were taken in each of the four cardinal directions. This was standardized using a tripod, with a height of 45 cm. The distance to the tree base was between 10 and 20 cm.

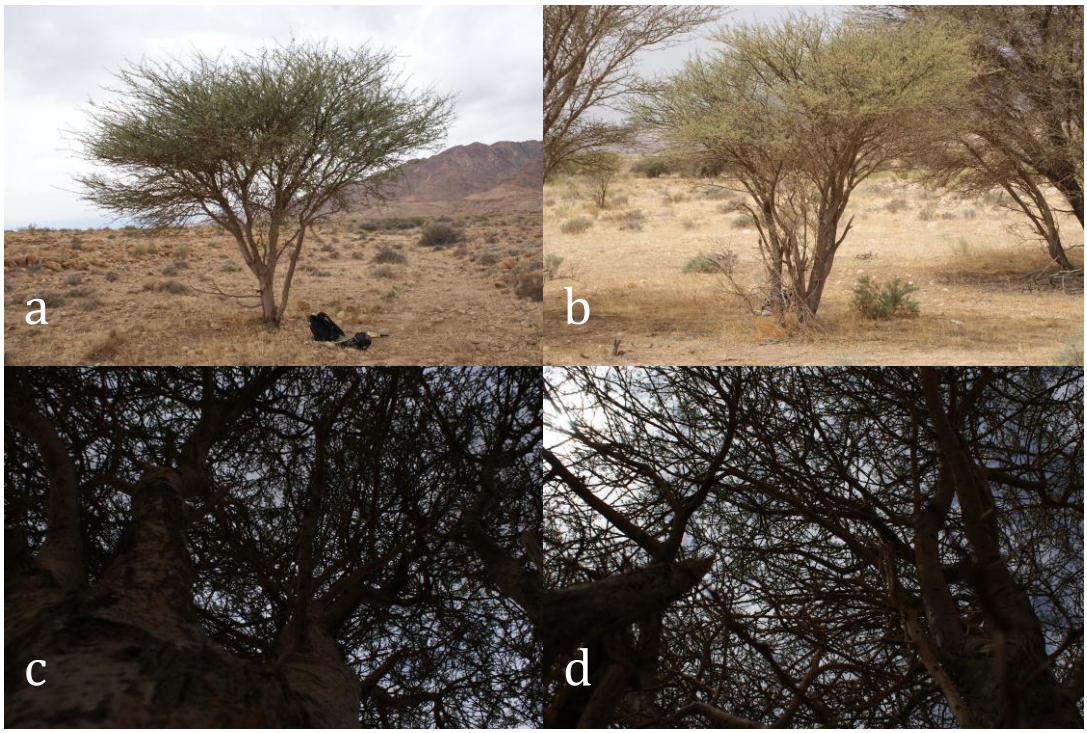

FIGURE 4: TWO EXAMPLES OF TREE HABIT (a AND b, BOTH EASTERN SIDE) AND IMAGES FOR TREE CROWN DENSITY ESTIMATION (c AND d, BOTH EAST)

ii Phenology

For each tree, the stage of leaf, flower and fruit development was noted based on the different stages proposed by Grouzis & Sicot (1980) (cited in Diouf & Zaafouri (2003)). The determination of the different stages was visually assessed (Table 4, Table 5 and Table 6).

TABLE 4: STAGE OF LEAF DEVELOPMENT (Grouzis & Sicot (1980) cited in Diouf & Zaafouri (2003))

Code	Stage of leaf development
V1	Swelling of buds, no developed leaves
V2	Leaf development (more than 10% and less than 50%)
V3	Majority of leaves developed
V4	Green leaves and dried leaves (or change in coloration) (more than 10% and less than 50%)
V5	More than 50% of the branches have dried leaves

TABLE 5: STAGE OF FLOWER DEVELOPMENT (Grouzis & Sicot (1980) cited in Diouf & Zaafouri (2003))

Code	Stage of flower development
f1	Only flower buds
f2	Flower buds and developed flowers (more than 10% and less than 50%)
f3	More than 50% of the branches carry flowers
f4	Flowers and dried flowers (more than 10% and less than 50%)
f5	Majority of flowers is dried

TABLE 6: STAGE OF FRUIT DEVELOPMENT (Grouzis & Sicot (1980) cited in Diouf & Zaafouri (2003))

Code	Stage of fruit development
F1	Fruit setting
F2	Evolution of fruit up to full-grown size
F3	Ripe fruits
F4	Ripe fruits and start of seed dispersal
F5	Fruits entirely dried

d VEGETATION

There is a positive influence of tree canopy on the herbaceous species composition and dry matter yields (Abdallah et al., 2008; Ludwig et al., 2004). For this reason, the vegetation under the tree canopy (vertical projection) and outside the tree canopy was recorded at each location. The zone outside the canopy is considered as a buffer zone and is the zone which is still being influenced by the tree shadow during the day. This buffer zone was 3 m for large trees (h > 1.3 m) and 1.5 m for small trees (h < 1.3 m) (arbitrarily chosen distances). A total of 40 species were identified, which mainly consist of perennial vegetation. This is explained by the time of the survey which was conducted in the second half of the dry season. After the first rains, lots of young sprouts were noticed but not recorded as the determination was often impossible. As fauna influence

the vegetation in one or another way, the presence of animal faeces and bird nests was also noted.

e SOIL ATTRIBUTES

Two different soil attributes were visually assessed for each tree (or tree group), using different distinctive classes. The first attribute is the *stoniness* of the soil (Day, 1983). The second is the presence of an *erosion crust* (under the canopy and in the buffer zone as defined for the recording of the vegetation).

TABLE 7: DIFFERENT CLASSES OF SOIL STONINESS (Day, 1983)

Code	Attribute	Surface occupied by stones (%)
#	Not applicable	-
0	Non stony land	<2
1	Slightly stony land	2-10
2	Moderately stony land	10-25
3	Very stony land	25-50
4	Exceedingly stony land	50-90
5	Excessively stony land	>90

TABLE 8: CLASSES OF EROSION CRUST

Code	Surface occupied by an erosion crust (%)
0	0-10%
1	10-25%
2	25-50%
3	50-75%
4	>90%

f DATABASE

When large amounts of data are to be analyzed, a management system can provide an increase in efficiency. A typical data management system is a relational database. For a database to be solid, the data have to be normalized, which is the splitting of data over multiple tables (Groh et al., 2007). Our data were normalized following the first three rules as mentioned in Groh et al., 2007:

1. Each cell of a table must contain only a single value and the table must not contain repeating groups of data.
2. Data not directly dependent on the table's primary key is moved into another table.
3. All fields that can be derived from data contained in other fields in the table or other tables in the database are removed.

All measurements were entered and compiled in a central database, using *Microsoft Office Access 2007* (addendum 4). Through the use of this relational database, data can easily be retrieved through the use of *queries*.

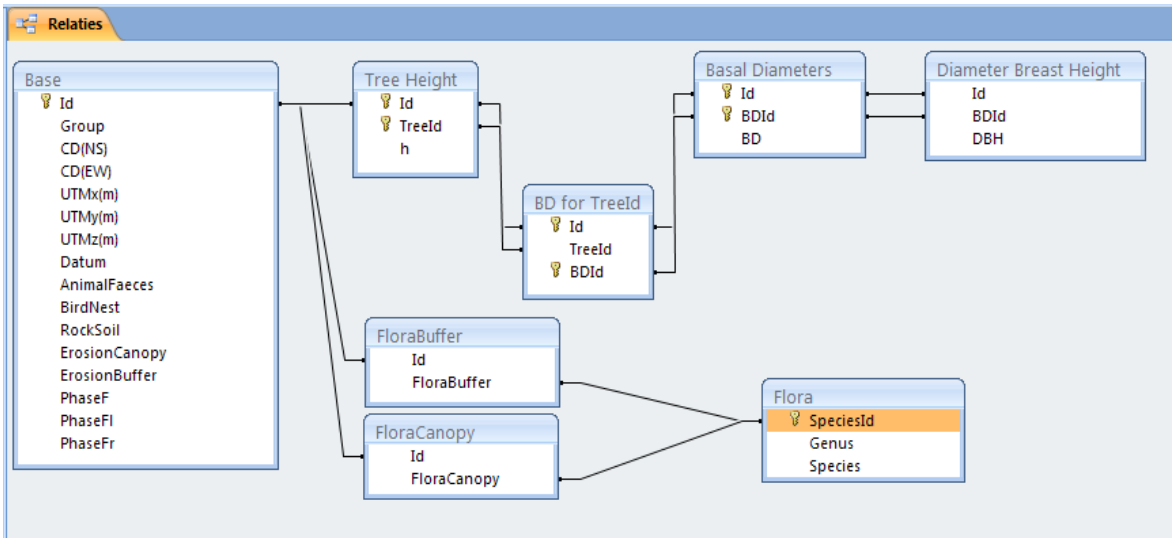

FIGURE 5: VISUALIZATION OF RELATIONS IN THE CREATED DATABASE

3 GeoEye: Image acquisition and characteristics

The GeoEye-1 (formerly known as OrbView-5) satellite was launched on September 6, 2008 and is the next-generation high-resolution imaging mission of GeoEye, Dulles, VA, USA. It follows a sun-synchronous circular orbit, at an altitude of 681 km (GeoEye, 2009; GIM, 2009; Kramer, 2009). The satellite is provided with a pushbroom imaging system. The panchromatic images have a resolution of 0.41 m (at nadir), which is resampled to 0.5 m for commercial customers. Multispectral (4 bands) images are available in 2 m resolution. The radiometric resolution is 11 bits per pixel (Eurimage, 2009; GIM, 2009).

The spectral range of the different bands is:

0.450 – 0.800 µm (panchromatic band)
0.450 – 0.510 µm (band 1 – Blue)
0.510 – 0.580 µm (band 2 – Green)
0.655 – 0.690 µm (band 3 – Red)
0.780 – 0.920 µm (band 4 – Near Infrared)

The GeoEye image used in this study was acquired on the 1st of August 2009 at 10:18 GMT. Cloud cover was 0%. The image was geometrically corrected by GeoEye Inc. The coordinate system is UTM (WGS 84). The image metadata is supplied in addendum 1, where all detailed information can be found.

4 SOFTWARE

For the implementation of the database, *Microsoft Office Access 2007* was used. Statistical analyses were performed with *SPLUS 8.0*. For calculations and graphs, *Microsoft Office Excel 2007* was used. Basic GIS operations, such as the determination of tree locations and subsequent delineation, were done with *Idrisi Andes Edition*. The automated analysis of tree crown density was also implemented in *Idrisi*. For segmentation, classification and calculation of object features, *Definiens eCognition Developer 8* (Definiens, 2009a) was used.

5 METHODOLOGY FOR IMAGE ANALYSIS

*Geographic Object-Based Image Analysis (*GEOBIA*)* is the methodology we adopted. The image analysis can be separated in two steps: sensor-specific analysis and scene-specific analysis (Benz et al., 2004). As the basic units of object-oriented image analysis are image objects (and not single pixels), these objects have to be created in a first step. This can be done by segmentation algorithms, of which multiple variants exist (Schiewe, 2002). These algorithms are generally based on image characteristics and use the information contained in the pixels. Of these resulting objects, object features and attributes can be extracted, which can be used for classification (Benz et al., 2004). The classified objects (trees) can then be used for the scene-specific analysis (e.g. estimation of forest stand attributes). An advantage of GEOBIA is that the created objects (and features) can be exported in *GIS-ready* format (Hay & Castilla, 2006; Schiewe, 2001).

The used algorithms will differ for the software used. As *Definiens eCognition Developer 8* (Definiens, 2009a) was used for the image analysis, the following methodology is therefore based on the algorithms available in eCognition.

a SEGMENTATION

Segmentation or the subdivision of an image into separate regions is the first step of the image analysis. The goal is to find regions of minimum heterogeneity (or maximum

homogeneity) (Benz et al. 2004). Definiens eCognition provides multiple segmentation algorithms, each with different strengths for different applications. Distinction is made between top-down and bottom-up strategies, the former cuts a bigger region into smaller sub-regions, while the latter merges smaller pieces to get a larger area (Definiens, 2009a). For the analysis of the GeoEye image, two different segmentation algorithms were sequentially used. First a *multiresolution segmentation* (bottom-up) was executed, followed by *contrast split segmentation* (top-down). The first algorithm is used to discriminate vegetation from the underlying soil. However smaller trees (mainly in dense plantations) are not always correctly delineated using *multiresolution segmentation,* as they are contained in larger segments with multiple trees and soil/vegetation in between. Hence, a subsequent segmentation was performed on the created segments, which are split if the contrast within the segment is adequately high and if the newly created segments are still large enough (determined by the algorithm's parameters).

i Multiresolution segmentation

The *multiresolution segmentation* algorithm merges pixels in an iterative way to form image objects. Single image objects of one pixel are identified and neighbouring pixels are merged (pair wise), based on relative homogeneity criteria (smallest growth). The homogeneity criterion is a combination of spectral and shape criteria. It is calculated as a combination of the colour and shape properties of the initial and resulting image objects. Colour homogeneity is based on the standard deviation of the spectral colours, while the shape homogeneity is based on the deviation of a compact shape. By using weights for colour, shape and compactness, the algorithm can be customized (Figure 6) (Benz et al. 2004).

Heterogeneity (f) is defined as follows in eCognition (Benz et al., 2004):

$$f = w_{colour} . \Delta h_{colour} + w_{shape} . \Delta h_{shape}$$

with w = weight parameters $\in [0,1]$ and $w_{colour} + w_{shape} = 1$

The difference in spectral heterogeneity Δh_{colour} and shape heterogeneity are defined as follows (Benz et al., 2004):

$$\Delta h_{colour} = \sum_{c} w_c \cdot \left[n_{merge} \cdot \sigma_{c,merge} - \left(n_{obj_1} \cdot \sigma_{c,obj_1} + n_{obj_2} \cdot \sigma_{c,obj_2} \right) \right]$$

$$\Delta h_{shape} = w_{compt} \cdot \Delta h_{compt} + w_{smooth} \cdot \Delta h_{smooth}$$

with Δh_{smooth} and Δh_{compt} defined as:

$$\Delta h_{smooth} = n_{merge} \cdot \frac{l_{merge}}{b_{merge}} - \left(n_{obj_1} \cdot \frac{l_{obj_1}}{b_{obj_1}} + n_{obj_2} \cdot \frac{l_{obj_2}}{b_{obj_2}} \right)$$

$$\Delta h_{compt} = n_{merge} \cdot \frac{l_{merge}}{\sqrt{n_{merge}}} - \left(n_{obj_1} \cdot \frac{l_{obj_1}}{\sqrt{n_{obj_1}}} + n_{obj_2} \cdot \frac{l_{obj_2}}{\sqrt{n_{obj_1}}} \right)$$

The subscript c refers to the considered image channel, with w_c the weight of the channel and σ_c, the standard deviation of channel c within the object. n_{merge} is the number of pixels within the merged object and n_{obj_i} is the number of pixels in object i. For the calculation of the smoothness heterogeneity (Δh_{smooth}) and the compactness heterogeneity (Δh_{compt}), l represents the perimeter of the object and b is the perimeter of the object's bounding box. The weight values are parameters to adapt the segmentation result to the considered application.

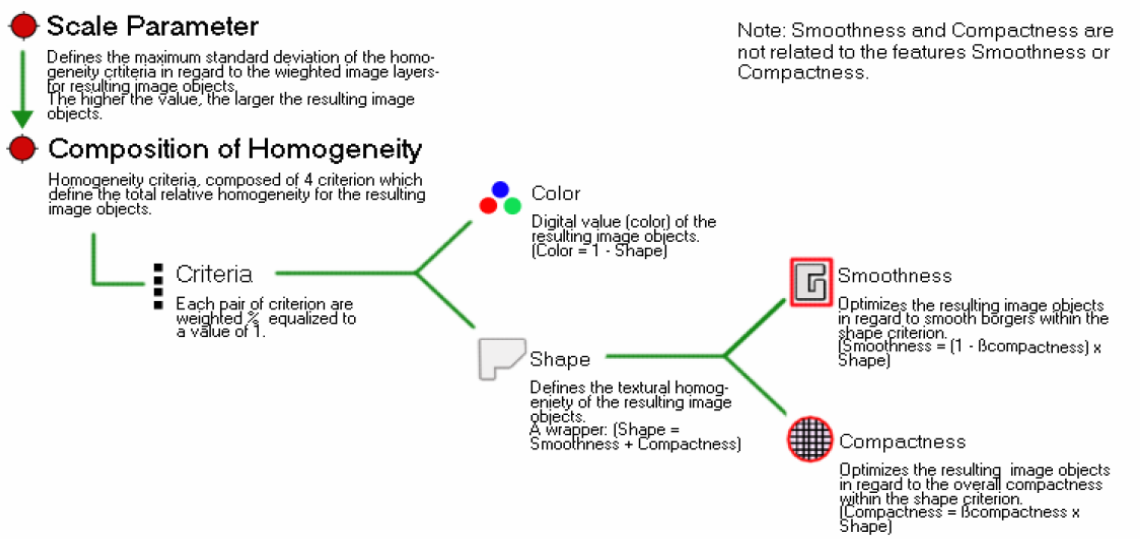

FIGURE 6: MULTIRESOLUTION CONCEPT FLOW DIAGRAM (Definiens, 2009b)

The size of the created objects is determined by the scale parameter of the algorithm (Definiens, 2009a). When the smallest growth exceeds the threshold defined by the scale

parameter, the process stops (Benz et al. 2004). Scale is a crucial aspect of image understanding. Although in remote sensing a certain scale is always presumed based on pixel resolution, the objects of interest often have their own inherent scale. At a certain scale, a particular class might be absent or appear differently (Benz et al. 2004). The larger the scale parameter, the more objects can be fused and the larger the objects grow (Benz et al. 2004).

The algorithm provides good results in various applications. However it puts high demands on the processor and memory, and is slower than some other segmentation techniques. Therefore, it may not always be the best choice (Definiens, 2009a).

ii Contrast split segmentation

Contrast split segmentation is based on the contrast between objects. It segments an image object into dark and bright regions, based on a threshold value that maximizes the contrast between the resulting bright objects (consisting of pixels with pixel values above the threshold) and dark objects (consisting of pixels with pixel values below the threshold). For each image object, the algorithm evaluates the optimal threshold. Optimization is achieved by considering different pixel values as potential thresholds. *Test* thresholds are considered in the range between the minimum and maximum pixel value. When a *test* threshold satisfies the minimum dark area and minimum bright area criteria, the contrast is evaluated and the threshold with the largest contrast is then chosen for splitting (Definiens, 2009a; Definiens, 2009b).

b CLASSIFICATION

In eCognition, a protocol is implemented to determine the optimal set of features to be used for classification. Through *Feature Space Optimization* (FSO), the combination of features can be found which are most suitable to separate the different classes. It is a global optimization algorithm that searches the combination of features that produces the largest average minimum distance between samples of the different classes. These samples have to be provided by the user (Definiens, 2009a). As this tool is designed for uncorrelated features, the results obtained through *Feature Space Optimization* will not necessarily be the optimum feature set (Groesz & Kastdalen, 2007).

The features provided are then used in the classification stage. *Nearest Neighbour (NN) Classification* is the classification procedure used (provided by eCognition). *Nearest Neighbour Classification* requires input from the user, as samples need to be created. It performs a supervised classification which, in contrast with unsupervised classification methods, requires training data (for full descriptions see e.g. Lillesand & Kiefer, 2004). *Nearest Neighbour Classification* uses a set of samples of different classes to assign membership values. The procedure consists of two major steps (Definiens, 2009a):

1. Teaching the system by defining training data (samples)
2. Classifying image objects based on their nearest sample neighbours

The classifier returns a membership value between zero and one, based on the image object's feature space distance to its nearest neighbour. When identical to a sample, the membership value becomes one. For each class selected, a membership value is returned (Definiens, 2009a). However these memberships are not probabilities, but possibilities as they are not normalized (sum not necessarily equal to 1). This type of classification is called fuzzy classification and is a very powerful soft classifier, which contains all information about the overall reliability, stability and class mixture. When a hard classification procedure is used, only the highest membership degree is considered (Benz et al., 2004). Fuzzy systems consist of three steps: fuzzification, combination of fuzzy sets and defuzzification. Fuzzification is the transition from a crisp system to a fuzzy system. Fuzzy object feature classes are defined by membership functions. Using these functions, a membership degree [0,1] is assigned to each object feature value, with respect to each object feature class. Different shapes of the membership functions will determine the transition between *full member* and *no member* (Figure 7).

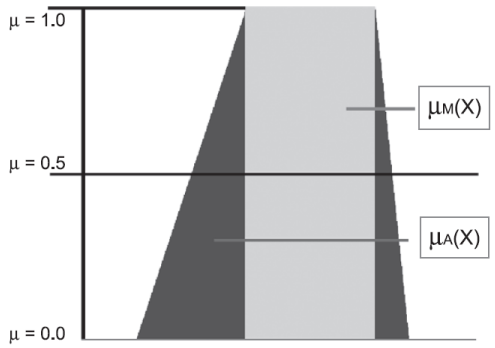

FIGURE 7: RECTANGULAR AND TRAPEZOIDAL MEMBERSHIP FUNCTIONS ON FEATURE X TO DEFINE A CRISP SET M(X), $\mu_M(X) \in [0,1]$ AND A FUZZY SET A(X), $\mu_a(X) \in [0,1]$ OVER THE FEATURE RANGE X (Benz et al. 2004)

The broader this membership function gets, the vaguer is the underlying concept. The lower the membership value, the more uncertain is the assignment of a certain value. More than one fuzzy set can be defined on one feature, e.g. to define the fuzzy sets *Acacia, soil* and *Eucalyptus* (Figure 8). The more the membership functions overlap, the vaguer the final classification will be. Based on these fuzzy sets, the membership value for each object is calculated and used for classification (Figure 9). The higher the membership degree for the most possible class, the more reliable is the assignment. When equal memberships occur, the classification is unstable and the object remains unclassified (Benz et al., 2004).

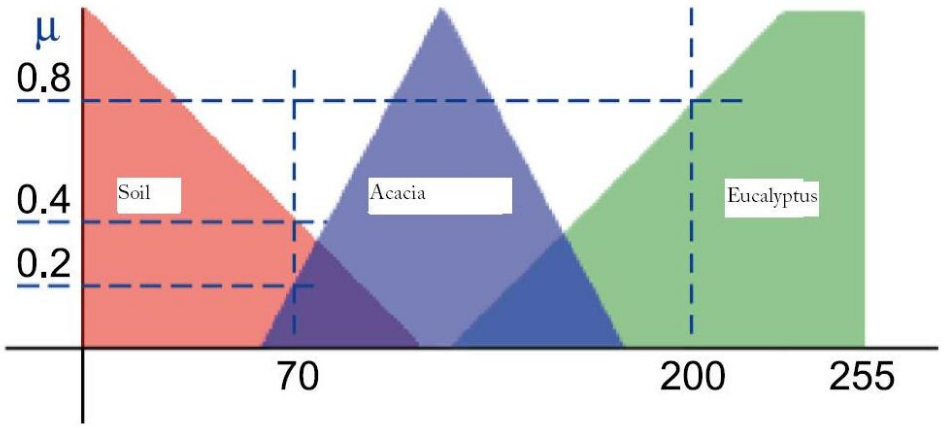

FIGURE 8: EXAMPLE FOR THREE FUZZY SETS ON FEATURE X. THE MEMBERSHIP FUNCTIONS ON FEATURE X DEFINE THE FUZZY SET *SOIL*, *ACACIA* AND *EUCALYPTUS* FOR THIS (FICTIOUS) FEATURE (ADAPTED FROM Benz et al., 2004)

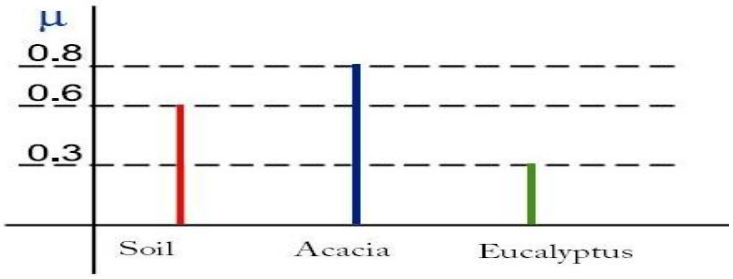

FIGURE 9: FUZZY CLASSIFICATION FOR THE CLASSES *SOIL*, *ACACIA* AND *EUCALYPTUS*. THE IMAGE OBJECT IS A MEMBER OF ALL CLASSES TO VARIOUS DEGREES (ADAPTED FROM Benz et al., 2004)

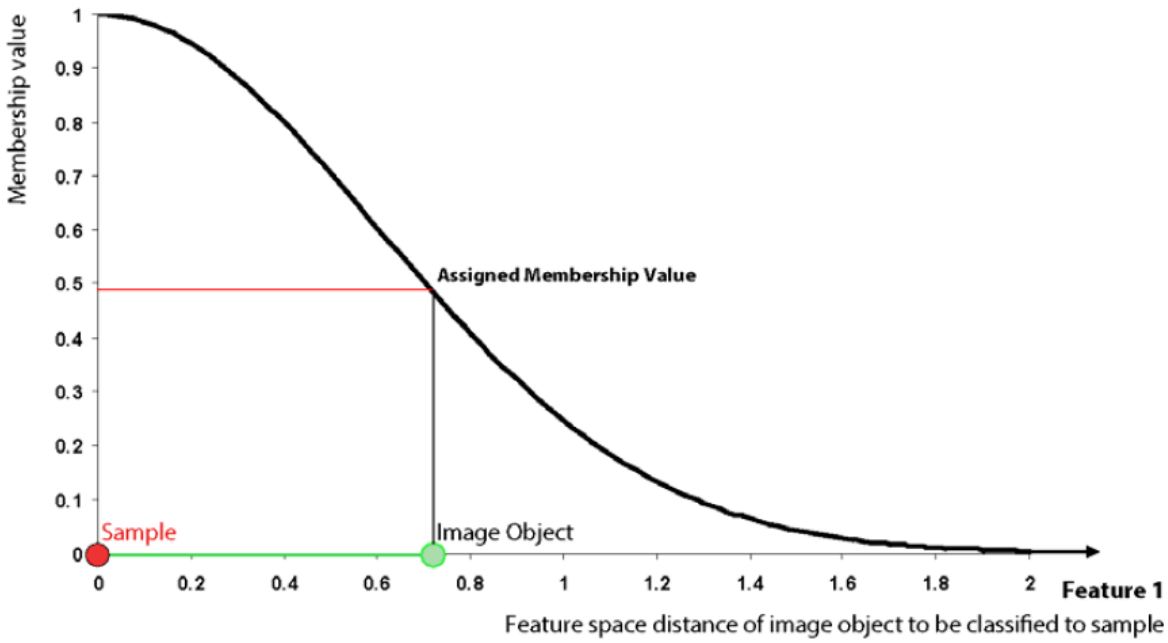

FIGURE 10: MEMBERSHIP FUNCTION CREATED BY NEAREST NEIGHBOUR CLASSIFIER (Definiens, 2009a)

In the classification procedure, only the nearest sample is used to evaluate its membership value. The effective membership function at each point in the feature space is a combination of fuzzy functions over all the samples of that class, as explained above. An illustration in one dimension is provided in Figure 10. When more dimensions are used, visualization becomes harder. A two dimensional illustration is shown in Figure 11. Samples are represented as small circles, surrounded by shading which represents the membership values. In areas where an object would be classified blue, the red membership value is ignored (and vice-versa). In zones where the membership value is below a threshold value (standard equal to 0.1), the objects will remain unclassified (Definiens, 2009a).

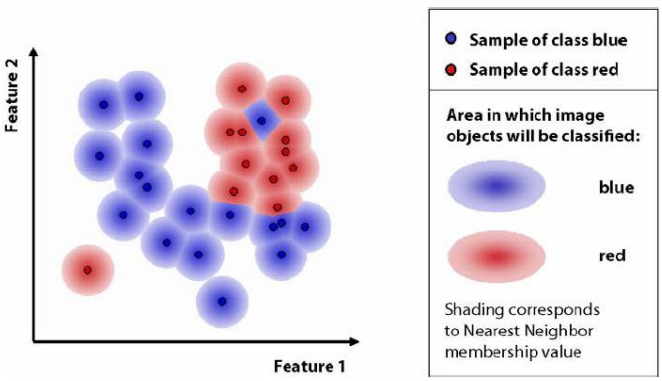

FIGURE 11: MEMBERSHIP FUNCTION ILLUSTRATING CLASS ASSIGNMENT IN 2 DIMENSIONS (Definiens, 2009a)

c CALCULATION OF OBJECT FEATURES

After the classification stage, all objects have a membership value for the three classes *soil*, *Eucalyptus* and *Acacia*. A next step consists of exporting the objects and object features in GIS format. As we are only interested in *Acacia* polygons, only those objects assigned to the *Acacia* class will be used. A large number of features can be calculated, which in turn are analyzed to assess relations with the ground truth.

d ACCURACY ASSESSMENT

The goal of the segmentation process is the replacement of manual digitizing of polygons. However segmentation results might not be entirely satisfactory. Manual editing of the created polygons is often necessary, making the (semi-)automated method less efficient if the amount of manual tweaking increases (Blaschke et al., 2008). Therefore, validation of segmentation is important to determine whether the proposed working strategy is valid. Several approaches can be used to evaluate segmentation quality (Benz et al., 2004):

- Reference polygons provided by manual digitizing can be used to test the automatic segmentation. The manual delineation for these polygons is then compared with the automatically created polygons through segmentation.
- The strength of segment borders for the entire image. The heterogeneity between the different segments is preferentially large. The *multiresolution segmentation* algorithm stops merging pixels if the increase in heterogeneity is too large. This increasing heterogeneity can be interpreted as a border between segments, to be overcome for merging. The higher this border for a certain segmentation parameter, the more stable the result. The ratio of strong borders to weak borders provides an indication of the quality of the results.

After the segmentation, a classification was performed. In eCognition accuracy assessment methods are provided, that produce statistical outputs to check the quality of the classification results. The following methods are provided (Definiens, 2009a):

- Classification stability
- Best classification result
- Error matrix based on TTA[15] mask
- Error matrix based on Samples

The *Classification Stability* measures the difference between the best and the second best class assignment (as a percentage). *Best classification result* is evaluated per class and returns basic statistical operations performed on the best classification result of the image objects of that particular class. The *error matrix* compares on a category by category basis, the relationship between known reference data (ground truth) and the corresponding results of an automated classification. It is a square matrix, with the number of rows and columns equal to the number of categories (Lillesand & Kiefer, 2004). This can be done based on test objects (using TTA Mask) or based on the samples if no test areas were defined.

Visual inspection of the classification can also provide valuable information. When the polygons are exported, a random subsection of a certain class can be selected and checked for commission errors (wrong classification). In a similar way this can be done for the unclassified objects, to check the omission errors (objects that should have been assigned to a certain class).

[15] Test and Training Area

Chapter 3: RESULTS AND DISCUSSION

In this section we present the results and our findings. First, a general analysis of dendrometric and ancillary variables is discussed. As there is also an image analysis part in this work, the next part of this section illustrates results acquired with the GeoEye-1 image. Next, empirical equations to estimate individual *Acacia raddiana* tree attributes are modeled, both through measured tree attributes and directly from image object features. Finally, the image analysis results and the modeled empirical equations are used to assess the structure of the *Acacia raddiana* population in Bou-Hedma National Park.

1 GENERAL ANALYSIS OF DENDROMETRIC AND ANCILLARY VARIABLES

The architecture of an adult tree is not only a reflection of the present conditions under which it is growing, but is the result of all the genetic and environmental factors that have been operating as the tree grows from seedling to maturity (Archibald and Bond, 2003). In general tree architecture is the result of a trade-off at the sapling stage between (rapid) vertical growth, and (often less rapid) lateral growth. In arid environments, trees are often widely scattered so that light interception is not the major selective force. Factors likely selecting for either vertical or horizontal growth in these environments are fire and herbivory (Archibald and Bond, 2003). A range of structural defenses against mammalian herbivory have been developed: spines (Gowda et al., 2003), highly branched shoots and wide canopies (Archibald and Bond, 2003). A highly branched cage-like structure can act in conjunction with spines to protect internal parts of a plant. In this section, field data is subject of a statistical analysis. Summary statistics are calculated and differences between ancillary grouping variables are assessed. Moreover, tree attributes for single-stemmed and multi-stemmed trees are compared.

During field survey, 433 random locations were visited in Bou-Hedma National Park. At these locations, tree attributes were measured as mentioned in the section 'Materials and methods'. At each of these locations, two possible types of habitus occurred: an individual tree or a group of trees. Individual trees were often multi-stemmed, making the discrimination with a tree group less clear. However in most of the cases, a clear distinction was possible based on the distance between the different stems: for an

individual tree this distance was very limited, while for tree groups this distance was large. When this distinction was not clear, the location was considered as a tree group. In approximately 10 % (43 out of 433) of the locations, a tree group was assessed. In this part, some statistical tests are used. A test is considered statistically significant if the p-value is lower than 0.05 (significant on the 5% level). If tests require normality, this normality is checked through QQ-plots and with the *Kolmogorov-Smirnov (K-S) Test for Normality* (H_0: samples are normally distributed). If necessary, data are transformed using the natural logarithm. When test for normality yields a p-value < 0.05, it is ensured that more than 30 data points are in the dataset, making it possible to perform the tests with lower power. To test homoscedacity, we use the *Modified Levene Test* (H_0: $\sigma_1^2 = \sigma_2^2 = \sigma_3^2 = \cdots$).

a DIRECTIONAL VARIATION IN CROWN DIAMETER

We considered individual trees and tree groups during field survey; hence this distinction will also be used in the subsequent analysis. Summary statistics for both crown diameter directions (North-South and East-West) are listed in Table 9. A *Two-Sample t-Test* (H_0: $\mu_1 = \mu_2$) is performed for both tree individuals and tree groups, yielding p-values of respectively 0.85 and 0.62. We conclude that on the 5 % significance level, there is no significant difference for both directions. Hence, no directional variation is considered and the arithmetic mean of these diameters will be used for further processing.

TABLE 9: SUMMARY STATISTICS OF CROWN DIAMETER IN TWO PERPENDICULAR DIRECTIONS

Statistic	CD in N-S direction (m)	CD in E-W direction (m)	Mean CD (m)
Tree individuals			
Mean	4.85	4.91	4.88
Standard Deviation	2.60	2.62	2.59
Minimum	0.50	0.54	0.52
Maximum	14.60	14.75	14.25
Tree groups			
Mean	9.85	10.31	10.08
Standard Deviation	5.01	3.56	3.91
Minimum	3.40	2.70	3.05
Maximum	32.75	17.40	24.93

b SAMPLE SUMMARY STATISTICS

Summary statistics are calculated and are presented in Table 10. Since the measured trees often had no single stem (nor at the base, nor at breast height), a representative measure is chosen to compare results. The maximum and the mean diameter are used for both basal diameter (BD) and diameter at breast height (DBH). A measure useful when measuring shrubs is the equivalent diameter, used to calculate total shrub plant diameter (Hoover, 2008; Noumi et al., 2010):

$$Equivalent\ Diameter = \sqrt{\sum_{i}^{n} d_i^2}$$

with n = total number of stems
d_i = diameter i

Although this representative diameter is used for shrubs, it can be used for trees with multiple stems as well (e.g. *Salix* sp.) (Hoover, 2008). Hence, we also calculate the equivalent diameter for both basal diameter and diameter at breast height.

A *Two-Sample t-Test* is used to compare the different tree attributes for tree individuals and tree groups. For all tree attributes p-values lower than 0.05 are found, so statistical significant differences are found between tree individuals and tree groups. For crown diameter this result is logical as total crown diameter was measured. Higher equivalent BD/DBH is also a logical consequence, as this measure aggregates all stems. Moreover, differences in tree height, mean and maximum DBH (and BD), are also observed. Tree height for a tree group is determined by the highest tree of the group. Light in (semi-) arid regions is generally not a strong affecting factor for tree architecture (Archibald and Bond, 2003). However, larger tree heights are found for tree groups compared to tree individuals, indicating interaction between trees in the tree group. Mean basal diameter was significantly higher for tree groups, but the difference is not marked (Table 10). DBH was also significantly higher for tree groups, which was not expected as trees subjected to light competition generally grow larger, with smaller bole diameters. However, the results might be influenced by an age factor, caused by the plantations. The majority of plantations are established in linear formations of individual trees, with a handful of exceptions. Hence, the tree groups in our dataset are probably old relicts of the ancient forest. Unfortunately, no data are available to discriminate between

plantations and relicts. Crown diameter is larger than tree height (Mihidjay, 1999), confirming that trees in arid environments generally grow wider (Archibald and Bond, 2003).

TABLE 10: SUMMARY STATISTICS OF TREE ATTRIBUTES FOR INDIVIDUAL TREES

Variable	Mean	Standard deviation	Minimum	Maximum
Tree individuals				
Crown diameter (m)	4.88	2.58	0.52	14.25
Tree height (m)	3.61	1.63	0.43	11.74
Mean basal diameter (cm)	19.1	15.2	1.1	120.0
Maximum basal diameter (cm)	21.4	15.2	1.6	120.0
Equivalent basal diameter (cm)	23.5	15.6	2.0	120.0
Mean DBH (cm)	7.7	6.6	1.4	54.0
Maximum DBH (cm)	13.0	9.1	1.5	54.0
Equivalent DBH (cm)	21.8	13.8	2.1	67.0
Tree groups				
Crown diameter (m)	10.08	3.91	3.05	24.93
Tree height (m)	5.19	1.46	1.90	8.82
Mean basal diameter (cm)	21.8	11.0	5.4	47.2
Maximum basal diameter (cm)	36.1	15.0	10.3	70.1
Equivalent basal diameter (cm)	52.3	20.9	14.6	126.5
Mean DBH (cm)	9.4	5.1	2.1	28.6
Maximum DBH (cm)	20.7	10.2	2.5	47.6
Equivalent DBH (cm)	44.8	20.7	4.1	120.3

c ANALYSIS OF ANCILLARY VARIABLES

i Stoniness and erosion crust

The stoniness of the soil and the presence of an erosion crust are graphically presented in Figure 12 and Figure 13. Stoniness class 2 (moderately rocky land, 10-25%) occurs the most, but the other classes cannot be ignored. This is consistent with field observations, as the plains have only few rocks, while the foot of the mountain chain is very rocky. The presence of an erosion crust is clearly influenced by the tree canopy. The biggest erosion crust class under the tree canopies is 0 (0-10% erosion crust), while in the buffer zone the largest class is 2 (25-50 % erosion crust). This shows that the tree canopy protects the underlying soil against the impact of the rain and therefore can be considered valuable for combating desertification. A *One-Way Analysis of Variances* (ANOVA) is performed with classes of stoniness and erosion crust as independent variables. This does not yield significant differences between the different tree attributes for classes of stoniness and erosion crust under the canopy. However a significant difference was found between erosion crust classes in the buffer zone between classes

0&2, 1&2 and 2&3. No logical explanation is found for these differences and they are considered an artifact of the used visual assessment of the classes.

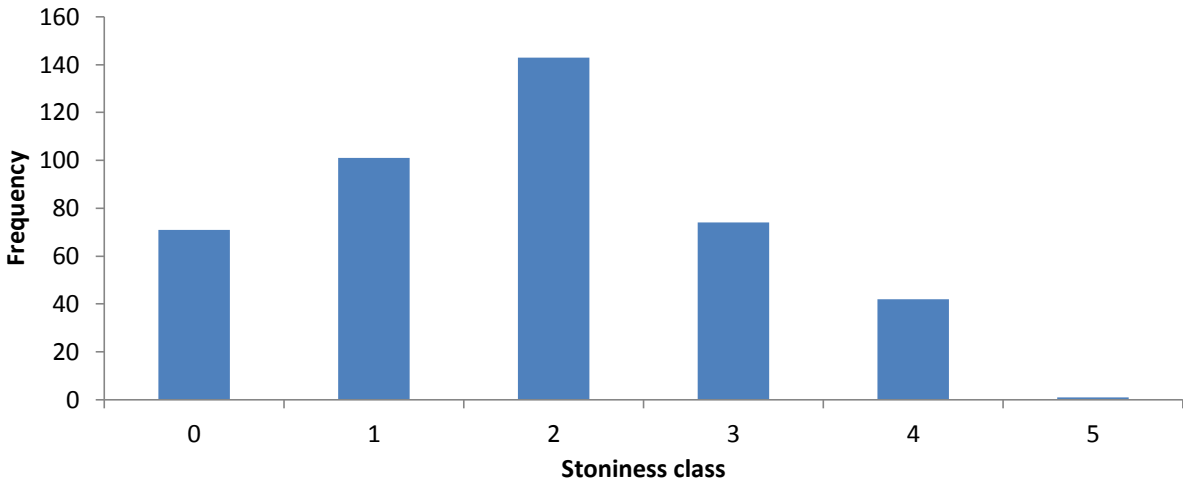

FIGURE 12: HISTOGRAM OF STONINESS CLASSES FOR INDIVIDUAL TREES

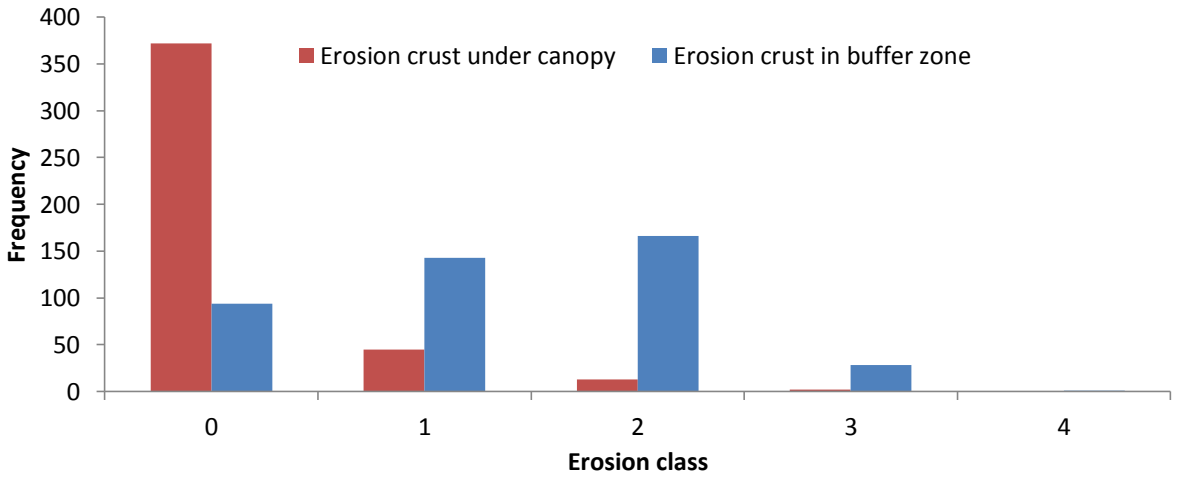

FIGURE 13: HISTOGRAM OF EROSION CRUST CLASSES FOR INDIVIDUAL TREES

ii Animal faeces

At the base of 62% of the individual trees (243 of 390 trees) animal faeces were found, while for tree groups this was 81% (35 of 43 tree groups). Bird nests (minimum one) were found in 6% of the individual trees (23 of 390 trees) and in 23% of the tree groups (10 of 43 tree groups). If tree groups are split based on the presence of animal faeces, less than 30 data points are present which have no animal faeces. Therefore no statistical analyses can be done. We limit the discussion to tree individuals. The Boolean variable is used as a grouping variable in the subsequent analysis. Both groups are thereafter analyzed for significant differences in tree attributes.

Summary statistics for both groups (presence and absence of animal faeces) are listed in Table 11. When a *Two-Sample t-Test* is performed, p-values for all variables are equal to zero, indicating a clear preference of the fauna. Larger trees, with a mean of 5.76 m are generally preferred. This difference was expected as larger crowns cast more shadow, attracting fauna in the national park (mainly *Oryx dammah*, *Addax nasomaculatus* and *Gazella* sp.), preferring shady locations for rumination. Higher values for tree height, basal diameter and diameter at breast height are also observed, which is also expected because of allometric relations. No consistent relationship is found between number of stems and the presence of animal faeces, though more than twice as much trees with a single stem were found with animal faeces at their base (Figure 14). This can be partially explained by the ease of access to these trees, as no branches hamper the animals.

TABLE 11: SUMMARY STATISTICS OF TREE ATTRIBUTES FOR INDIVIDUAL TREES, GROUPED BASED ON THE PRESENCE OR ABSENCE OF ANIMAL FAECES

Variable	Mean	Standard deviation	Minimum	Maximum
Animal faeces absent				
Crown diameter (m)	3.41	2.19	0.52	14.25
Tree height (m)	2.76	1.34	0.43	7.96
Mean basal diameter (cm)	11.7	10.8	1.1	61.6
Maximum basal diameter (cm)	13.4	11.0	1.6	61.6
Equivalent basal diameter (cm)	15.0	11.3	2.0	61.6
Mean DBH (cm)	5.2	3.8	1.4	23.1
Maximum DBH (cm)	8.4	6.6	1.5	43.0
Equivalent DBH (cm)	14.2	11.3	2.1	62.8
Animal faeces present				
Crown diameter (m)	5.76	2.41	0.98	13.38
Tree height (m)	4.12	1.58	0.78	11.74
Mean basal diameter (cm)	23.4	15.8	1.3	120.0
Maximum basal diameter (cm)	26.2	15.5	2.2	120.0
Equivalent basal diameter (cm)	28.6	15.6	2.8	120.0
Mean DBH (cm)	9.0	7.3	1.4	54.0
Maximum DBH (cm)	14.7	9.4	1.6	54.0
Equivalent DBH (cm)	25.5	13.5	3.1	67.0

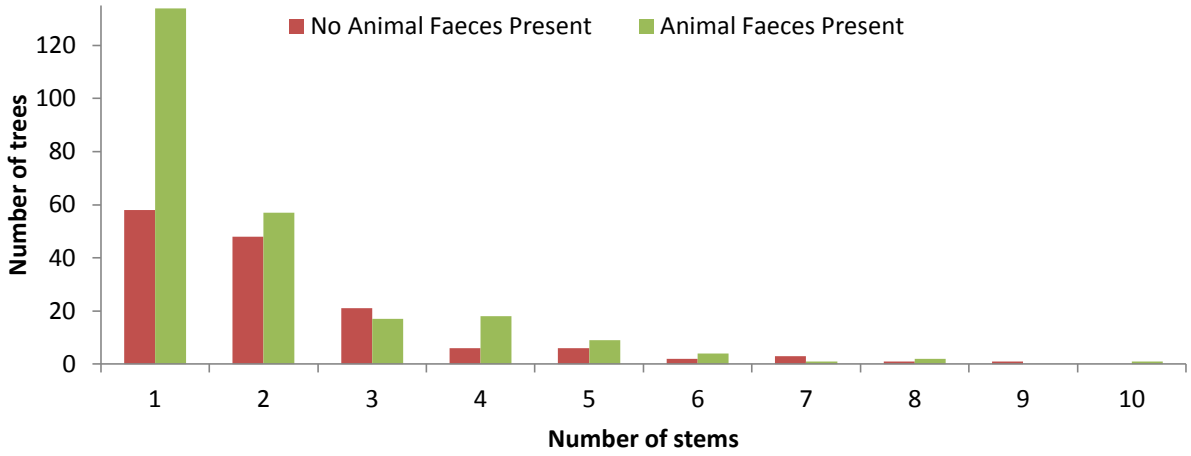

FIGURE 14: HISTOGRAM OF NUMBER OF STEMS IN FUNCTION OF THE PRESENCE OF ANIMAL FAECES

d VOLUME

Bole diameter was measured at two different heights: basal diameter (10-15 cm above the ground) and diameter at breast height (130 cm above the ground). Number of stems at breast height was generally larger than the basal number, caused by a strong bifurcation of the branches at low heights. Diameter at breast height is generally not measured for *Acacia raddiana* because of the density of branches at that particular height (with spines). An advantage of performing both measures is that the transition from the base to breast height is known. This can be used to estimate the volume of the wood from the base to 1.30 m above the ground. However, bifurcation height is very irregular and was not measured. Hence, only a biased volume estimation can be performed based on the equivalent BD and equivalent DBH. We do not have any indications for the shape of the trunk, so we calculate the volume of a truncated cone:

$$v = \frac{\pi}{4} h \left(\frac{d_0^2 + d_0 d_b + d_b^2}{3} \right)$$

with v = volume truncated cone (m^3)
d_0 = basal diameter (m)
d_b = diameter at breast height (m)
h = breast height (1.30 (m))

e *MULTI- VERSUS SINGLE-STEMMED TREES*

Acacia raddiana shows a large variation of appearances in the field. Some individuals have a more bushy appearance. According to Mihidjay (1999), the bushy aspect is explained by the fact that young individuals are multi-stemmed from the base. At a certain age (starting from approximately 10 years), one of the axes becomes the trunk while others are inhibited. The inhibited axes degenerate afterwards (Mihidjay, 1999). Sometimes the bifurcation at the base remains (2 to 3 branches), however these individuals seem more retarded in their growth (Mihidjay, 1999). It is however hard to derive a general rule as in the field also aged, large trees are found with multiple stems (Noumi[16], Bensaid[17] & De Smet, personal communication; own observations).

Growing single-stemmed is a characteristic used in taxonomy to classify *Acacia raddiana* (Brenan, 1983; AbdElRahman & Krzywinski, 2008). The morphological features used to separate taxa in the *Acacia* complex are largely overlapping and the taxa display high phenotypic plasticity (AbdElRahman & Krzywinski, 2008). However the morphological characters may very well be phenotypic expressions of ecological factors (AbdElRahman & Krzywinski, 2008). For instance, *Acacia karroo* had the highest average stem number in arid shrubland compared to a forest and a savanna population (Archibald & Bond, 2003). In general, *A. raddiana* grows with a single trunk. However the terminal buds often disappear, caused by animal browsing or by drought, inducing growth of lateral buds (Bensaid, personal communication). This results in the typical bushy aspect of the tree. When trees are cut for wood, new growth is also induced from the base. In reality all these situations are observed in the field.

The hypothesis formulated by Mihidjay (1999) is not generally accepted (Noumi, Bensaid & De Smet, personal communication), and the multiple stems are considered a characteristic of the species (De Smet & Hamdi, personal communication). We test the above hypothesis with our data. Therefore we split the dataset based on the number of stems. Tree groups are not used in the subsequent analysis, hence 390 tree individuals remain. The histogram is shown in Figure 15, illustrating that almost 50 % (193 out of 390 trees) of the sampled trees has a single stem. Less than 10 % of the individuals have

[16] Zouhaier Noumi, Université de Sfax, Faculté des Sciences, Laboratoire de Biologie et d'Ecophysiologie des végétaux en milieu aride, Tunisia
[17] Sahraoui Bensaid, Unité de recherche sur les zones arides, Algeria

more than 4 stems. Based on this distribution, we consider 4 classes of trees: 1 stem, 2 stems, 3 stems and ≥4 stems. This guarantees that more than 30 samples are present in each class, required for statistical analyses. Summary statistics were calculated for each of the four defined classes, indicating lower tree attribute means for trees with more than 1 stem (Table 12).

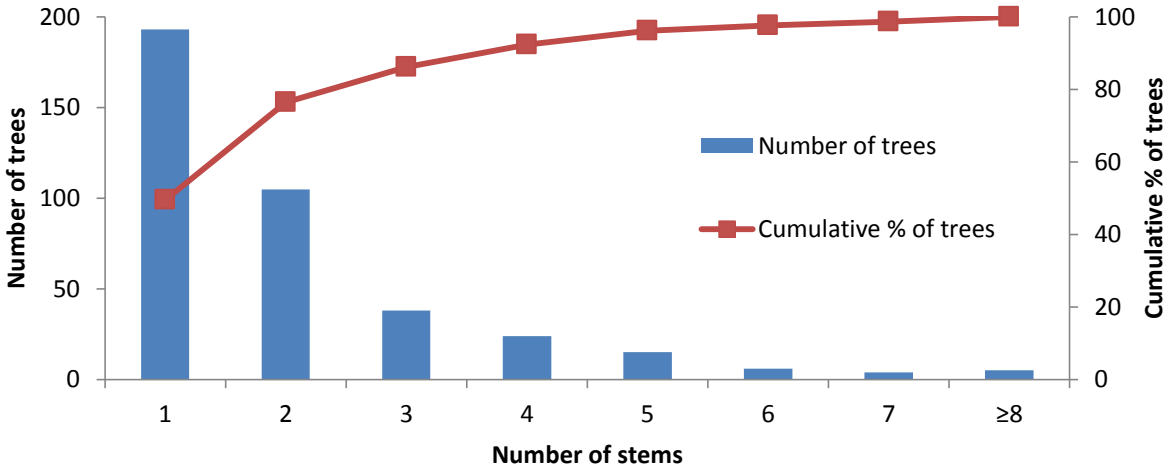

FIGURE 15: HISTOGRAM OF NUMBER OF STEMS

Next, we use a One-Way ANOVA to compare means of two or more samples, yielding p-values smaller than 0.05 for all variables. Hence, we conclude on the 5 % level of significance, that differences between the different classes (number of stems) are significant for at least two classes. In order to know which classes are significantly different, we use the *Tukey Method*. Significant differences between the means of each of the considered classes for the different tree variables are indicated in Table 12. Means followed by different letters (superscript) are considered significantly different as determined by the Tukey Method. These results reveal a clear difference between trees with a single stem (class 1) and trees with multiple stems (classes 2, 3 & 4) for the variables tree height, mean and maximum DBH, and maximum BD. Single-stemmed trees show larger attribute values than multi-stemmed individuals. For crown diameter, no significant difference is found between class 1 and class 4, this can be explained by the fact that 4 or more stems significantly increase crown diameter.

For mean BD, significant differences are found between class 1 and the other classes. Moreover a significant difference was found between trees with 2 and 3 stems. Trees with 2 stems have a significantly larger mean BD, while for maximum BD no significant differences were found between these classes. Equivalent BD shows other results as

well. While class 1 is significantly different from class 2 & 3, this was not the case compared to class 4. Moreover, class 3 and class 4 are significantly different according to the *Tukey Method*. Class 4 shows higher values for the equivalent BD, hence occupying more basal area. This is in analogy with the results found for crown diameter, as both variables are expected to be correlated.

For DBH, a clear discrimination between single-stemmed trees and multi-stemmed trees exists, except for the equivalent DBH. Again significant differences were found between class 1 and classes 2 & 3, but not with class 4, which should not be surprising considering the higher equivalent BD for this class.

Looking at the volume, only statistical differences are found between one-stemmed trees and trees with 2 or 3 stems. Differences between trees with one stem and 4 or more stems are not significant. The hypothesis of Mihidjay (1999) cannot be rejected, nor accepted. We notice significant lower values for trees with 2 or 3 stems in comparison with the single stemmed trees. However these results cannot be generalized for trees with more than 3 stems.

FIGURE 16: *Acacia raddiana* TREE INDIVIDUAL WITH 3 STEMS AT THE BASE WITH A TOTAL TREE HEIGHT OF 4.35 M AND CROWN DIAMETER OF 8.3 M

TABLE 12: SUMMARY STATISTICS OF TREE ATTRIBUTES FOR EACH OF THE DEFINED CLASSES (NUMBER OF STEMS)[18]

Number of stems class	Mean	Standard deviation	Minimum	Maximum
Crown diameter (m)				
1	5.6[ac]	2.64	0.79	14.25
2	3.94[b]	2.21	0.84	12.45
3	3.79[b]	2.27	0.52	9.10
≥4	4.86[c]	2.49	1.16	11.10
Tree height (m)				
1	4.18[a]	1.69	0.63	11.74
2	3.02[b]	1.35	0.56	10.25
3	2.82[b]	1.51	0.43	7.62
≥4	3.26[b]	1.29	0.82	7.14
Mean basal diameter (cm)				
1	27.5[a]	16.5	2.1	120.0
2	12.1[b]	8.0	1.5	44.1
3	9.2[c]	7.1	1.1	28.1
≥4	9.3[bc]	5.9	1.3	27.0
Maximum basal diameter (cm)				
1	27.5[a]	16.5	2.1	120.0
2	15.7[b]	11.6	2.0	72.2
3	13.1[b]	9.9	1.6	43.1
≥4	16.7[b]	10.9	2.1	43.8
Equivalent basal diameter (cm)				
1	27.5[ad]	16.5	2.1	120.0
2	18.2[bc]	12.5	2.2	73.3
3	17.1[b]	12.9	2.0	53.0
≥4	23.8[cd]	15.1	2.8	62.2
Mean DBH (cm)				
1	9.6[a]	7.8	1.6	54.0
2	5.8[b]	4.5	1.4	30.9
3	5.0[b]	2.8	1.5	10.7
≥4	5.7[b]	3.0	1.4	13.5
Maximum DBH (cm)				
1	15.1[a]	10.2	2.1	54.0
2	9.5[b]	7.2	1.5	44.4
3	9.2[b]	5.7	2.2	19.8
≥4	10.7[b]	5.8	1.6	24.0
Equivalent DBH (cm)				
1	22.7[a]	14.5	2.3	67.0
2	16.8[bc]	11.6	2.1	60.5
3	17.5[bc]	11.8	4.3	50.3
≥4	22.2[ac]	13.0	2.7	54.6
Volume (dm^3)				
1	94.8[a]	109.1	1.2	891.5
2	49.0[bc]	71.4	2.2	459.0
3	51.4[bc]	61.0	3.6	272.3
≥4	79.2[ac]	81.9	2.4	336.9

[18] Mean values which are not followed by the same letter are significantly different ($p < 0.05$) as determined by Tukey's method.

f PHENOLOGY

Field measurements were done during a limited period of the year (mainly September – October), so only data on phenology for this period are available. Hence, no full evaluation of tree phenology can be performed. The number of trees in the different development stages for leaves, flowers and fruit is listed in Table 13. These results show that the majority (91.6 %) of the trees was in leaf development stage 3, indicating maximum presence of leaves. The tree is considered semi-deciduous (see addendum 2), however no trees were sampled with more than 10 % dried leaves, although we were in the dry and hot season. For the remaining part of trees, leaf development was in an early stage. Flowering was very variable, depending on individuals; in the field individuals close to each other even showed large differences. For about one third of the sampled locations, the majority of flowers were dried, introducing the formation of fruits. For 12.3 % (53 individuals) no distinct flowering stage was observed. Fruit setting was only observed during the last weeks of October, which were also the last days in the field. Hence, no full grown fruits were observed, except for remains of the previous year (86.7 % of the individuals had not started fruit setting). These observations confirm the phenologic cycle assessed by Mihidjay (1999) and Wahbi (2006) in Bou-Hedma National Park.

TABLE 13: NUMBER OF TREES FOR THE DIFFERENT STAGES OF V, f AND F (SEPTEMBER - OCTOBER 2009, 430 SAMPLES)

	V		f		F	
Stage	Number of trees	%	Number of trees	%	Number of trees	%
1	7	1.63	51	11.63	35	8.14
2	29	6.74	53	12.33	22	5.12
3	394	91.63	75	17.44	0	0.00
4	0	0.00	57	13.26	0	0.00
5	0	0.00	142	33.02	0	0.00

g TREE CROWN DENSITY

During the field survey, pictures of the tree crowns were taken in vertical position (looking upwards) in the four cardinal locations. This was only possible for trees with sufficient height. Although the procedure was standardized, pictures taken during different times of day (and between consecutive days) are quite different. As a result, leaves are not always clearly visible on the pictures (caused by strong illumination). However this could be fixed by illumination correction on the camera. Moreover, often

leaning trees were encountered, covering a large portion of the picture with our used method.

Nevertheless the pictures are analyzed with unsupervised classifiers, creating a binary mask with branches and leaves on the one side, and sky (sometimes with clouds) on the other side (Figure 17). To analyze the pictures, they are imported in *Idrisi* and separated in 3 different bands (RGB) for further analysis. Next, we use both the modules *Cluster* (based on histogram peak technique) and *IsoClust* (similar to K-means) in *Idrisi* to classify the images based on the 3 separated bands. As for each tree, 4 images are available, the process demands lots of computational time, hence the process is automated. Because of the variation between the pictures and the unsupervised working strategy, no consistent classification is obtained. Hence manual supervision of each picture is done for each tree and for each of the four cardinal locations, which is a very time-consuming task. After classification the number of pixels assigned to each class (tree/sky) is calculated. Based on the total number of pixels in the images, the percentage tree cover is determined. The arithmetic mean was thereafter calculated, resulting in a measure for tree crown density.

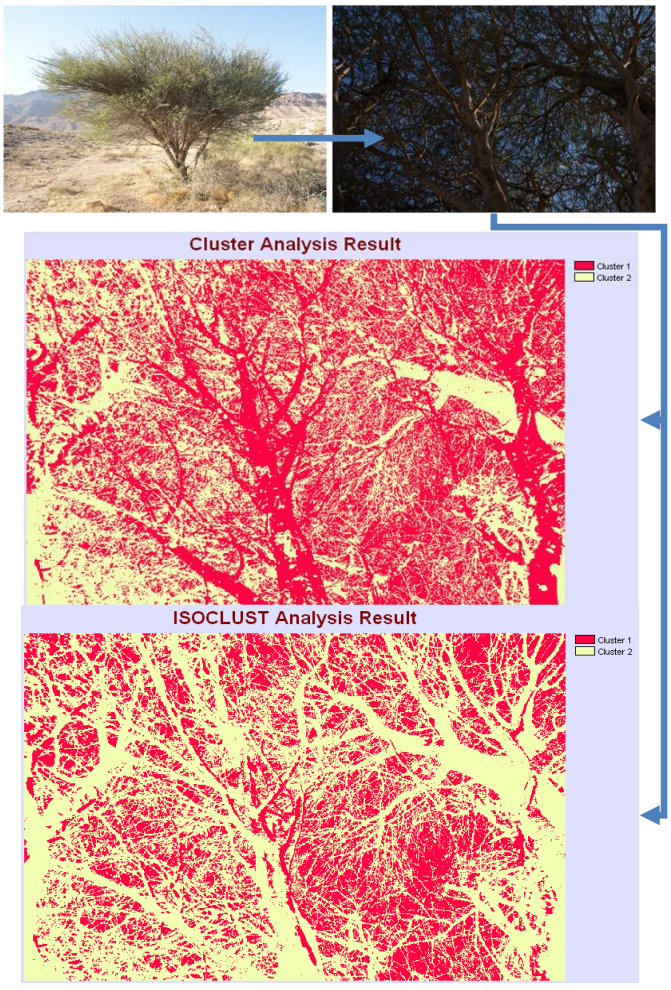

FIGURE 17: ILLUSTRATION OF TREE CROWN DENSITY ANALYSIS RESULTS

2 IMAGE ANALYSIS

a OPTIMAL TIME OF IMAGE ACQUISITION

Information concerning phenology is particularly interesting to determine the optimal time of image acquisition, in order to increase spectral difference between soil and *Acacia* trees. However no exact recommendations can be given, as the cycle is highly dependent on climatic conditions. Vegetative buds start to grow at the beginning of June, with a limited growth of vegetative branches up to mid-September. When fruit setting starts, vegetative growth is also initiated and continues up to the end of January. In Bou-Hedma National Park, more than 500 plant species (from 71 plant families) can be found (addendum 3). A large part of the vegetation is annual. However, during the dry season, annuals are hard to find. Some perennial species occur in the entire area. During field survey, 40 species were recorded (included in the database, addendum 4). The majority of species was perennial, which was expected considering the time of the year (hot and dry season). At the end of the field survey, a temperature drop and the first rains induced the growth of annual vegetation growth. However, species identification was not possible.

The optimal time of image acquisition, is determined at the time at which discrimination between trees, soil and vegetation is the largest. The dry season is considered optimal, as no lush vegetation is present, increasing the separability of trees from the soil. Moreover, cloud cover is generally very low. Exact figures on the development of the vegetation are not available; hence no quantitative analysis is performed. The image is ideally acquired, when the leaves of the trees are fully developed. According to the observed phenology (addendum 2), this is from the end of July to the end of January. The GeoEye-1 image we used was acquired on the 1st of August 2009. As the time of acquisition overlaps with the dry season and with the period of maximum leaf development, the distinction between trees and soil is high (Figure 18).

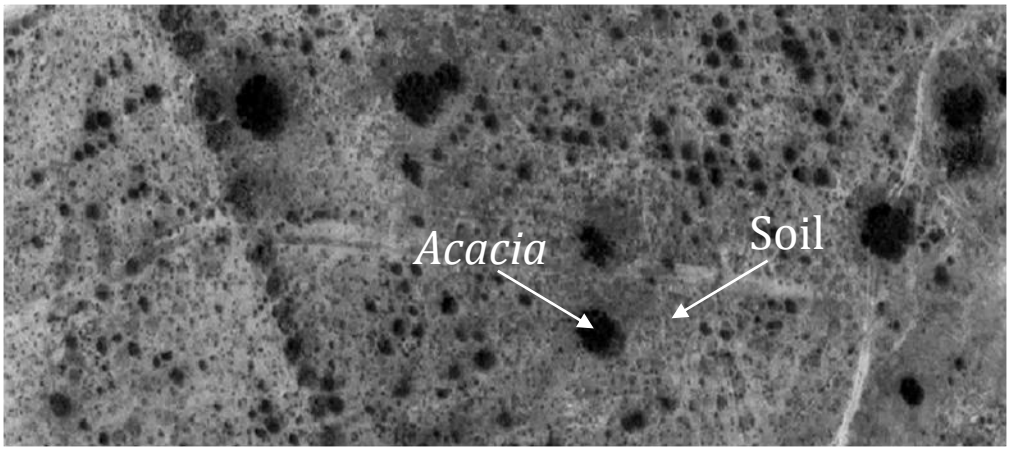

FIGURE 18: ILLUSTRATION OF TREE/SOIL SEPARABILITY (GEOEYE-1, PANCHROMATIC BAND, 0.5 M SPATIAL RESOLUTION)

b SEGMENTATION

For both the *multiresolution* and *contrast split segmentation* the algorithms' parameters are determined by trial and error on a subset of the image, containing both appearances of *Acacia raddiana* (natural versus plantation) and *Eucalyptus* sp. Best segmentation results are acquired by solely using the panchromatic band (mainly driven by its more suitable spatial resolution in the context of individual tree delineation). After several runs of the *multiresolution segmentation* algorithm with different scale parameters, a scale parameter of 40 was considered optimal. The homogeneity criterion is determined by two parameters: shape and compactness. These are respectively set to 0.2 and 0.5. This results in an initial segmentation, correctly delineating larger trees. However smaller trees are not segmented, but are included in larger segments with multiple smaller trees and soil/vegetation in between. Therefore a sequential segmentation is performed on the initial segments. For the greater part *contrast split segmentation* is able to isolate smaller trees (Figure 19). The split is based on the contrast present in the panchromatic band using the parameters mentioned in Table 14 (for a full description of parameters we refer to Definiens (2009b)).

The sample trees were manually delineated in order to visually compare segmentation results with the manual delineations (Figure 20). When we compare both delineations, it is clearly visible that the manual delineations are larger than the segmentation results. It seems that the segmentation result is closer to reality than the manually delineated polygons, as irregular crown edges are also observed on the field. When crown diameter is measured on these polygons and compared to the ground truth data, the manually

delineated polygons represent an overestimation. However, some trees that were delineated manually are not isolated by the segmentation algorithm. The tree right above (indicated with an arrow) in Figure 20, not detected through segmentation, has a ground truth crown diameter of 1.82 m.

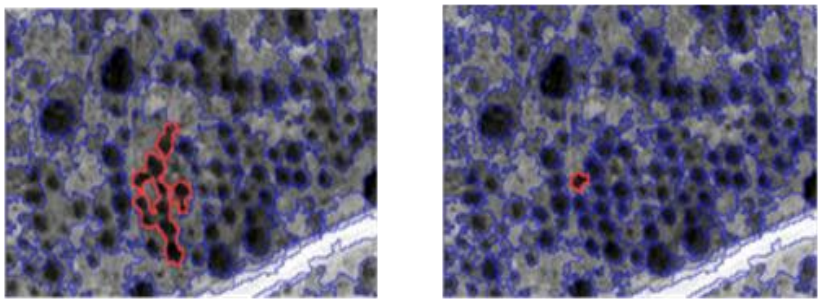

FIGURE 19: RESULTS OF THE INITIAL MULTIRESOLUTION SEGMENTATION (LEFT) AND SUBSEQUENT CONTRAST SPLIT SEGMENTATION (RIGHT) (FOR USED PARAMETERS SEE TEXT)

TABLE 14: PARAMETERS USED FOR CONTRAST SPLIT SEGMENTATION

Parameter	Value
Contrast mode	Edge difference
Minimum relative area dark	0.1
Minimum relative area bright	0.1
Minimum contrast	0
Minimum object size	10

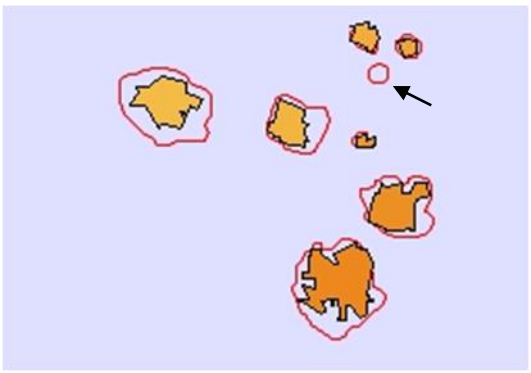

FIGURE 20: COMPARISON OF SEGMENTATION RESULTS (FILLED POLYGONS) AND MANUAL DELINEATIONS (OUTLINES IN RED)

c CLASSIFICATION

In order to separate *Acacia raddiana* trees from soil and other vegetation, the created segments have to be classified. Therefore, three classes of interest are considered (*Acacia, Eucalyptus* and *soil*). Initially, only the panchromatic band is used for classification. However, low separation distances between classes are found. When

multispectral wavebands are added, separation distance increases, emphasizing the importance of multispectral wavebands to discriminate between different tree species (*Eucalyptus* sp., *Acacia* sp.) and soil segments. Through *Feature Space Optimization* (FSO) an optimal feature set of 34 object features (out of 20 categories) is determined (Figure 21) on an image subset. Maximum separation distance is 9.71. In Table 15, feature categories used for classification are listed. A detailed list is provided in addendum 5. The Forest Discrimination Index (FDI) (Bunting & Lucas, 2006) is adjusted for the GeoEye-1 image (FDI=NIR-(R-B)). Initial classification results on a subset show good results with these object features. Hence a full classification is performed, with as many *Acacia* samples as soil samples (randomly selected over the study area). However this does not yield satisfying results, as many soil polygons are classified as *Acacia,* especially soil polygons with vegetative cover. Next, the sample pool of soil segments is increased, which yields better results. Though closer inspection of the classification reveals a large number (order of magnitude 10,000 on 500,000 segments) of small soil segments, classified as *Acacia*. A subset of these soil segments is therefore selected as soil samples, which yields satisfying results. Finally, 170 *Acacia* samples, 37 *Eucalyptus* and 5,153 soil samples are selected. The low number of *Acacia* samples is explained by the fact that only representative samples are retained for classification. Some trees were not detected or included in a soil polygon and therefore not included for classification.

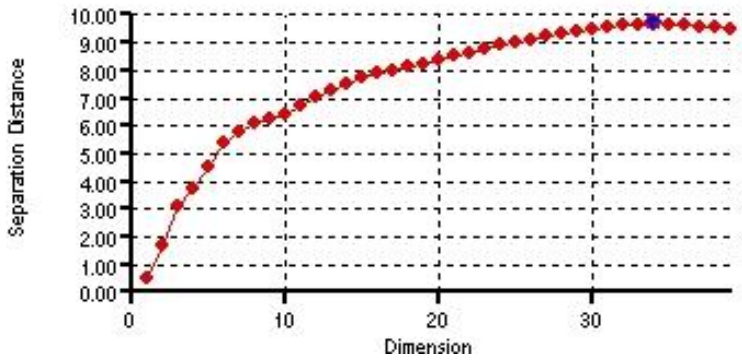

FIGURE 21: RESULT CHART OF FEATURE SPACE OPTIMIZATION WITH 34 DIMENSIONS AS OPTIMUM

TABLE 15: FEATURE CATEGORIES USED FOR CLASSIFICATION

Type	Feature
Customized	FDI, SAVI, NDVI
Layer Values	Mean, Min, Max, Mean of outer border, Border contrast, Contrast to neighbour pixels, Edge contrast of neighbour pixels, StdDev to neighbour pixels, Circular mean
Geometry	Assymetry, Density, Compactness
Texture after Haralick	Homogeneity, Mean, Correlation, Ang 2nd moment, Entropy

The three classes of interest are rendered in colours with *Eucalyptus* sp. in red, *A. raddiana* in green and *soil* in brown. The remaining non classified image objects are buildings and roads (Figure 22). Because of the limited number of *A.raddiana* samples, no test samples were selected (all of them were used for training). However only statistics of the samples are used in the classification process (samples are not automatically assigned to their class). Therefore a (biased) accuracy assessment, based on the samples, is performed yielding a KIA of 0.96 indicating that not all samples were correctly classified. In fact 16 of the 170 *Acacia* samples were classified as *Eucalyptus*. All *Eucalyptus* samples were correctly classified. Only one of the soil samples was misclassified as *Eucalyptus.* Based on the number of samples, classification results can be considered as satisfactory. Mean of the *best classification result* for all objects of *Acacia, Eucalyptus* and *soil* was respectively 0.62, 0.38 and 0.64. The low value for *Eucalyptus* is caused by the low number of samples for the *Eucalyptus* class. Mean *classification stability* (percentage difference between best and second best class assignment) was 0.20, 0.11 and 0.15 for respectively *Acacia, Eucalyptus* and *soil*. The higher these values, the more stable the classification. Hence, we conclude that the *Acacia* class is more stable than the other classes, which is favorable for our analysis.

The strongly iterative procedure of this classification method, limits the efficiency as 500,000 segments had to be classified. In fact, initial classification demanded about 1 week of computational time[19]. Subsequent classification runs were only performed on *Acacia* segments, as only soil segments were incorrectly classified as *Acacia*. Computational time for these classifications was between 50 and 70 hours. Possible improvements are the use of alternative classification algorithms (such as artificial neural networks) or the efficient selection of samples. Random sampling apparently did not include enough variance for the soil samples. Hence an intensive sampling in a selection of regions over the entire study area could produce better results.

[19] Hardware configuration: Intel® Core^2 ™ Quad CPU, Q9550 @ 2.83 Ghz, 3.25 GB of RAM

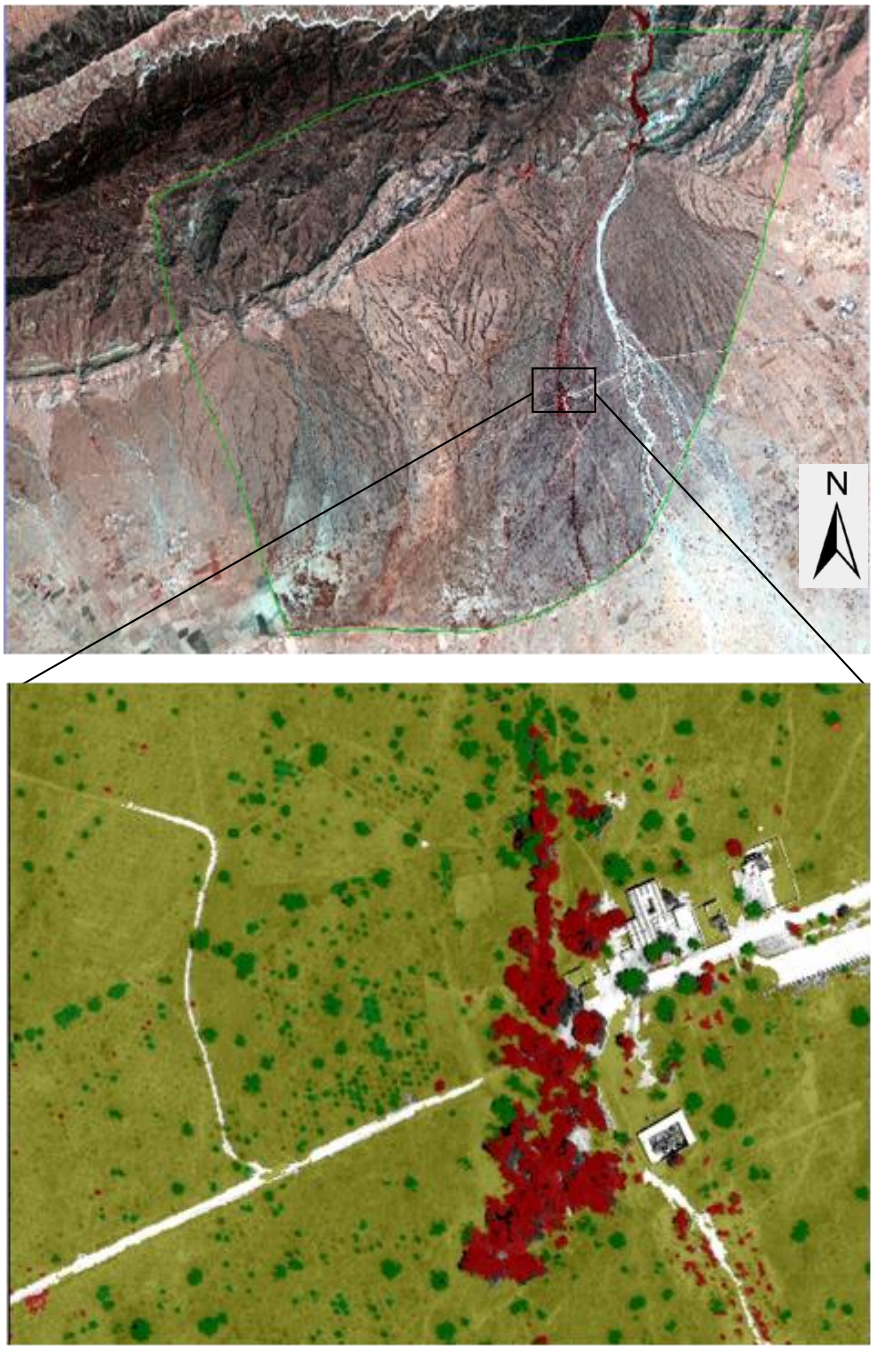

FIGURE 22: STUDY AREA (ABOVE) AND CLASSIFICATION OF IMAGE SUBSET (RED = *Eucalyptus* sp., GREEN= *Acacia raddiana*, BROWN=*soil*).

3 EMPIRICAL EQUATIONS TO ESTIMATE INDIVIDUAL *ACACIA RADDIANA* TREE ATTRIBUTES

a ALLOMETRIC RELATIONS

Tree attribute values are often correlated and therefore it is possible to model allometric relationships. These models are useful to estimate variables that are hard to measure or take considerable time to measure (e.g. tree height). The goal is to estimate tree attribute values for individual trees. Typical forest inventory error varies between 15 % and 20 % (Kayitakire et al., 2006). Pearson correlation coefficients were calculated for the different tree attributes (and derived attributes) by way of exploratory analysis. We used 329 samples for calculation of correlations, which does not include all trees. This is caused by missing data, e.g. diameter at breast height for trees smaller than 1.30 m. A correlation of 0.79 is found between tree crown density (TCD) determined with *Cluster* and with *IsoClust*. As both methods try to measure the same variable, this correlation is highly expected. Low correlations are found between TCD and other tree attributes, especially for the *Cluster* method (maximum correlation of 0.32). For the *IsoClust* method, higher correlations are found with crown diameter (0.48), maximum BD (0.40), equivalent BD (0.43) and equivalent DBH (0.46), indicating that a relation is present. However no satisfying relationship can be modeled between these attributes (low R^2 values, order of magnitude 0.25). The variation between pictures on different times of the day, are a possible reason for the low correlations. Next, we first consider correlations between crown diameter and other tree attributes, keeping in mind possible applications in the subsequent image analysis. A relation between DBH and BD is also presented, followed by the estimation of volume and tree height from BD.

i Estimating bole diameter through crown diameter

High correlations are found between crown diameter and all three derived BD measures. Correlations for mean BD, maximum BD and equivalent BD are respectively 0.81, 0.88 and 0.92. These correlations give an indication of the linear relationship between both variables. As crown diameter can be directly estimated from satellite imagery, we use crown diameter as dependent variable and BD as independent variable. Forest trees usually exhibit a significant relationship between their crown diameters and bole diameters. For many species the relationship between both variables has been modeled using a linear relationship (Hemery et al., 2005). When crown diameter versus mean BD

is modeled (linear function) for tree individuals with a different stem number (1, 2, 3 or more stems), a clearly different model emerges. For a fixed crown diameter, tree individuals with more than 1 stem, show a lower mean basal diameter. This difference is bigger for larger crown diameters, although overlapping data points exist (Figure 23). However, based on the satellite imagery, we are not able to discriminate between those different classes. Hence, it would be useful if a representative value based on the basal diameter could be derived from crown diameter. Modeling crown diameter versus maximum basal diameter already decreases the difference between the classes. Though, best results are found with the equivalent BD (Figure 24). The clear difference between different classes is not present for this relation. The deviation at larger crown diameters can be neglected, considering the large standard deviations (Table 12). Moreover, comparing the regression slopes (using a *student t-test*) of the four modeled linear regressions in Figure 24, yields p-values > 0.05. Hence we conclude that no significant differences exist between the four regressions.

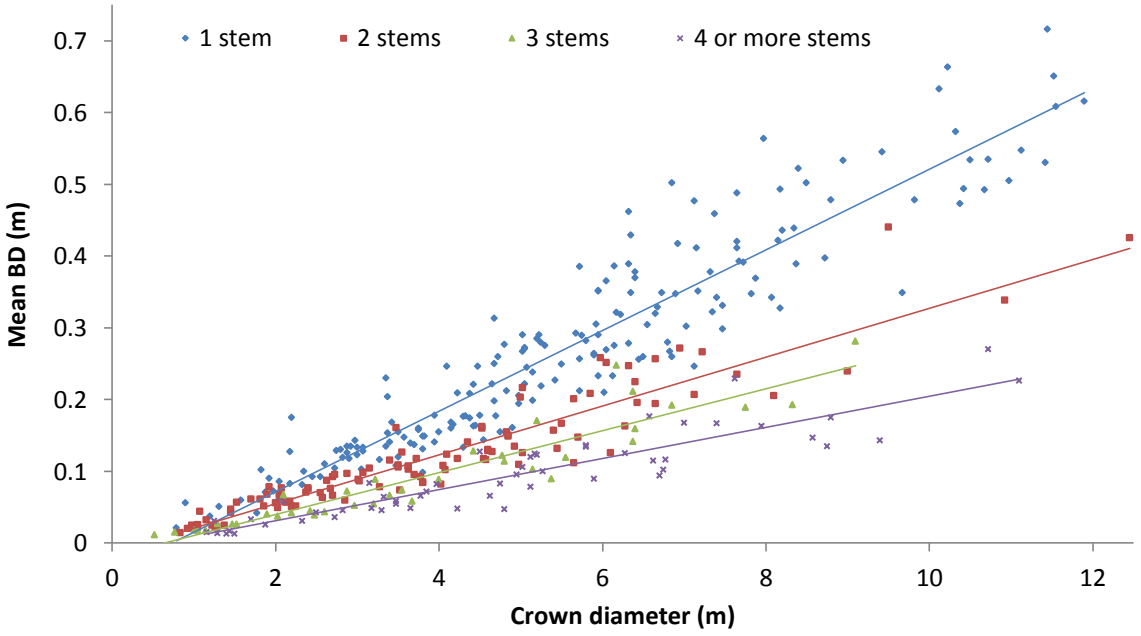

FIGURE 23: MEAN BASAL DIAMETER (m) IN FUNCTION OF CROWN DIAMETER (m)

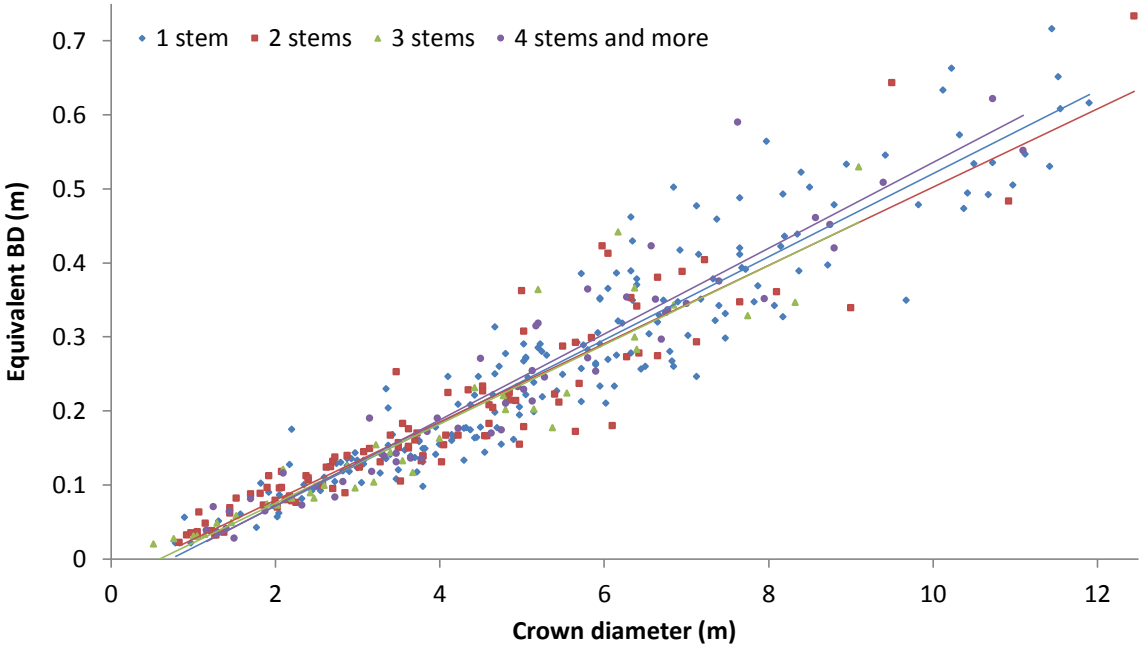

FIGURE 24: EQUIVALENT BASAL DIAMETER (m) IN FUNCTION OF CROWN DIAMETER (m)

As no significant differences were found between the four regressions, we combine the four classes in one class to model the relation between crown diameter and equivalent BD. For accuracy assessment, data is split in a training and test subset, respectively 70 % and 30 % of the data set (mentioned in addendum 4). We use a random number generator to split the 390 tree individuals in 269 trees for training and 121 trees for testing the models. Both sets will remain the same for all further analyses as well, unless otherwise explicitly mentioned. We use the Root Mean Square Error (RMSE) and Mean Absolute Percentage Error (MAPE) as accuracy assessment tools.

$$RMSE = \sqrt{\frac{\sum_{i=1}^{n}(f(x_i) - y_i)^2}{n}}$$

$$MAPE = \frac{1}{n}\sum_{i=1}^{n}\left|\frac{f(x_i) - y_i}{y_i}\right|$$

with $f(x_i)$ = estimated value
y_i = actual value
n = number of test data points

Equivalent diameter modeled in function of crown diameter, yields the following equation, with a R^2 of 0.90:

$$Equivalent\ BD\ (m) = 0.0543 \times crown\ diameter\ (m) - 0.0321 \qquad \text{(Figure 24)}$$

The RMSE and MAPE have values of respectively 0.070 m and 17.4 %. We notice an increasing variance, with increasing crown diameter.

The same analysis strategy was used for bole diameter at breast height. For the mean DBH, the different classes were less distinctive. Equivalent DBH in function of crown diameter for the different classes shows three overlapping point clouds with no significant differences in regression slopes, hence the data are combined again yielding the following model (R^2 = 0.92, RMSE = 0.038 m and MAPE = 18.2 %):

$$Equivalent\ DBH\ (m) = 0.0551 \times crown\ diameter\ (m) - 0.0678 \qquad \text{(Figure 25)}$$

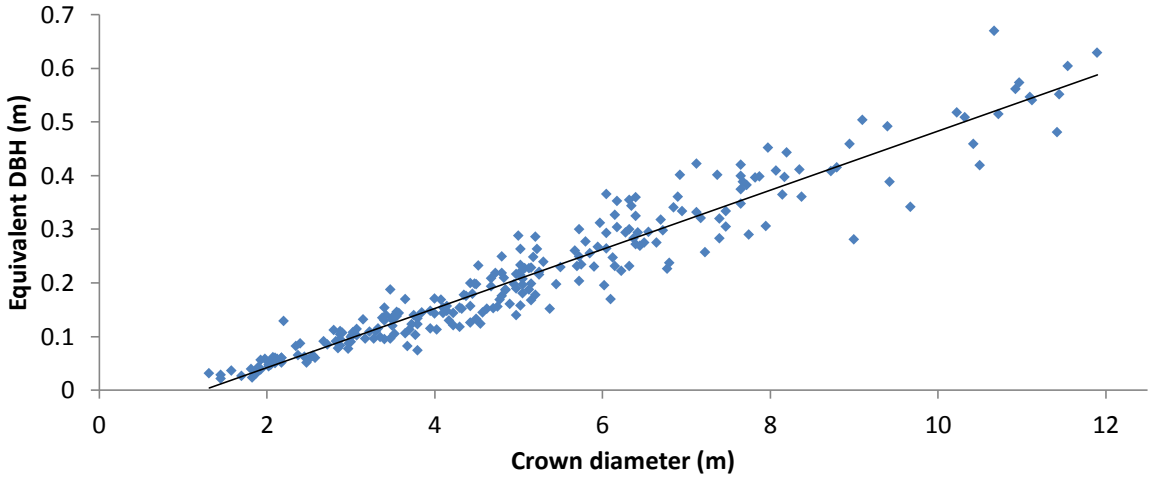

FIGURE 25: EQUIVALENT DIAMETER AT BREAST HEIGHT (m) IN FUNCTION OF CROWN DIAMETER (m)

ii Estimating volume from crown diameter

A strong relation also exists between the estimated volume from base to 1.30 m above the ground and crown diameter. It results in a model with a R^2 of 0.93, with a RMSE and MAPE of respectively 45.989 dm^3 and 31.7 %.

$$Volume\ (dm^3) = 0.8319 \times crown\ diameter\ (m)^{2.503} \qquad \text{(Figure 26)}$$

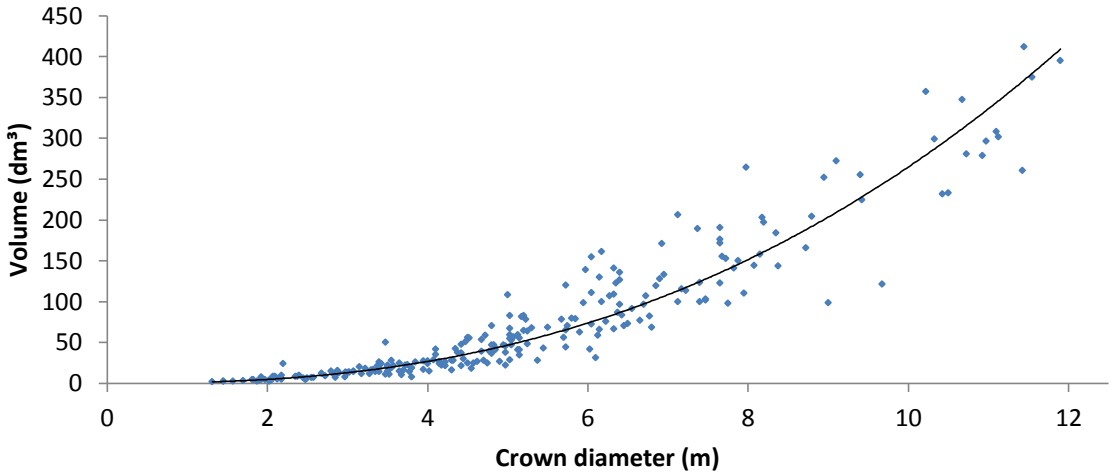

FIGURE 26: VOLUME (dm³) IN FUNCTION OF CROWN DIAMETER (m)

iii Estimating tree height from crown diameter

Although *Acacia raddiana* does not feature marked height development, a good relation is found between crown diameter and total tree height. The resulting model has a R^2 of 0.86, RMSE of 0.770 m and MAPE of 15.7 %. In Figure 27, an increasing variance with increasing crown diameter is noticed. The relation between crown diameter and tree height follows a ¾ power law.

$$Tree\ Height\ (m) = 1.1332 \times crown\ diameter\ (m)^{0.7439} \qquad \text{(Figure 27)}$$

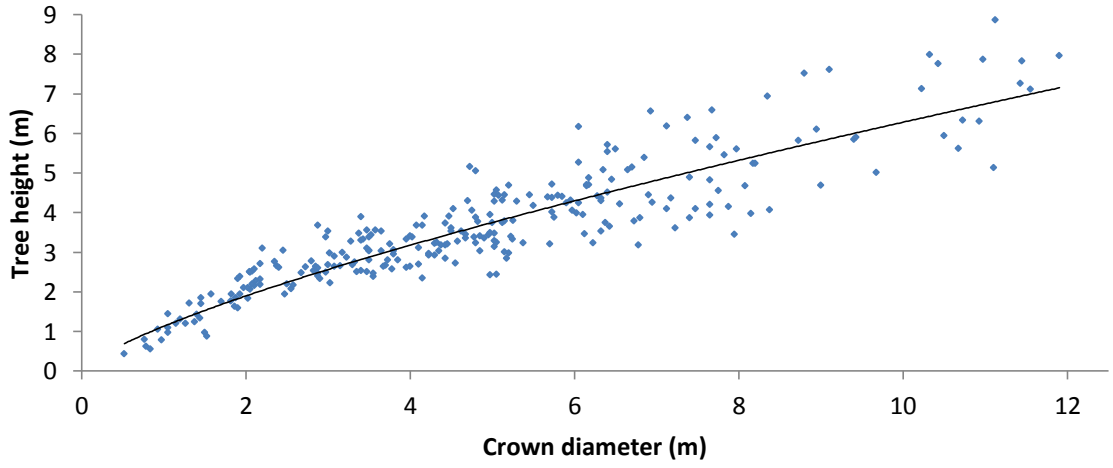

FIGURE 27: TREE HEIGHT (m) IN FUNCTION OF CROWN DIAMETER (m)

iv Estimating equivalent DBH from equivalent BD

Diameter at breast height is very hard to determine for *Acacia raddiana* as lots of stems have to be measured. The density of the branches (with spines) makes it very difficult to measure trees at breast height. Rarely only one stem was present at breast height: of the 390 tree individuals only 12 had a single stem at breast height. Basal diameter is much easier and faster to measure. However during field survey both diameters were measured. Correlation between the equivalent basal diameter and equivalent diameter at breast height is strong, which is of course not surprising. It however means that by measuring the basal diameter, we can estimate the equivalent diameter at breast height with relative high accuracy as the resulting linear relation has a R^2 of 0.94, RMSE of 0.0578 m and MAPE of 17.3 %. A linear model is used, based on the scatter plot (Figure 28). Moreover in literature, the relation between stump diameter and DBH is found to be linear (Ozcelik et al., 2010; Shrivastava & Singh, 2003).

$$Equivalent\ DBH\ (m) = 0.9401 \times Equivalent\ BD\ (m) - 0.0167 \qquad \text{(Figure 28)}$$

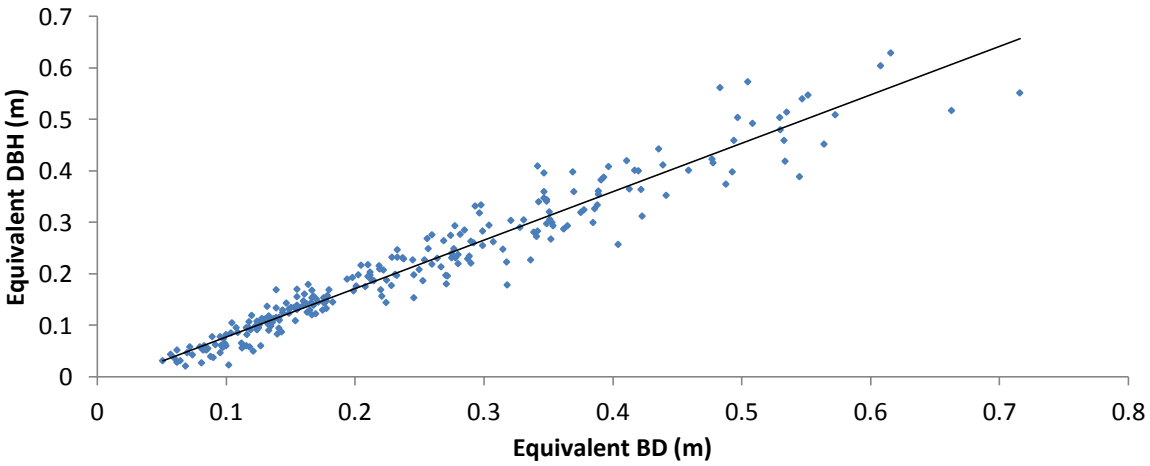

FIGURE 28: EQUIVALENT DIAMETER AT BREAST HEIGHT (m) IN FUNCTION OF EQUIVALENT BASAL DIAMETER (m)

v Estimating volume from equivalent BD

Based on the created model between equivalent DBH and equivalent BD, the equation to calculate the volume can be adapted, resulting in volume estimation, with only BD as argument with d_b, d_0 in m and v in m^3. Analogue analysis could result in a model to estimate volume in function of DBH, which is however harder to measure.

$$\begin{cases} v = \frac{\pi}{4} h \left(\frac{d_0^2 + d_0 d_b + d_b^2}{3} \right) \\ d_b = 0.9401 \times d_0 - 0.0167 \end{cases}$$

$$v = 0.9611 d_0^2 - 0.0164 d_0 + 9.4917 \times 10^{-5}$$

vi Estimating tree height from bole diameter (height-diameter curve)

Correlation between tree height and equivalent BD/equivalent DBH is also present. We use the *Näsland formula* to fit the height-diameter curve, yielding following equation (R^2=0.86, RMSE=0.8964 m and MAPE=15.4 %):

$$Tree\ height\ (m) = 1.30 + \frac{Equivalent\ BD\ (m)^2}{(72.4541 + 0.3178 \times Equivalent\ BD\ (m))^2} \quad \text{(Figure 29)}$$

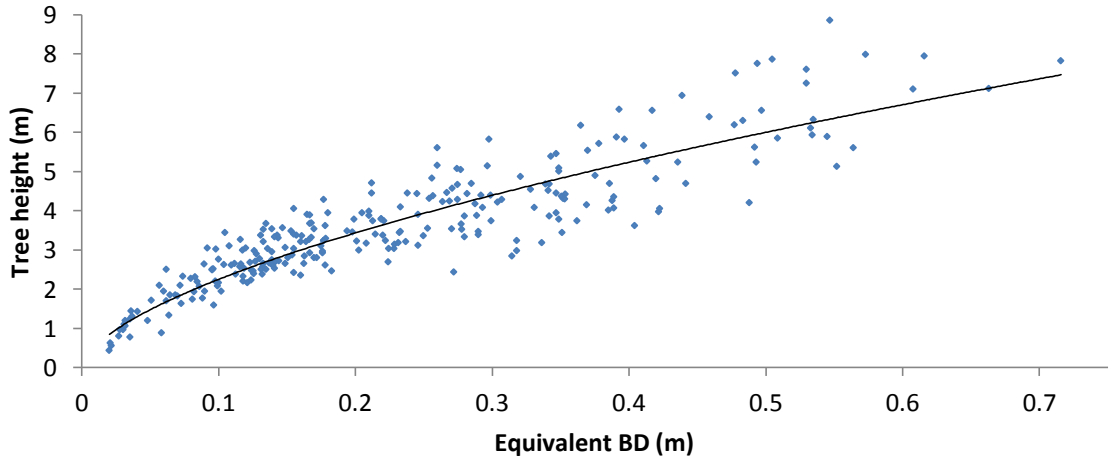

FIGURE 29: TREE HEIGHT (m) IN FUNCTION OF EQUIVALENT BASAL DIAMETER (m)

b *RELATIONS WITH CALCULATED IMAGE OBJECT FEATURES*

If tree attributes are to be estimated from features derived from the GeoEye-1 image at the object level, models have to be empirically built based on field measurements. As segmentation errors occur, especially for trees smaller than 3.5 m, those segments are eliminated from the dataset before modeling. After elimination, 344 trees (scattered over the entire study area) remained in the dataset. This dataset is randomly divided in a training and test set, respectively 226 and 118 data points (different from the points considered in the previous section). More than 200 features are thereafter extracted from the *Acacia* objects for both the training and test set (e.g. elliptic fit, number of pixels, texture measures after Haralick (1973)). For each of these features, correlations are calculated with measured tree attributes.

Based on the computed object features, we first tried to discriminate between tree groups and tree individuals. As only 39 tree groups are present in the dataset, no test set is used for this part of the analysis. Low correlations are found between the Boolean variable *group* and the calculated object features. Decision tree analysis is used to distinguish between tree groups and tree individuals. However, no satisfying results are found as only 19 of 39 tree groups are successfully identified. Hence, none of the extracted features could be considered meaningful for the discrimination between tree groups and individuals. We therefore only consider tree individuals in the subsequent analysis.

i Crown diameter estimation

A high correlation is found between the crown diameter (CD) and the feature *area* of the *Acacia* segments, which is calculated as the number of pixels. Based on the theoretic relation between crown area and crown diameter, a power function is fitted through the training data points (Figure 30). The regression results in a model, with a R^2 of 0.64, RMSE of 1.67 m and MAPE of 21.6 %.

$$CD\ (m) = 0.9095 \times area(pixels)^{0.4183} \qquad \text{(Figure 30)}$$

Additionally, the correlation dataset also reveals a strong relationship between the feature *area* and *GLCM entropy layer 4 (90°)* (with layer 4 being the NIR band and 90° the horizontal direction for calculation based on GLCM (Haralick et al., 1973)). The

observed relationship is exponential (Figure 31). Regression results in a model, with a R^2 equal to 0.96 and a RMSE of 14.7 pixels (MAPE of 13.0 %).

$$area(pixels) = 1.8367 \times e^{1.2718 \times GLCM\ Entropy\ Layer\ 4\ (90°)} \qquad \text{(Figure 31)}$$

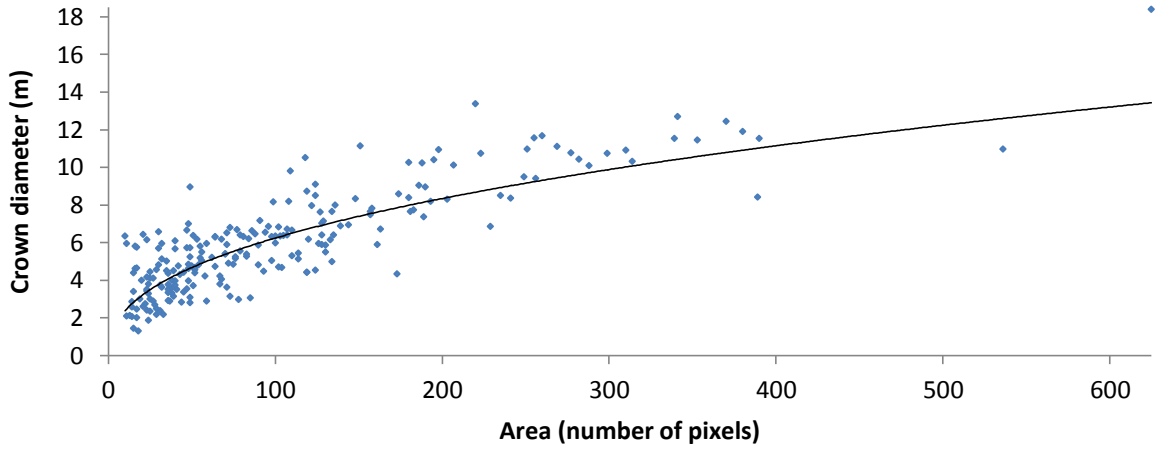

FIGURE 30: ESTIMATION OF CROWN DIAMETER (m) USING THE AREA FEATURE

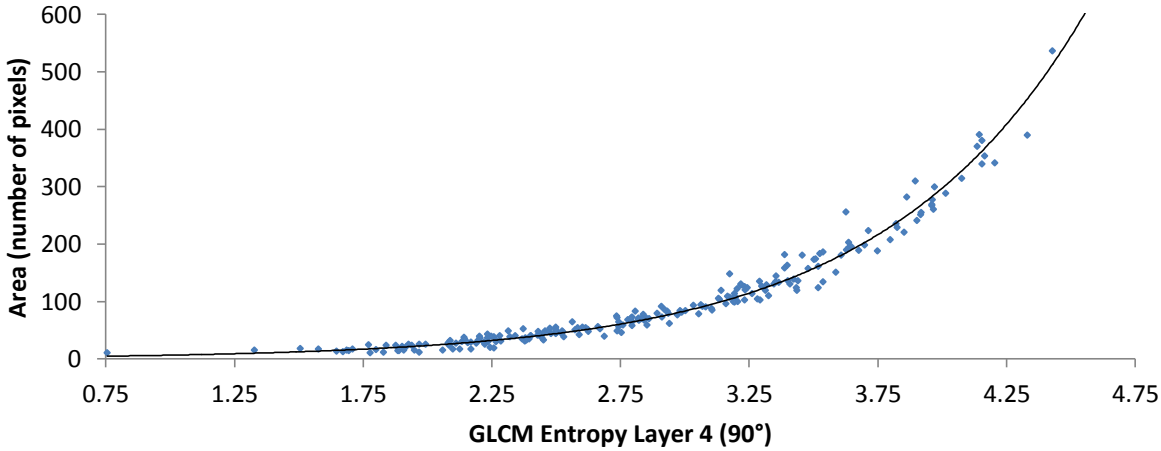

FIGURE 31: RELATION BETWEEN GLCM ENTROPY LAYER 4 (90°) AND AREA

As both models feature acceptable RMSE and MAPE values (considering a typical forest inventory error of 15 % to 20 %), both equations are combined to build a model, directly predicting crown diameter based on *GLCM Entropy Layer 4 (90°)* (Figure 32). The RMSE between predicted and measured crown diameter is 1.61 m (MAPE of 22.0 %, R^2=0.58).

$$CD\ (m) = 1.1758 \times e^{0.5320 \times GLCM\ Entropy\ Layer\ 4\ (90°)} \qquad \text{(Figure 32)}$$

When crown diameter classes for the test set are visualized in a histogram (Figure 33), derived diameter classes through our models show acceptable results. An overestimation (> 50 % overestimation) of crown diameter class]4,6] is however

observed for both models. Furthermore, larger crown diameter classes are underestimated.

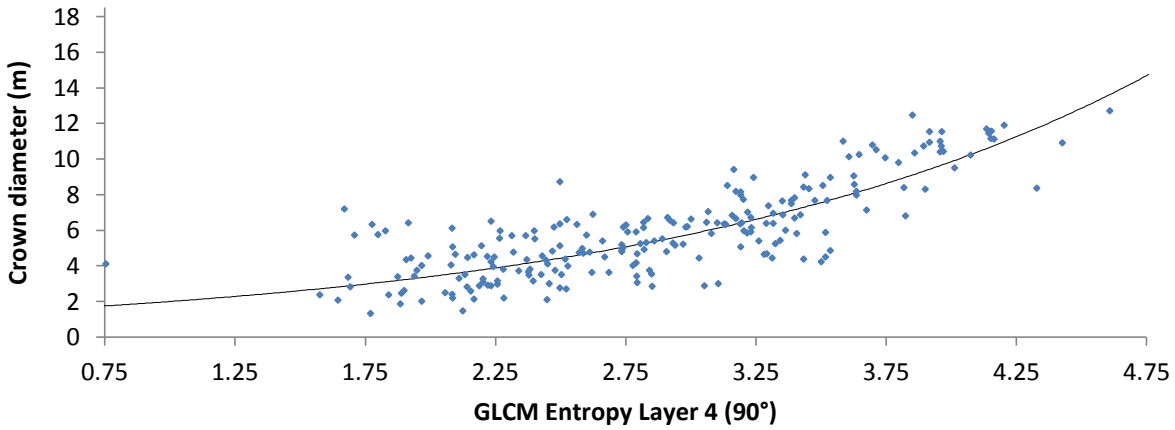

FIGURE 32: ESTIMATION OF CROWN DIAMETER (m) USING THE GLCM ENTROPY LAYER 4 (90°) FEATURE

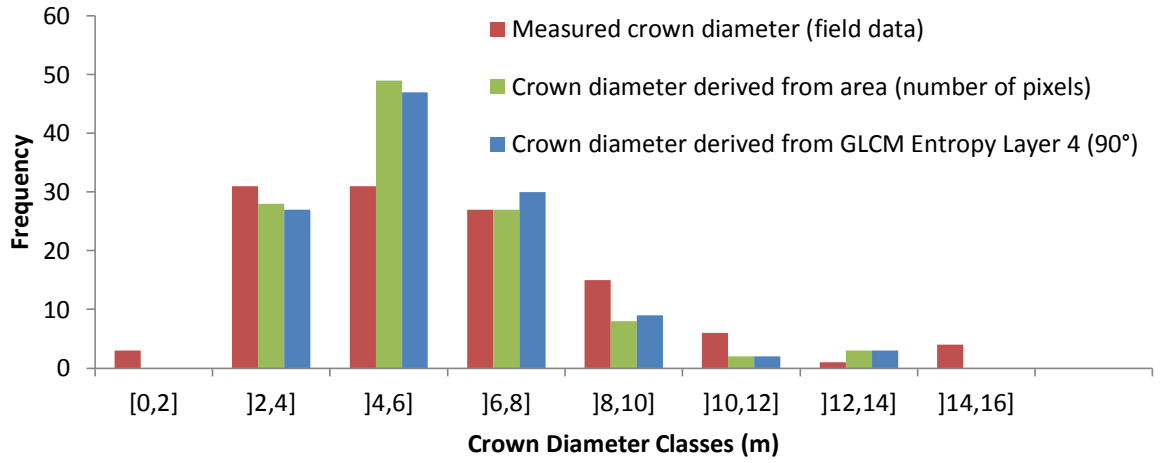

FIGURE 33: MEASURED VERSUS DERIVED CROWN DIAMETER CLASSES (m)

ii Tree height estimation

When focusing on tree height, the correlation dataset shows a high correlation between tree height and the features *area* and *GLCM Entropy Layer 4 (90°)*. Considering the high correlation between both features, analogous reasoning leads to a model for the estimation of tree height through the entropy feature (Figure 34). A RMSE value of 0.92 m was found, with a MAPE of 20 % and a R^2 of 0.58. Comparison of derived versus measured three heights shows good resemblance. Smaller tree heights were however not detected with our model (Figure 35).

$$Tree\ height\ (m) = 1.3822 \times e^{0.3689 \times GLCM\ entropy\ layer\ 4\ (90°)}$$ (Figure 34)

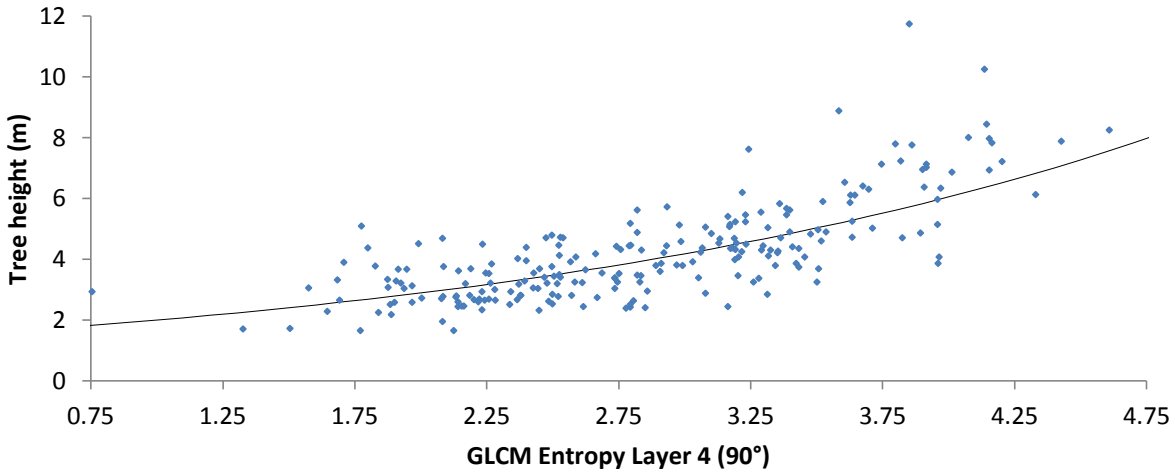

FIGURE 34: ESTIMATION OF TREE HEIGHT (m) USING THE GLCM ENTROPY LAYER 4 (90°) FEATURE

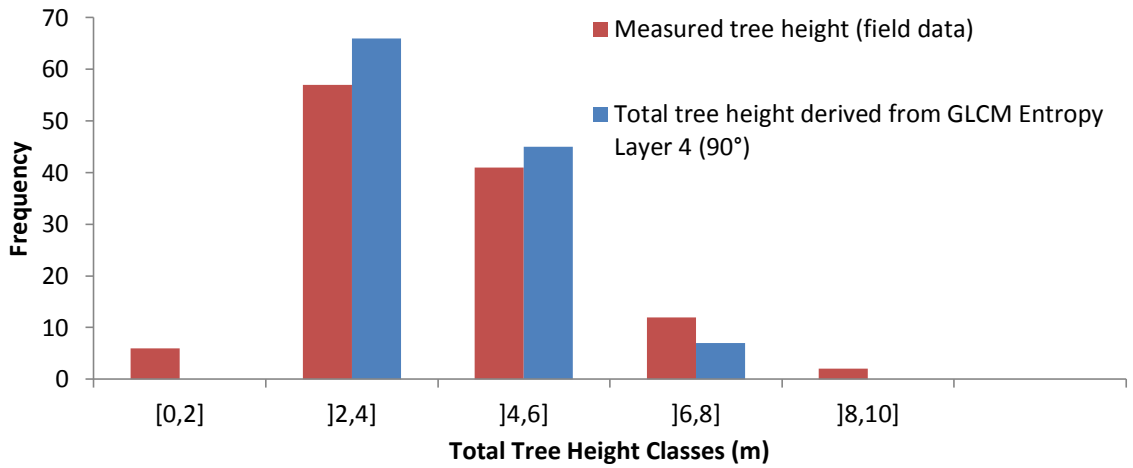

FIGURE 35: MEASURED VERSUS DERIVED TREE HEIGHT CLASSES (m)

iii Bole diameter estimation

Similar reasoning leads to equations to estimate bole diameter, based on calculated features. Once again high correlation is found for the feature *area*. Using the relation between *area* and *GLCM Entropy Layer 4 (90°)*, models are created to estimate BD and DBH through the entropy feature. For BD, the model results in a RMSE of 0.099 m, MAPE of 32.6 % and a $R^2$of 0.63. For DBH, RMSE was lower (0.087 m), MAPE was 48.7 % and R^2=0.63.

$$Equivalent\ BD\ (m) = 0.0406 \times e^{0.6472 \times GLCM\ Entropy\ Layer\ 4\ (90°)} \quad \text{(Figure 36)}$$

$$Equivalent\ DBH\ (m) = 0.0276 \times e^{0.7249 \times GLCM\ Entropy\ Layer\ 4\ (90°)} \quad \text{(Figure 37)}$$

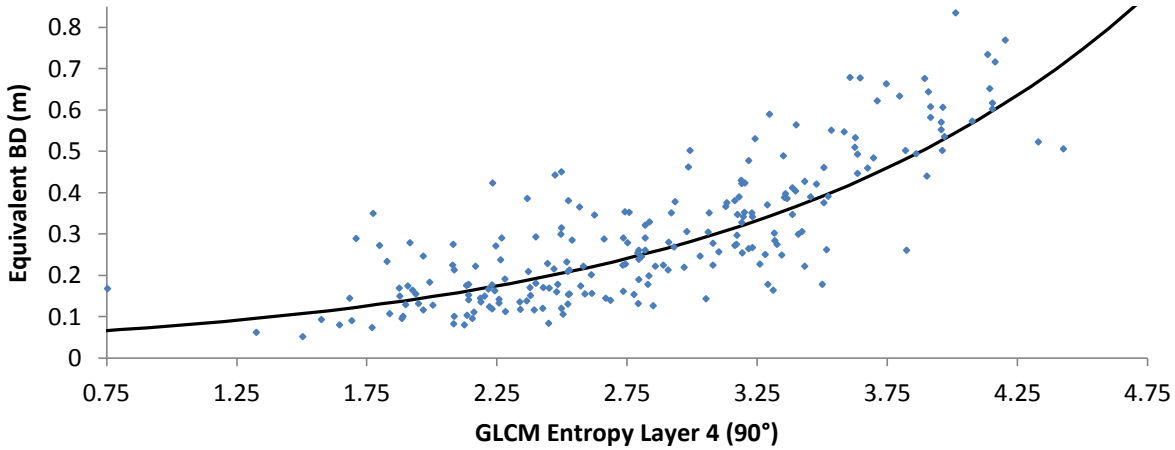

FIGURE 36: ESTIMATION OF EQUIVALENT BASAL DIAMETER (m) THROUGH GLCM ENTROPY LAYER 4 (90°)

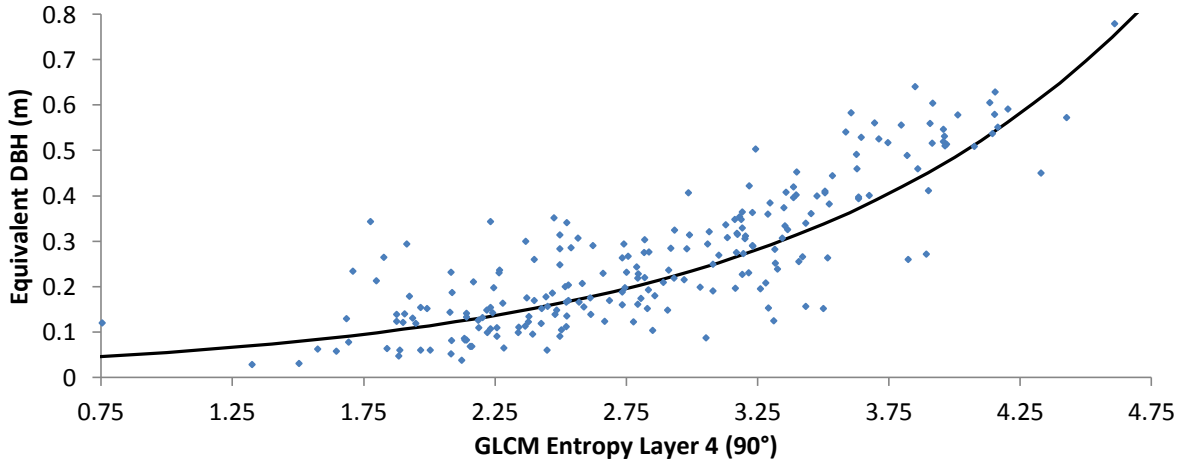

FIGURE 37: ESTIMATION OF EQUIVALENT DIAMETER AT BREAST HEIGHT (M) THROUGH GLCM ENTROPY LAYER 4 (90°)

4 STRUCTURE OF BOU-HEDMA NATIONAL PARK

The terminology *Acacia* forest steppe was for the first time used in Tunisia by Doûmet-Adanson in 1874, describing the *Acacia raddiana* forest of Bled Talah. Nowadays it is used to designate preforest formations in arid zones (Zaafouri et al., 1996). The forest steppe of Bou-Hedma, suffered for over a century from overexploitation of natural resources by an intensification of agricultural activities. Through reforestation and protection programs, the original vegetation is gradually restored. Characteristics of the original forest steppe, described between 1900 and 1925 by different explorers are listed in Table 16.

TABLE 16: CHARACTERISTICS OF THE ORIGINAL FOREST STEPPE IN BOU-HEDMA, DESCRIBED BETWEEN 1900 AND 1925 (Zaafouri et al., 1996)

Attribute	Value
Total tree height	9 to 10 m (maximum 10 m)
Trunk height	3 to 4 m at most
Mean basal diameter	15 to 20 cm
Basal diameter of biggest trees	2,3 to 3 m
Density	4 to 25 trees/ha

A forest is characterized by its origin (seeds or vegetative), its structure (arrangement of ages or diameters), its height and its density (Zaafouri et al., 1996).

a ORIGIN

The origin of the forest remains doubtful (Zaafouri et al., 1996): there are claims from the local population that the species was introduced in Tunisia through faeces of camels at the beginning of the 11th century. Some scientists consider the forest as a tropical relict (Lavauden, 1927), while others consider the introduction of *A. raddiana* from Ghdamès (Zaafouri et al., 1996). Other authors think that *A. raddiana* is not native of Tunisian steppe zones but originates in Southern Africa, with a centre of diversification in Northern Africa (Ouarda, et al. 2009). As a part of protection and restoration programs, reforestation actions were undertaken (in the integral protection zone 1) in 1963, 1966/67, 1994/1995/1996 and 2000/2001 (Hamdi, personal communication; Wahbi, 2006). The population of Bled Talah also shows natural regeneration, albeit very limited in the protection zone. The forest is considered natural. Many factors have been discussed to explain the low level of regeneration of the *A. raddiana* tree. First, the semi-parasitic mistletoe *Loranthus acacia* is suspected to cause drying and mortality of *Acacia*

trees (Noumi et al., 2010). Secondly *A. raddiana* trees suffer from extraordinarily high infestation of seed beetles (mostly Bruchidae, *Bruchidius raddianae* and *Caryedon palaestinicus*) (Grouzis & Le Floc'h, 2003). Moreover, the protection of the Bou-Hedma National Park from browsing, which may cause disturbance and trampling of the soil, favours the development of surface pellicle in the soil, which inhibits seeds germination because water cannot infiltrate in the ground (Noumi et al., 2010). Hence, recruitment might be seriously limited when no action of animals (such as browsing) is present. This low regeneration of *Acacia* seeds in protected areas raises a real problem, not only in Tunisia, but also in other regions of the world (Noumi et al., 2010).

b STRUCTURE

We know that the forest steppe population in Bou-Hedma National Park has an uneven-aged structure (all ages and bole diameters are present). During the classification process 21,912 segments were classified as *Acacia*. These segments do not necessarily represent individual trees, as tree groups are also included. There are approximately 27,000 tree individuals in Bou-Hedma National Park (Noumi, personal communication). The underestimation of trees is caused by the fact we could not split tree groups in tree individuals and the bad segmentation of smaller tree crowns. No reliable distinction was found to discriminate between individuals and tree groups. Hence results will be biased, but this strategy can be justified as groups are only a limited fraction of the total population (approximately 10%, based on our random sampling). Moreover, we expect this bias to be visible for larger tree crown diameters, as tree groups generally have a larger crown diameter.

The distribution of crown diameters derived from the GeoEye-1 image, shows a clear presence of crown diameter classes 3 to 4 and 4 to 5 m (Figure 38). An exponential decrease is present for larger crown diameters. Smaller crown diameter classes seem to be less present. This is in accordance with field observations, however it is probable that smaller trees are not all detected by the segmentation or the classification algorithms, especially for crown diameter class 0 to 2 m. Moreover this structure is highly influenced by reforestation actions, which were undertaken in 1963, 1966/1967, 1995/1996 and 2001 (Hamdi, personal communication). Unfortunately, no exact data is available on their number or location.

In Figure 39, the distribution of equivalent BD classes is illustrated. Equivalent BD was estimated directly from *GLCM Entropy Layer 4 (90°)*, from CD through *GLCM Entropy Layer 4 (90°)* and from CD through *area*. The distribution of BD classes also shows exponential behavior for the three methods, validating the uneven-aged forest structure. Zaafouri et al. (1996) found similar results for a population in Haddej (an integral protection zone, part of the same Biosphere Reserve), based on field measurements. The same researchers also found an irregular structure for the population outside the protection zone. The resulting structure in Bou-Hedma National Park is caused by the elimination of external pressure (mainly anthropogenic). However natural regeneration remains scarce. Only two seedlings were found during field survey. Noumi et al. (2010) only found two seedlings beneath 300 adult trees of *A. raddiana* in protected zones in one year. Though, for size class distribution of *Acacia raddiana* in different plant communities, Noumi et al. (2010) found the class with bole diameter between 0 and 10 cm to be the largest class.

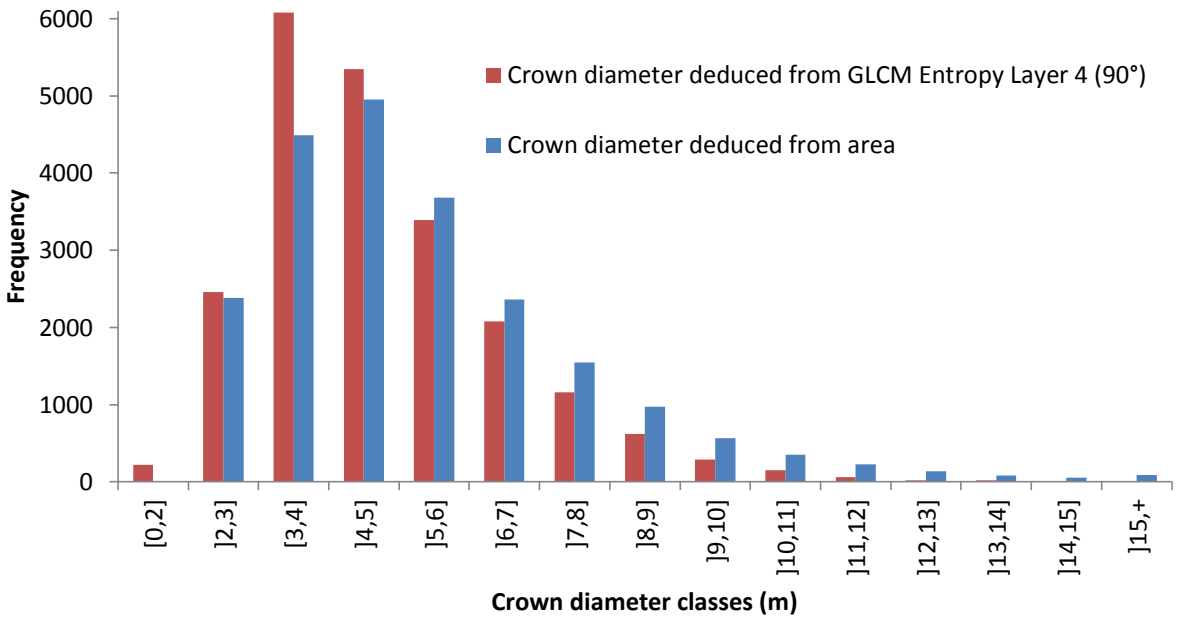

FIGURE 38: DISTRIBUTION OF CROWN DIAMETER CLASSES (m) IN BOU-HEDMA NATIONAL PARK

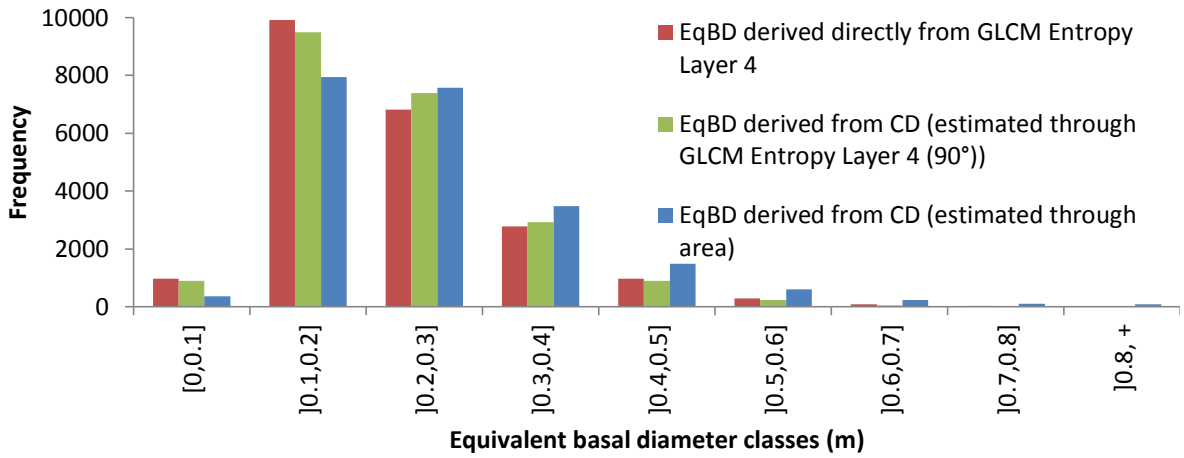

FIGURE 39: DISTRIBUTION OF EQUIVALENT BASAL DIAMETER CLASSES (m) IN BOU-HEDMA NATIONAL PARK

c HEIGHT

Tree height was also determined using three methods (directly from GLCM Entropy Layer 4 (90°) and from derived crown diameter). The distribution of tree height classes estimated from the GeoEye-1 image is shown in Figure 40. A good resemblance is found between tree height directly estimated through the entropy feature and tree height derived from estimated crown diameter. As crown diameter estimated through GLCM Entropy Layer 4 (90°) and area are similar, tree height estimation is also similar for both methods.

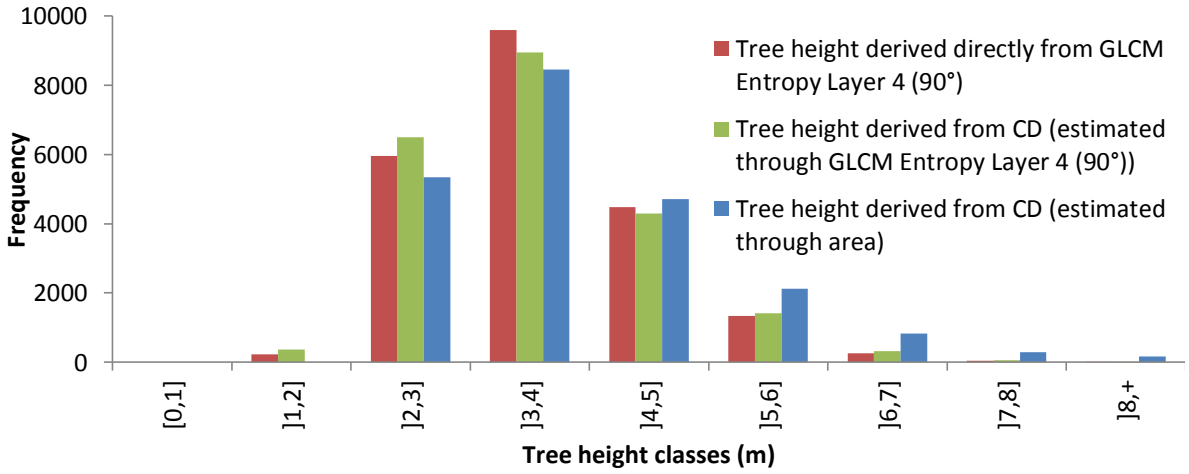

FIGURE 40: DISTRIBUTION OF TREE HEIGHT CLASSES (m) IN BOU-HEDMA NATIONAL PARK

d DENSITY

Density can be determined by calculating the number of trees per hectare. We use a kernel of 1 hectare (200×200 pixels, 0.5 m resolution) to determine tree density. A total of 2,596 non-overlapping kernels were used. In order to exclude border effects, kernels stayed 100 pixels (50 m) from the limits of the park. In 760 of the hectare plots, no trees were present. We find a mean density of 8.4 trees per ha for the entire national park, with a median value of 5.0 trees per ha. A maximum density of 95 trees per hectare was found, which can be found in dense plantations close to the *Bordj*. These values are in accordance with forest density values mentioned in Table 16.

We did not consider different zones in our analysis. However structure was found to be significantly different between the *glacis* and the *sandy plain* by Noumi et al. (2010). The differences were mainly due to variations in soil water availability and the pressure of anthropogenic disturbances such as browsing.

CONCLUSIONS

The major objective of this MSc. thesis was to assess the amount of *Acacia raddiana* in Bou-Hedma National Park and estimation of crown diameter classes. As we collected a large amount of field data, these were compiled in a relational database. Next, dendrometric and ancillary data were statistically analyzed. We found no directional variation in crown diameter between the N-S and the E-W orientation; hence the arithmetical mean was calculated and used for further processing.

Significant differences in tree attributes were found between tree individuals and tree groups, with higher values for tree groups. However the majority of the plantations are linear formations, while groups are likely to be relicts of the ancient forest. Hence, the resulting differences between tree groups and tree individuals might be caused by an age factor.

Comparing the frequency of the different erosion crust classes, under and outside tree canopy, revealed that the percentage erosion crust under the tree canopy was limited (in most cases between 0 % and 10 %). In the buffer zone, larger percentage values were found, with a percentage cover of 25-50 % as largest group. When splitting the dataset based on the presence of animal faeces, significant differences were found for all tree attributes, indicating a clear preference of the herbivorous fauna.

A hypothesis formulated by Mihidjay (1999), stated that young *Acacia raddiana* individuals are multi-stemmed from the base and that from a certain age, one of the axes becomes the trunk while others are inhibited. We tested this hypothesis with our measurements. The dataset was split in classes: trees with one stem, two stems, three stems and four stems and more. We then used ANOVA, followed by a comparison of means (Tukey method). Significant differences were found between tree attributes of the different classes. However differences were not consistent for all tree attributes. Hence, we cannot confirm nor reject the hypothesis of Mihidjay (1999).

In a next stage, allometric equations were modeled. These allometric equations make it possible to determine hard to measure or time-consuming measurements to be estimated through easy to measure tree attributes. These models are also useful in the image processing stage, to estimate tree attributes through crown diameter. Hence we modeled equivalent basal diameter, equivalent diameter at breast height, volume and tree height in function of crown diameter. Mean absolute percentage errors were lower than 30 %, except for volume estimation through crown diameter. We also modeled a relationship between equivalent DBH and equivalent BD (MAPE < 30 %), making it possible to estimate volume directly from basal diameter. Finally, a height-diameter curve was modeled, also resulting in MAPE lower than 30 %.

In order to estimate the amount of *Acacia*'s, a Geographic Object-Based Image Analysis (GEOBIA) working strategy was used. Two subsequent segmentation algorithms were used: *multiresolution segmentation* and *contrast split segmentation*. Parameters were determined by trial and error. Best segmentation results were acquired by solely using the panchromatic band (mainly driven by its more suitable spatial resolution in the context of individual tree delineation). Both large trees and small trees were correctly segmented. However some trees that were manually delineated, were not detected by the segmentation procedure. For the resulting segments, > 200 object features were calculated. Based on correlations between object features and tree attributes, relations were modeled to estimate crown diameter with the *area* (number of pixels) feature and the *GLCM Entropy* feature. In analogy, we also modeled tree height and equivalent basal diameter in function of the *GLCM Entropy* feature.

Next, optimal features for image classification were determined, based on ground truth measurements. Initially, only the panchromatic band was used for classification. However, low separation distances between classes were found. When multispectral wavebands were added, separation distance increased, emphasizing the importance of multispectral wavebands to discriminate between different tree species (*Eucalyptus* sp., *Acacia* sp.) and soil segments. Satisfying classification results were obtained (KIA based on samples of 0.96), correctly classifying *Eucalyptus* sp., *Acacia* sp. and soil polygons. Classification results were then used to determine the structure of the population in Bou-Hedma National Park. In total 21,912 segments

were classified as *Acacia*. Our results indicate an uneven-aged forest structure, with a lack of small individuals. Reasons for the lack of small individuals are limited natural regeneration and no visual detection of small individuals. Density was determined by simply counting the number of *Acacia*'s (both groups and individuals) per ha. A mean density of 8.4 trees per ha was found, in line with the historical density of the forest (4 to 25 trees/ha).

The optimal time of image acquisition could not be quantitatively determined, as no data are available on the seasonal evolution of the vegetation. Moreover, the contribution of soil characteristics to enhance results could not be researched, as no detailed soil map is available. Tree crown density was determined by using unsupervised classification algorithms. However this did not yield satisfying results as correlations with other tree attributes were low. Moreover, efficiency of the applied method was low, as the image processing demanded manual checking of each classified image.

A number of research issues need to be elaborated in the future. The image processing procedure could be optimized by efficient sampling for the Nearest Neighbour classification procedure. More specifically, number of iterations might be reduced by intensive sampling in a limited number of regions (instead of random sampling over the entire study area). Moreover, the classification procedure could be performed using other algorithms (such as Artificial Neural Networks) outside eCognition.

We determined the structure of the population in Bou-Hedma National Park, by using high resolution satellite imagery. Moreover all trees have been measured by a Tunisian PhD student in an intensive field campaign (Noumi, personal communication). Hence, comparison between both the intensive field campaign and the (semi-)automated image processing procedure could give a validation of our results, if the above mentioned data would become available.

As data concerning the evolution of the vegetation over the different seasons, was lacking, it could be interesting to permanently survey plots in the field. Together with data on tree phenology, this could provide a quantitative answer which time of acquisition is optimal to estimate amount of *Acacia*'s and their attributes.

REFERENCES

Abdallah, L., Chaïeb, M. & Zaafouri, M.S. (1999) Phénologie et comportement in situ d'*Acacia tortilis* subsp. r*addiana*. *Revue des régions arides*, 11(1/99), 60-69.

Abdallah, F., Noumi, Z., Touzard, B., Belgacem, A.O., Neffati, M. & Chaieb, M. (2008) The influence of *Acacia tortilis* (Forssk.) subsp. *raddiana* (Savi) and livestock grazing on grass species composition, yield and soil nutrients in and environments of South Tunisia. *Flora,* 203**,** 116-125.

Abdelkebir, H. (2005) Elaboration de la carte des aménagements CES et de lutte contre l'ensablement dans l'observatoire de Haddej Bou Hedma par la technique de SIG. Thesis, Université de Jendouba, Ecole Supérieure des Ingénieurs de l'Equipement Rural de Medjez-El-Bab, 83 p.

AbdElRahman, H.F. & Krzywinski, K. (2008) Environmental effects on morphology of *Acacia tortilis* group in the red Sea Hills, North-Eastern Sudan and South-Eastern Egypt. *Forest Ecology and Management*, 255, 254-263.

Archibald, S. & Bond, W. J. (2003) Growing tall vs growing wide: tree architecture and allometry of *Acacia karroo* in forest, savanna, and arid environments. *Oikos,* 102, 3-14.

Bagnouls, F. & Gaussen, H. (1953) Saison sèche et indice xérothermique. *Bull. Soc. Hist. Nat.* Toulouse, 88, 193–239.

Benz, U.C., Hofmann, P., Willhauck, G., Lingenfelder, I. & Heynen, M. (2004) Multi-resolution, object-oriented fuzzy analysis of remote sensing data for GIS-ready information. *ISPRS Journal of Photogrammetry and Remote Sensing,* 58**,** 239-258.

Blaschke, T., Lang, S. & Hay, G.J (2008) Object-Based Image Analysis. Spatial concepts for knowledge-driven remote sensing applications. Berling Heidelberg: Springer-Verlag, 801 p.

Boukchina, R., Ouled Belgacem, A., Taamallah, H., Ouessar, M., Dhaoui, M. & Selmi, S. (2006) Surveillance biophysique dans l'observatoire de Haddej Bou Hedma – Tunisie. Institut des Régions Arides, Médenine, Tunisia, 145 p.

Brack, C.L. (1999) Forest Measurement and Modeling - Measuring trees, stands and forests for effective forest management. http://sres-associated.anu.edu.au/mensuration/ (consulted February 25, 2010).

Brenan, J.P.M. (1983) Manual on taxonomy of *Acacia* species. Present taxonomy of four species of *Acacia* (*A. albida, A. senegal, A. nilotica, A. tortilis).* Rome: FAO, 47 p.

Bunting, P. & Lucas, R. (2006) The delineation of tree crowns in Australian mixed species forests using hyperspectral Compact Airborne Spectrographic Imager (CASI) data. *Remote Sensing of Environment,* 101**,** 230-248.

Caron, S. (2001) Suivi écologique de l'Oryx algazelle (*Oryx dammah*) dans le parc National de Bou-Hedma (Tunisie) et notes sur les autres Ongulés sahélo-Sahariens du parc. Travail

de fin d'étude en vue de l'obtention du grade académique de Diplôme d'Etudes Supérieures Specialisées. Université des Sciences et Technologies de Lille (France).

Chen, X.X., Vierling, L., Rowell, E. & DeFelice, T. (2004) Using lidar and effective LAI data to evaluate IKONOS and Landsat 7 ETM+ vegetation cover estimates in a ponderosa pine forest. *Remote Sensing of Environment,* 91**,** 14-26.

Chubey, M.S., Franklin, S.E. & Wulder, M.A. (2006) Object-based analysis of Ikonos-2 imagery for extraction of forest inventory parameters. *Photogrammetric Engineering and Remote Sensing,* 72**,** 383-394.

Day, J.H. (1983) Expert Committee on Soil Survey. Manual for describing soils in the field. Ottawa, Ontario, The Canada Soil Information System (CanSIS), 97 p.

Definiens (2009a) eCognition Developer 8. User Guide. München: Definiens AG.

Definiens (2009b) eCognition Developer 8. Reference Book. München: Definiens AG.

Diouf, M. & Zaafouri, M. (2003) Phénologie comparée d'*Acacia raddiana* au nord et au sud du Sahara. In : Grouzis, M. & Le Floc'h, E. (2003) éd. *Un arbre au désert*. *Acacia raddiana.* Paris : IRD éditions, 103-118.

Dupuy, N., Detrez, C., Neyra, M., De Lajudie, P. & Dreyfus, B. (1991) Les *Acacias* fixateurs d'azote du Sahel. *La Recherche*, 22(233), 802-804.

Eurimage (2009) GeoEye-1: The world's highest resolution commercial satellite. *Eurimage products and service guide, GeoEye-1.* 4 p.

Falkowski, M.J., Wulder, M.A., White, J.C. & Gillis, M.D. (2009) Supporting large-area, sample-based forest inventories with very high spatial resolution satellite imagery. *Progress in Physical Geography,* 33**,** 403-423.

GeoEye (2009) GeoEye-1 Fact Sheet. http://launch.geoeye.com/LaunchSite/about/fact_sheet.aspx (consulted February 25, 2010).

GIM (2009) Technische info – GeoEye-1.http://www.gim.be (consulted December 7, 2009).

Gougeon, F.A. & Leckie, D.G. (2006) The individual tree crown approach applied to Ikonos images of a coniferous plantation area. *Photogrammetric Engineering and Remote Sensing,* 72**,** 1287-1297.

Gowda, J.H., Albrectsen, B.R., Ball, J.P., Sjoberg, M. & Palo, R. T. (2003) Spines as a mechanical defence: the effects of fertiliser treatment on juvenile *Acacia tortilis* plants. *Acta Oecologica-International Journal of Ecology,* 24**,** 1-4.

Greenberg, J.A., Dobrowski, S.Z. & Ustin, S.L. (2005) Shadow allometry: Estimating tree structural parameters using hyperspatial image analysis. *Remote Sensing of Environment,* 97**,** 15-25.

Groesz, F.J. & Kastdalen, L. (2007) Mapping trees and thicket with optical images. Testing the use of high resolution image data for mapping moose winter food resources. *Oppdragsrapport (5),* Hedmark University College, 36 p.

Groh, M.R., Stockman, J.C., Powell, G., Prague, C.N., Irwin, M.R. & Reardon, J. (2007) *Microsoft Office Access 2007 Bible.* Indianapolis: Wiley Publishing, 1356 p.

Grouzis, M. & Le Floc'h, E., éd. (2003) Un arbre au désert, Acacia raddiana. Paris: IRD Editions, 313p.

Hall, F. G., Shimabukuro, Y.E. & Huemmrich, K.F. (1995) Remote-sensing of forest biophysical structure using mixture decomposition and geometric reflectance models. *Ecological Applications,* 5**,** 993-1013.

Haralick, R. M., Shanmuga, K. & Dinstein, I. (1973) Textural features for image classification. IEEE *Transactions on Systems Man and Cybernetics,* SMC3**,** 610-621.

Hay, G.J. & Castilla, G. (2006) Object-based image analysis: Strengths, Weaknesses, Opportunities and Threats (SWOT). 1st International conference on object based image analysis (OBIA 2006), July 4-5, 2006, Salzburg University, Austria.

Hay, G.J. & Castilla, G. (2008) Geographic Object-Based Image Analysis (GEOBIA): A new name for a new discipline In : Blaschke, T., Lang, S. & Hay, G.J. (2009) Object-Based Image Analysis: spatial Concepts for Knowledge-Driven Remote Sensing Applications. Berlin Heidelberg: Springer-Verlag, 75-89.

Hemery, G. E., Savill, P.S. & Pryor, S.N. (2005) Applications of the crown diameter-stem diameter relationship for different species of broadleaved trees. *Forest Ecology and Management,* 215**,** 285-294.

Hirata, Y. (2008) Estimation of stand attributes in *Cryptomeria japonica* and *Chamaecyparis obtusa* stands using QuickBird panchromatic data. *Journal of Forest Research,* 13**,** 147-154.

Hoover C.M. (2008) Field Measurements for Forest Carbon Monitoring. A Landscape-Scale Approach. New York: Springer Science + Business Media B.V.

Intergovernemental Panel on Climate Change (IPCC) (2000) Special report on land use, land use change and forestry. http://www.ipcc.ch/ipccreports/sres/land_use/index.htm (consulted March 7, 2010).

Kane, V.R., Gillespie, A.R., McGaughey, R., Lutz, J.A., Ceder, K. & Franklin, J.F. (2008) Interpretation and topographic compensation of conifer canopy self-shadowing. *Remote Sensing of Environment,* 112**,** 3820-3832.

Karem, A., Ksantini, M., Schoenenberger, A. & Waibel, T. (1993) Contribution à la régénération de la végétation dans les Parcs Nationaux en Tunisie aride. Eschborn: GTZ, 201p.

Karem, A. (2001) Le rôle des parcs nationaux et les réserves naturelles dans la conservation de la biodiversité. *Rev. Régions Arides*, 2001, 293-302.

Katoh, M., Gougeon F.A. & Leckie D. (2009) Application of high-resolution airborne data using individual tree crowns in Japanese conifer plantations. *Journal of Forest Research,* 14**,** 10-19.

Kayitakire, F., Hamel, C. & Defourny, P. (2006) Retrieving forest structure variables based on image texture analysis and IKONOS-2 imagery. *Remote Sensing of Environment,* 102**,** 390-401.

Ketterings, Q.M., Coe, R., van Noordwijk, M., Ambagau, Y. & Palm, C.A. (2001) Reducing uncertainty in the use of allometric biomass equations for predicting above-ground tree biomass in mixed secondary forests. *Forest Ecology and Management*, 146, 199-209.

Kramer, H.J. (2009) GeoEye-1 (OrbView-5). http://directory.eoportal.org/presentations/223/13708.html (consulted April 8, 2010).

Lavauden, L. (1927) Les forêts du Sahara (Extrait de la *Revue des Eaux et Forêts*). *Revue Eaux et Forêts*, Berger-Levrault, Nancy-Paris-Strasbourg, 26 p.

Lavauden, L. (1928) La forêt de gommiers du bled talha (Sud-tunisien). *Revue des Eaux et Forêts*, 66, 699-713.

Leboeuf, A., Beaudoin, A., Fournier, R.A., Guindon, L., Luther, J.E. & Lambert, M.C. (2007) A shadow fraction method for mapping biomass of northern boreal black spruce forests using QuickBird imagery. *Remote Sensing of Environment,* 110**,** 488-500.

Le Floc'h, E. & Grouzis, M. (2003) *Acacia raddiana*, un arbre des zones arides à usages multiples. In : Grouzis, M. & Le Floc'h, E. (2003) éd. *Un arbre au désert*. *Acacia raddiana*. Paris : IRD éditions, 21-58.

Le Houerou, H.N. (2001) Biogeography of the arid steppeland north of the Sahara. *Journal of Arid Environments*, 48, 103-128.

Leckie, D.G., Gougeon, F.A., Tims, S., Nelson, T., Burnett, C.N. & Paradine, D. (2005) Automated tree recognition in old growth conifer stands with high resolution digital imagery. *Remote Sensing of Environment,* 94**,** 311-326.

Lillesand, M. and Kiefer, R.W. (2004) Remote sensing and image interpretation. New York: Wiley, 763 p.

Ludwig, F., de Kroon, H., Berendse, F. & Prins, H.H.T. (2004) The influence of savanna trees on nutrient, water and light availability and the understorey vegetation. *Plant Ecology*, 170, 93-105.

Maltamo, M., Mustonen, K., Hyyppa, J., Pitkanen, J. & Yu, X. (2004) The accuracy of estimating individual tree variables with airborne laser scanning in a boreal nature reserve. *Canadian Journal of Forest Research-Revue Canadienne De Recherche Forestière,* 34**,** 1791-1801.

Mihidjay, A.S. (1999) Etude de la morphogenèse d'*Acacia tortilis* (Forsk.) Hayne ssp. *raddiana* (Savi) Brenan et essais de regeneration *in vitro*. Memoire de diploma d'études approfondies en physiologie vegetale. Université de Tunis II (Tunisia).

Needham T. & Peasley N. (2003) The ASDM Stand Interventions Encyclopedia. The Forestry Resource Book of the Future – Today. http://www.unb.ca/standint/ (consulted April 8, 2010).

Nizinski, J., Morand, D. & Fournier, C. (1992) Le rôle du couvert ligneux sur le bilan hydrique d'une steppe (Nord du Sénégal). *Cah. Orstom, Sér.Pédol.*, 27 (2), 225-236.

Ndour, P. & Danthu, P. (1998) Effet des contraintes hydriques et salines sur la germination de quelques *acacias* africains. In : Campa, C., Grignon, M., Gueye, M. & Hamon, S. (1998) Colloques et séminaires : l'acacia au sénégal. Orstom Edition, 105-122

Noumi, Z., Touzard, B., Michalet, R. & Chaieb, M. (2010) The effects of browsing on the structure of *Acacia tortilis* (Forssk.) Hayne ssp. *raddiana* (Savi) Brenan along a gradient of water availability in arid zones of Tunisia. *Journal of Arid Environments,* 74**,** 625-631.

Ozcelik, R., Brooks, J.R., Diamantopoulou M.J. & Wiant, H.V. (2010) Estimating breast height diameter and volume from stump diameter for three economically important species in Turkey. *Scandinavian Journal of Forest Research,* 25**,** 32-45.

Ouarda, H.E., Walker, D.J., Khouja, M.L. & Correal, E. (2009) Diversity analysis of *Acacia tortilis* (Forsk.) Hayne ssp *raddiana* (Savi) Brenan (Mimosaceae) using phenotypic traits, chromosome counting and DNA content approaches. *Genetic Resources and Crop Evolution*, 56, 1001-1010.

Ozdemir, I. (2008) Estimating stem volume by tree crown area and tree shadow area extracted from pan-sharpened Quickbird imagery in open Crimean juniper forests. *International Journal of Remote Sensing,* 29, 5643-5655.

Palace, M., Keller, M., Asner, G.P., Hagen S. & Braswell, B. (2008) Amazon forest structure from IKONOS satellite data and the automated characterization of forest canopy properties. *Biotropica,* 40**,** 141-150.

Popescu, S.C. (2007) Estimating biomass of individual pine trees using airborne lidar. *Biomass & Bioenergy,* 31**,** 646-655.

Running, S.W., Loveland, T.R. & Pierce, L.L. (1994) A vegetation classification logic-based on remote-sensing for use in global biogeochemical models. *Ambio,* 23**,** 77-81.

Saharaoui, B.S., Ait Mohand L. & Echaib B. (1996) Evolution spatio-temporelle des peuplements d'*Acacia tortilis* (Forsk.) Hayne *raddiana* (Savi) Brenan dans les monts Ougarta (Sahara nord-occidental). *Sécheresse*, 7, 173-178.

Schiewe, J., Tufte L. & Ehlers M. (2001) Potential and problems of multi-scale segmentation methods in remote sensing. *Geographische informationssysteme*, 6, 34-39.

Schiewe, J. (2002) Segmentation of high resolution remotely sensed data – Concepts, applications and problems. Joint international symposium on geospatial theory, processing and applications. Ottawa, Canada.

Schoenenberger, A. (1987) Rapport phytoécologique sur le Parc National de Bou Hedma. Projet GTZ N° 82.2045, 42 p.

Sghari, A. (2009) À propos de la présence d'une steppe tropicale au Jebel BouHedma en Tunisie présaharienne : approche géomorphologique. Quaternaire, 20, 255-264.

Shrivastava M.B. & Singh R.A. (2003) Interrelationships among crown diameter, diameter at breast height and stump diameter of silver fir trees. http://www.fao.org/DOCREP/ARTICLE/WFC/XII/0902-B4.HTM#P28_106 (consulted May 28, 2010).

Suarez, J.C., Ontiveros, C., Smith, S. & Snape, S. (2005) Use of airborne LiDAR and aerial photography in the estimation of individual tree heights in forestry. *Computers & Geosciences,* 31**,** 253-262.

Tarhouni, M. (2003) Cartographie des systèmes écologique et étude de la dynamique de l'occupation des terres dans le parc national de Bou Hedma. Thesis, Université de Sfax pour le Sud, Faculté des Sciences de Sfax, 94 p.

Tarhouni, M., Ouled Belgacem, A., Neffati, M. & Chaieb, M. (2007) Dynamique des groupements végétaux dans une aire protégée de Tunisie mériodinale. *Cahiers Agriculture*, 16 (1), 7.

Vassal, J. (2003) Introduction. In : Grouzis, M. & Le Floc'h, E. (2003) éd. *Un arbre au désert*. Acacia raddiana. Paris : IRD éditions, 13-17.

Wahbi, J. (2006) Régénération de l'*Acacia tortilis* ssp *raddiana* dans le parc national de Bou Hedma et son adaptation aux différentes contraintes abiotiques au stade de germination. Mémoire de mastère. Institut national agronomique de Tunisie.

Wulder, M. (1998) Optical remote-sensing techniques for the assessment of forest inventory and biophysical parameters. *Progress in Physical Geography,* 22**,** 449-476.

Wulder, M.A., Kurz, W.A. & Gillis, M. (2004) National level forest monitoring and modeling in Canada. *Progress in Planning,* 61**,** 365-381.

Wulder, M.A., White, J.C., Goward, S.N., Masek, J.G., Irons, J.R., Herold, M., Cohen, W.B., Loveland T.R. & Woodcock, C.E. (2008) Landsat continuity: Issues and opportunities for land cover monitoring. *Remote Sensing of Environment,* 112**,** 955-969.

Zaafouri, M.S., Zouaghi, M., Akrimi N. & Jeder H. (1996) La foret steppe a *Acacia tortilis* sbssp. *raddiana* var. *raddiana* de la Tunisie aride: dynamique et evolution. Actes du séminaire international. Acquis scientifiques et perspectives pour un développement durable des zones aride. Jerba, 5-6-7 Décembre 1996, 258-271.

ADDENDA

All addenda are available online at http://users.telenet.be/kevin.delaplace/thesis/ . On request they can be obtained on CD-ROM, by contacting the author[20].

Addendum 1: GeoEye-1 metadata

Addendum 2: *Acacia raddiana* (Savi)

Addendum 3: Flora of Bou-Hedma National Park (provided by ir. Lazhar Hamdi)

Addendum 4: Microsoft Office Access 2007 Database

Addendum 5: Features used for image classification

Addendum 6: Paper submitted for GEOBIA 2010

[20] Kevin Delaplace
Rekkemsestraat 291
8510 Marke
Belgium
kevin.delaplace@gmail.com
0032 498 20 92 07